STEADY STATE STRENGTH BEHAVIOR OF GANGA SAND

A Thesis submitted

in Partial Fulfillment of the requirements

for the Degree of

Master of Technology
in
Civil Engineering

by

Abhik Datta

under the guidance of

Dr. P. K. Basudhar and Dr. N. R. Patra

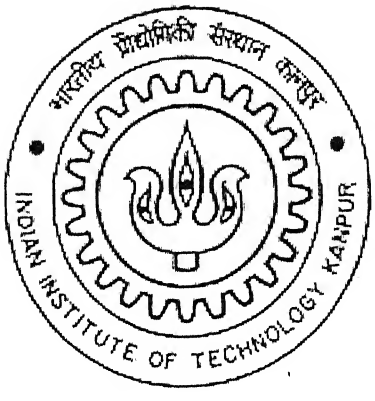

DEPARTMENT OF CIVIL ENGINEERING
INDIAN INSTITUTE OF TECHNOLOGY KANPUR
MAY 2005

ABSTRACT

Steady state of deformation for any mass of particles is that state in which the mass is continuously deforming at a constant volume, constant normal effective stress, constant shear stress and constant velocity. Variations in steady state strength are seen to cause sharp variations in post-earthquake stability analysis indicating that they are critical for determining whether flow failure occurs or not. The present methods of evaluation of steady-state strength have either got certain limitations or are too sophisticated for use in all cases. An alternative effective stress approach allows the assessment of steady state strength from conventional drained triaxial tests. This method allows a geotechnical laboratory with the capability of performing traditional drained tests with volume change measurements, to participate in static liquefaction and residual strength assessment. This method is used to study the steady state strength behavior of Ganga sand in the present study and this is validated with stress-controlled consolidated undrained test result. The steady state strength behavior of Ganga sand is compared with that of Toyoura sand and also with the predicted behavior from a model.

ACKNOWLEDGEMENT

I would like to take this opportunity to express my deepest reverence to my teacher and thesis supervisor Prof. P. K. Basudhar who suggested the present problem and gave his valuable guidance throughout the course of this work. I would also like to tender the most sincere gratitude to my thesis supervisor Prof. N. R. Patra and my teacher Prof. Sarvesh Chandra for providing tips and encouragement during this work.

I am sincerely thankful to Mr. A. K. Srivastava for letting me use the facilities and providing with the materials necessary for all the tests conducted. I would also like to express my heartfelt gratitude to Mr. K. P. Yadav, Mr. Sanjay Gupta, Mr. Gulab Chand and Mr. Ram Parsuram for providing me with all the helps I needed for carrying out the experiments.

I would forever remember the warmth and affection I received from my friends and well-wishers who made my stay here memorable and pleasant.

Finally I would like to thank my parents and my brother, who, though far away from me, remained my source of support and encouragement.

CERTIFICATE

It is certified that the work contained in the thesis entitled "Steady State Strength behavior of Ganga Sand", by Abhik Datta, has been carried under our supervision and that this work has not been submitted elsewhere for a degree.

P. K. Basudhar
Department of Civil Engineering
Indian Institute of Technology Kanpur
Kanpur, May 2003

Dr. N. R. Patra
Department of Civil Engineering
Indian Institute of Technology Kanpur
Kanpur, May 2003

CONTENTS

CHAPTER 1

INTRODUCTION

1.1. General: Mechanism of Steady State Strength

Liquefaction is the condition where a loose saturated sand or silt loses shear resistance due to pore-water pressure build-up when subjected to undrained loading, whether that be monotonic, cyclic or dynamic. However different from earlier consideration of liquefaction, it is now recognized that loose sand does not necessarily lose all its strength during liquefaction.

Study of the liquefaction behavior of soils under cyclic loading is complicated and requires sophisticated equipments. Also, the behavior of soil during liquefaction cannot always be explained based on the results of cyclic triaxial tests only. This led to the development and use of the concept of steady state strength, which can be measured, although with some difficulty, in the laboratory with triaxial apparatus.

The steady state strength concept is very important in understanding the liquefaction problem. Steady state of deformation for any mass of particles is that state in which the mass is continuously deforming at a constant volume, constant normal effective stress, constant shear stress and constant velocity. The words 'steady state' come from the analogy with a steady state flow in fluid mechanics and the word 'deformation' comes to signify the fact that the steady state exists so long as the deformation exists. Continuous shear after the residual strength is reached in drained tests on clays or sands are examples of steady-state deformation. The steady state of deformation is achieved only after all particle orientation has taken place and particle breakage, if any, is complete, so that the shear stress needed to continue deformation and the velocity of deformation remain constant. These conditions are achieved only at large strains, well beyond those that normally are reached in undrained triaxial tests. As already stated, steady state of deformation requires a constant velocity of deformation and the steady state exists only so long as deformation continues. The structure of a specimen during steady-state deformation is very special and quite different from both its initial structure and the structure of the specimen before steady

state is reached. The steady state strength is the shear strength of the soil during steady state deformation. A plot of void ratio against mean effective confining stress is called the steady state line. A soil whose initial state falls above its steady state line would undergo liquefaction, if subjected to a shear stress over and above its steady state strength.

The steady state concept is solely important for problems of liquefaction under monotonic loading. For more common dynamic or earthquake loading problems also, the determination of undrained steady state strength is critical for indicating whether the soil in question is susceptible to liquefaction. To determine whether liquefaction would be triggered by a given earthquake, one should perform cyclic tests in which the driving shear stresses are less than the in-situ steady state strengths.

Variations in steady state strength are seen to cause sharp variations in post-earthquake stability analysis indicating that they are critical for determining whether flow failure occurs or not. The present methods of evaluation of steady-state strength have either got certain limitations or are too sophisticated for use in all cases. An effective stress approach allows the assessment of undrained stress-strain curve and the undrained effective stress path of a monotonic test up to large strain level from drained triaxial tests. This method provides the conditions for the development of complete versus limited liquefaction. Since, steady state strength or soil behavior at large strains are difficult to be measured, this simplified method makes it possible for geotechnical laboratories with the capability of performing traditional drained tests with volume change measurements to participate in static liquefaction and residual strength assessment. There are hardly a few Indian sands whose steady state characteristics have been published. Sitharam, et al. (2004) reported some studies on the silty sand from Bhuj region after the Bhuj earthquake. They studied stress-strain behavior of the mentioned sand upto large strain levels, in monotonic as well as cyclic undrained triaxial tests at three relative densities of 8.9%, 56.5% and 80%. Till now no work on steady state characteristics of Ganga sand has yet been reported and, as such, can be taken up and studied to provide some idea by this alternative method about its steady state strength as a measure to evaluate the possibility of liquefaction if the in-situ void ratio at a site composed of this sand, is known. To give some idea about the work done to date on the subject and frame the plan of action of the present study a brief literature review is presented in the following section.

1.2. Literature Review

A brief review of literature in the field of steady state strength of soils, both experimental and analytical, is presented in this section.

1.2.1. Experimental Studies

1.2.1.1. Laboratory Studies

Casagrande (1936) first established the importance of volumetric strain in the soil behavior and introduced the term liquefaction. He performed a series of drained strain-controlled triaxial tests and discovered that initially loose and dense specimens at the same confining pressure approached the same density when sheared to large strains. The void ratio corresponding to this density was called the critical void ratio which was found to vary with the effective confining pressure.

Castro (1969) introduced the importance of steady state in liquefaction after performing a series of undrained, stress-controlled triaxial tests. He plotted the relationship between effective confining pressures and void ratios at large strains for these undrained, stress-controlled tests and referred to the curve produced by this plot, which is similar to the critical void ratio line for the drained strain controlled tests performed by Casagrande (1936), as the Steady State Line (SSL).

Castro, Poulos and Leathers (1985) and Castro, Seed and Keller (1992) did series of laboratory tests and performed a steady state strength analysis for the lower San Fernando dam slide following the earthquake of 1971. Previous analyses were based on the results of cyclic triaxial stresses and evaluation of seismic shear stresses only and failed to explain certain key features which were explained by these analyses. They recommended that for assessing the seismic stability analysis of a dam, determination of the undrained steady state strength should be included in the experimental program. This type of analysis indicates whether the soil in question is susceptible to liquefaction. To determine whether liquefaction would be triggered by a given earthquake, one should perform cyclic tests in which the steady state strength is overcome by the driving shear stress. If due to densification the steady state strength

values of the undisturbed specimens increase beyond the driving shear stress then the soil cannot provide information on the cyclic loads required to trigger liquefaction.

There have been some experimental studies on the dependence of steady state strength on different factors. They are being discussed here. Castro et al. (1985), Poulos et al. (1985), Fear and Robertson (1995) studied the effect of grain characteristics and grain size compositions of soils on the position and slope of the steady state line. The vertical position of the steady state line is chiefly influenced by the grain size distribution, also generally, it is seen that the void ratio range is more effective than the conventional parameters from gradation curves like mean grain size, uniformity coefficient and coefficient of curvature. The slope of the steady state line is said to be dependent predominantly on the shape of the grains with steeper slope expected for more angular grains.

Been and Jefferies (1985), Sladen et al. (1985), Pitman et al., (1994) studied the influence of fines on the position and slope of the steady state line. The presence of plastic or clayey fines is generally considered to increase the steady state strength of a soil. Numerous field studies have shown that soils with more than 10 or 20 percent of plastic fines tend not to liquefy during earthquakes depending on the plasticity of the fines. Soils meeting the plasticity requirement tend to undergo a cyclic mobility form of failure that results in only minor strength loss and small deformations of the soils mass. Soils not meeting the plasticity requirement tend to undergo flow liquefaction that results in significant strength loss and very large deformations. The understanding of the steady state behavior and liquefaction of sands containing non-plastic fines is less complete with contradictory results in the literature.

Negussy and Islam (1994) on tailing sand, Verdugo and Ishihara (1996) on Toyoura sand, Riemer and Seed (1997) on Monterey sand, Ishihara et al (1998) on sand fraction of Masado soil, Cubrinovski et al (1999) on Kasumigaura sand have conducted various types of laboratory tests including triaxial tests in compression and tension, simple shear tests and ring shear tests with several methods of soil sample preparation and studied the effect of mode of deformations, method of sample preparations, drainage conditions, forms of consolidation, bedding orientation etc. on the liquefaction behavior and steady state strength of soils. Cubrinovski et al (1999) noted no significant change in undrained strength determined by triaxial compression and extension tests. However Yoshimine and Ishihara (1998) pointed out that

undrained strength in triaxial compression is considerably higher than that in triaxial tension, while simple shear test gives a value in between them. The literature is not unanimous on the effect of sample preparation method on steady state behavior also. Most authors suggest that there is no effect of the method of sample preparation on the steady state behavior. Verdugo (1992) applied three methods of sample preparation on Toyoura sand and unique steady state line was obtained in three cases. However, there exist some experimental results (DeGregorio, 1990) that indicate effect of fabric on its position. According to available literature, form of consolidation, over-consolidation ratio and bedding orientation have practically no effect on the apparent position of the steady state line (Verdugo, 1992 and Kato et al, 2001).

Norris et al. (1997) presented an effective stress approach for the evaluation of the whole undrained stress-strain response including peak and residual strength values from traditional drained triaxial tests with volume change measurements. This method provides a simple approach for determining steady state strength and liquefaction susceptibility.

1.2.1.2. Field Tests

Seed et al. (1985) provided empirical relationships between corrected standard penetration test (SPT) blow counts and the post-earthquake residual strength as established from case-histories of embankment slope failures. Seed and Harder (1990) provided additions of residual strength prediction data from SPT values, to the original data.

Stark and Mesri (1992) provided a critical review of Seed's correlations. They stated that the mobilized strength back-calculated by Seed (1987), Seed et al. (1988) and Seed and Harder (1990) may reflect partial drainage and may not be the undrained strength sought.

Dorby (1995) provided a variation of Seed's case study approach by taking the residual strength as a ratio of the vertical effective stress and suggested that the ratio lies in the range 0.04 to 0.20.

Ishihara (1993) studied the undrained behavior of Japanese saturated sand, and proposed some new index parameters to quantify undrained behavior better. The

laboratory established criteria for contractive or dilative behavior was expressed in terms of cone penetration tip resistance value.

Stark and Olson (1995) presented relationships between cone penetration tip resistance and the liquefaction potential of sandy soils. The relationships were based on 180 liquefaction and non-liquefaction case histories where Cone Penetration Tests were performed.

Juang et al. (2002) investigated the soil liquefaction case histories of liquefied soil and examined three methods namely Robertson method, Olsen method and Juang method, using the case histories of the Chi-chi earthquake. The results of comparisons showed that Juang method is more accurate than the other two.

1.2.2. Theoretical Studies

Roscoe and Poorooshasb (1963) were the first to emphasize the importance of the combined influence of density and normal stress for modeling of soil behavior. On the basis of both theoretical and experimental considerations, they introduced the critical state of the soil as a reference for quantification of the effects of the initial state on soil behavior.

Poulos (1981) provided a comprehensive explanation of the concept of the steady state of deformation in particulate media with particular reference to soil. Poulos et al. (1985) provided a critical review of the concept of steady-state deformation and its relevance to the evaluation of the undrained stability of saturated sand. They defined the critical void ratio line as the relationship between void ratio and mean effective stress at steady state deformation under drained shear condition and the steady state line (SSL) as the relationship between void ratio and mean effective stress deformation under undrained shear condition. The quasi steady state is the temporary steady state, which is lost due to dilative tendency or strain-hardening behavior until the final steady state is obtained. It indicates the transfer from contractive to dilative behavior. The relationship between void ratio and effective mean stress at these quasi steady states in undrained shear test gives the quasi steady state lines (QSSL).

Alarcon-Guzman et al. (1988) provided a detailed study on the conditions leading to limited or steady-state flow deformation under monotonic loading and the state conditions marking the initiation of strain-softening behavior under either

monotonic or cyclic undrained loading. They noted that the phase transformation lines (distinguishing the transformation from contractive to dilative behavior) are defined by the values of mobilized friction angle at which dilation prevails on loading within the strain-hardening region of the state diagram.

In a similar vein, Been and Jefferies (1985), Bolton (1986), Verdugo (1992) and Ishihara (1993) have reported extensive studies on the combined influence of the initial density and normal stress on sand behavior. A distinctive feature of these studies is that particular indices and parameters serving as measures for the effects of the initial state on sand behavior have been proposed. Been and Jefferies (1985) defined the state parameter (Ψ) as the difference between the current void ratio (e) and the void ratio at the steady state (e_c). Bolton (1986) proposed a relative dilatancy index (I_R), which can be expressed as $I_R = \frac{D_R}{100}(Q - \ln p_p') - 1$, where D_R is the relative density, Q = an empirical constant that varies with the crushing strength of the grains, p_p' = the mean effective stress at peak deviator stress. Verdugo (1992) and Ishihara (1993) defined the state index (I_s) as $I_s = \frac{e_U - e}{e_U - e_Q}$ where e_Q is the void ratio of the quasi steady state line (QSS-line) and e_U is the void ratio of the upper reference line (UR-line), both at the initial mean normal stress p' as referred to in Fig. 1.1. When a line is extended to the flat slope of quasi steady state or steady state line at low pressures, it gives rise to the upper reference line. Obviously at any effective mean stress, void ratio corresponding to UR-line would be higher than that corresponding to QSS-line. Thus, the state index is a direct measure for the relative initial e-p state with respect to the QSS-line and UR-line and quantifies the link between the relative initial state and the normalized stress- strain curve.

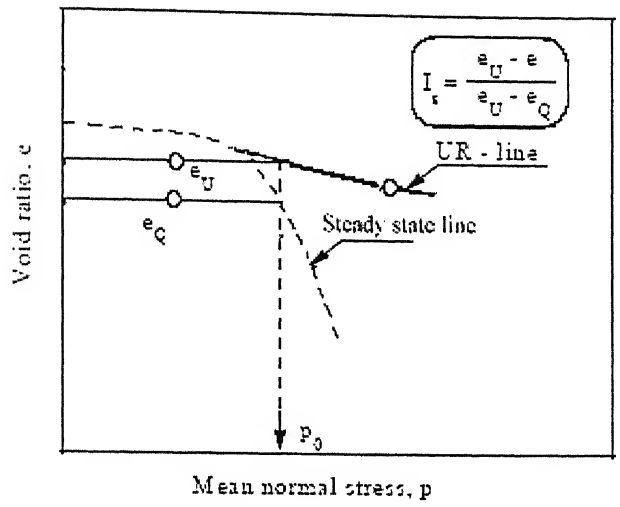

Fig 1.1: State index

Several attempts have been made to use these parameters for modeling steady state strength behavior of sands. Jefferies (1993) incorporated the state parameter (Ψ) as a hardening parameter in the cam clay model to describe the monotonic behavior of sand. Wood et al. (1994) used the same parameter for modeling drained monotonic stress-strain behavior associated with strain softening. However Ishihara (1993) pointed out that Ψ, which is the difference between the in-situ void ratio (e) and the void ratio at the steady state (e_c), is useful for quantifying the behavior of medium to dense sand, but its use becomes less tenable for cases of low confining stress and high void ratios.

Cubrinovski and Ishihara (1998 and 2000) gave a stress-strain dilatancy model based on the state index. This model is designed for modeling both monotonic and cyclic undrained behavior of sand and analysis of liquefaction problems. They concluded that the position of SSL shifts towards the void ratio-axis with decrease in void ratio range ($e_{max} - e_{min}$) and the slope of the SSL become steeper with more angularity of particles.

1.3. Motivating factors of the present study:

Thus, it is seen that even though the importance of steady state strength in evaluating the post liquefaction behavior of sands has been recognized as early as 1969, apart from a few studies on measuring the reserve strength of different sands, especially in USA (Monterey sand by Reimer and Seed (1997)) and Japan (Toyoura sand by

Yoshimine and Ishihara (1998), Kasumigaura sand by Kubrinovski et al. (1999)) not much studies have been undertaken on the subject. Some studies have been made to develop theoretical models most notably by Cubrinovski and Ishihara (1998 and 2000) to predict steady state strength and the behavior of Toyoura sand at large deformation based on common physical properties (e.g. emax, emin, grain shape and size etc) of the sand. Efforts to validate these models with experimental data are scanty. As such, for such models to be useful, data needs to be generated for various local sands in earthquake prone areas of the world for hazard mitigation. Once the models successfully match a large pool of experimental data they can be used for predicting steady state behavior of sands. Till to date in India, no serious efforts have been made to study the steady strength characteristics of local river sands collected from different strata of the river basins. Thus it is necessary to initiate such a study. As such, an effort has been made in this direction in this thesis.

1.4. Thesis Structure

The contents of the thesis are as follows:

Chapter 1: Introduction: Here there is a brief introduction to the concept of steady state strength and its relevance to liquefaction study, followed by a literature review on the subject.

Chapter 2: Experimental Details: Here the present methods of evaluation of steady state strength behavior, sample preparation, material used, the methods adopted in the present study with relevance is discussed.

Chapter 3: Results, discussions and scope of future work: Here the results are showed with brief discussion. Conclusions have been drawn and the scope of future work is discussed.

Appendix: Finally in the Appendix, experimental data for the various tests are provided.

CHAPTER 2

EXPERIMENTAL DETAILS

2.1. General

At present there are three methods for assessing the steady-state strength of liquefying sand. One method (Seed et al, 1985) uses an empirical correlation between corrected SPT blow-count and the post-earthquake residual strength as established from case histories of embankment slope failures involving liquefied materials. Response based on actual field evidence is preferred. However, too few field cases have been properly studied and those too with back-figured strengths (averaged over too large a volume of soil) for the development of empirical relations (e.g. method proposed by Seed et al., 1985) to be reliable. While there have been additions to the original data (Seed and Harder, 1990), the band for residual strength versus blow-count in this relationship is simply too wide. This suggests that the residual strength is a more complex function of volume change tendencies of the sand that can be expressed as a simple correlation with the corrected blow-count value. A variation of Seed's approach is to take the residual strength as a ratio of the vertical effective stress (Dorby, 1995). Unfortunately, the ratio suggested ranges from 0.04 to 0.20 though Stark and Mesri (1992) differentiate its dependence upon corrected blow-count.

A second method (Poulos et al., 1985) involves the evaluation of residual strength from static consolidated undrained test on reconstituted and undisturbed samples and interpretation of such data. In regard to the second method, a basic understanding of why peak and residual strengths ensue is necessary; otherwise such testing becomes merely an exercise in black box testing. The strain level at which steady state is obtained is usually high and the strain rate required to achieve the steady state is very high also. Thus, it is impossible to achieve the steady state by normal or conventional strain-controlled triaxial test. Stress-controlled triaxial tests with pore-pressure measurement must be done to study steady-state behavior. Even

then dynamic recording equipment with rapid measuring capabilities and a pneumatic system or a closed-loop electro-hydraulic system loading equipment is desirable.

The third method, first proposed by Bishop et al (1971), involves a ring-shear apparatus which provides shear by way of torsion. The ring-shear apparatus is specifically designed for testing stress-strain characteristics at large strain levels and is suitable for steady state strength studies. But one problem with this apparatus, like direct shear test, is that failure occurs in a predefined plane. Also few laboratories or geotechnical firms possess such equipment.

Hence, an alternative method was proposed by Norris et al (1997), by which steady state strength behavior can be examined through conventional drained triaxial tests with volume change measurement. This has been used to study the steady state characteristics of Ganga sand and was checked by the second method of stress-controlled consolidated undrained triaxial test.

2.2. Sample Preparation

Soils which possess little or no cohesion are difficult if not impossible to trim into a specimen. If undisturbed samples of such materials are available in sampling tubes, satisfactory specimens can usually be obtained by freezing the sample to permit cutting out suitable specimens. Samples should be drained before freezing. The frozen specimens are placed in the triaxial chamber, allowed to thaw after application of the chamber pressure, and then tested as desired. Some slight disturbance probably occurs as a result of the freezing, but the natural stratification and structure of the material are retained. In most cases, however, it is permissible to test cohesionless soils in the remolded state by forming the specimen at the desired density. Even then, controlling the density of the sample inside such small diameter of 38 mm is difficult.

A forming jacket consisting of a split mold which encloses a rubber membrane is required for cohesionless soils. The inside diameter of the mold minus the double thickness of the membrane is approximately equal to the diameter of the specimen prepared. A funnel or spoon for placing the material inside the jacket along with a tamping hammer and a suction pump are also necessary for preparation of cohesionless soil sample.

Samples at three relative densities of around 20%, 45% and 75% were prepared varying a) the amount of suction, b) amount of tamping, c) height of fall, d) number of layers and e) initial moisture content. Generally moist tamping with no or little suction was the method used to achieve the low relative density samples. 160 gm of dry sand was mixed with 5 to 7% of water content, i.e. 8 to 10 gm of water. This was roughly divided in five equal parts. Each part was poured into the circular split-mold by a spoon, with no suction or vibration. After placing of each part, around 10 gentle blows were provided by a 10 mm diameter tamping rod. For preparing medium dense sand, 170 gm of dry sand was weighed and placed inside an 8 cm diameter funnel. It was then poured from the funnel inside the split mold from approximately 30 mm height over the sand level. No tamping was done here, but all the while suction was provided along the circumference of the specimen. For preparing dense sample, 180 gm of dry sand was put in a bowl. They were dropped inside the membraned split mould by a spoon. After dropping each spoon, around 10 blows were provided by a 10 mm diameter tamper. All the while, suction was provided along the circumference of the specimen as was done for the earlier case.

2.3. Details of Method 1

This method was proposed by Norris et al. (1997). The method is discussed below stepwise.

Step 1: A sample is isotropically consolidated to a particular consolidation pressure σ_{3C} and particular void ratio e_C .

Step 2: The sample is rebounded to a higher void ratio say e_1 by decreasing cell pressure to σ_{3_1} from σ_{3C}. The volume change due to rebound ($\varepsilon_{V_{Isotropic}}$) is measured.

Step 3: Now drained triaxial test is performed on the sample and stress vs. strain curve and volumetric strain vs. axial strain curve are drawn.

Step 4: The above process is repeated for several samples, the rebounded void ratio or reduced cell pressure being different in different cases.

Step 5: For any particular rebounded sample, Fig. 2.2 is entered with the corresponding measured $\varepsilon_{V_{Isotropic}}$ of step 2 and moved horizontally until it cuts the volumetric strain-axial strain curve of the corresponding sample.

Step 6: Now moving vertically up to Fig. 2.1 until it intersects stress-strain curve of the corresponding sample the point on required undrained response is located. For example, let the third rebound curve be considered. If the volumetric strain during rebound from σ_{3c} to $\sigma_3'\Big|_3$ is $\varepsilon_{V_{Iso}}\Big|_3$ then Fig. 2.2 is entered with $\varepsilon_{V_{Iso}}\Big|_3$ and moving horizontally till the third rebound curve is intersected, point A is obtained. From point A moving vertically till the third rebounded stress-strain curve of Fig. 2.1 is intersected, point B can be found out, which is a point on the undrained curve.

The logic behind the above procedure is discussed now. The undrained (constant volume) behavior in a consolidated undrained test is the result of opposing volume change tendencies from isotropic and deviatoric stress changes accompanying the change in the effective confining pressure. During undrained shear of loose sand the applied deviator stress (σ_d) will cause an undrained pore-water pressure buildup (Δu_d). Consequently a drop occurs in the effective confining pressure to $\sigma_3' = \sigma_{3c} - \Delta u_d$. Suppose one assumes a value of Δu_d (without at this time knowing the corresponding value of σ_d) and obtain the associated (drained) σ_3' curve of Fig 2.1. In the undrained test the decrease in σ_3 (from σ_{3c} to σ_3') will mean that the sample would like to expand by an

amount $\varepsilon_{V_{iso}}$. However, the total or undrained volumetric strain (ε_V) due to both effective confining pressure (σ_3') and deviator stress (σ_d) must be equal to zero [i.e. $\varepsilon_V = \varepsilon_{V_{iso}} + \varepsilon_{V_{Shear}} = 0$]. Consequently, the volumetric strain due to deviator stress ($\varepsilon_{V_{Shear}}$) in Fig 2.1 must be equal and opposite (compressive) to $\varepsilon_{V_{iso}}$. Therefore if one enters the volumetric change curve with $\varepsilon_{V_{Shear}} = -\varepsilon_{V_{iso}}$ and moves horizontally, until $\varepsilon_{V_{Shear}}$ for the curve at the reduced pressure σ_3' is intersected, then a vertical

line should intersect the stress-strain curve at the associated σ_d of the given σ_3' curve.

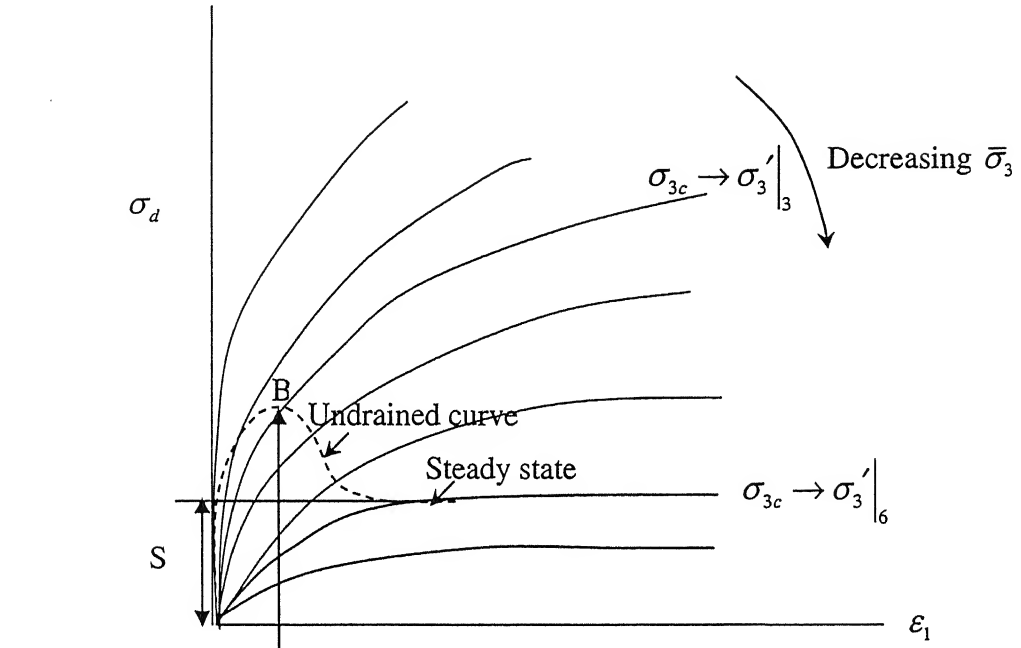

Fig. 2.1: Stress-strain behavior

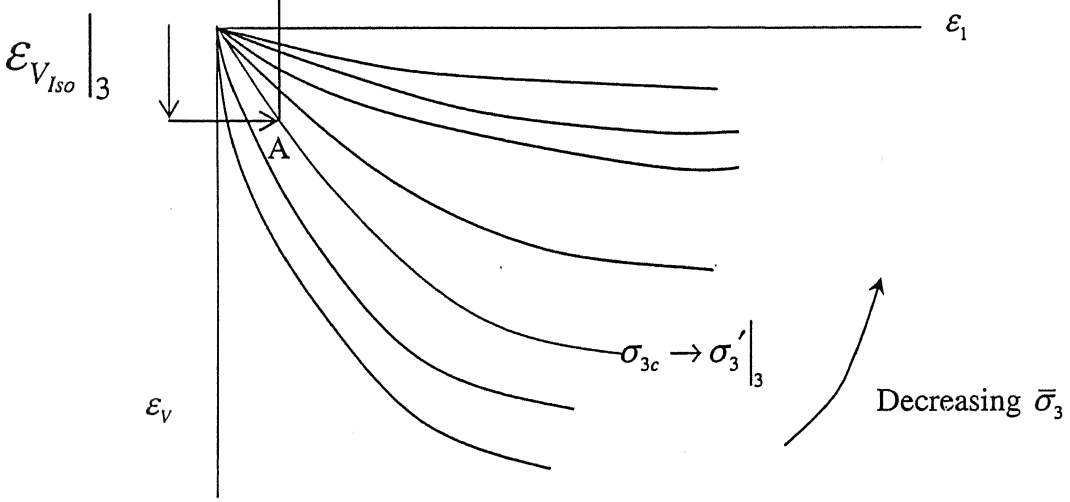

Fig. 2.2: Volume change behavior

Step 7: The process is repeated for all the rebounded samples. These points are joined to get the whole undrained response. The point at or beyond which the associated drained response becomes horizontal gives the steady state strength. At the same time the corresponding point (p ', q) on the undrained effective stress path can be assessed

as $p' = \sigma_3' + \sigma_d/2$ and q = $\sigma_d/2$ and plotted with taking the rebounded cell pressure of the drained stress-strain curve where the steady state is obtained. For example, in Fig 2.1 the steady state is obtained over the sixth curve which was for a sample rebounded from σ_{3c} to say $\sigma_3'\Big|_6$, then the steady state strength is S/2 + $\sigma_3'\Big|_6$.

Step 8: If the steady state is felt like reaching between two rebounded curves, an intermediate value between these two rebounded cell pressures can be taken by interpolation. The initial void ratio and the steady state strength as calculated above, give rise to a point on the steady state line (SSL). We can repeat the procedure for a few more initial relative densities to get the whole SSL. Now for any stress encountered we can tell whether the soil is susceptible to flow liquefaction by checking whether its state falls above the SSL and whether the stress is greater than the steady state strength.

Fig. 2.3 shows a prepared sample while the experimental set up to do strain controlled consolidated drained tests on samples rebounded to different cell pressures are shown in Fig 2.4 and Fig 2.5.

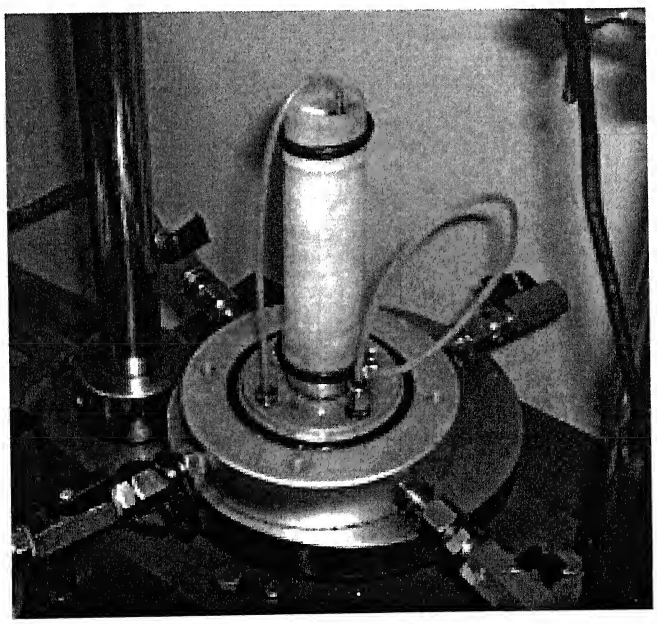

Fig. 2.3: A prepared sample

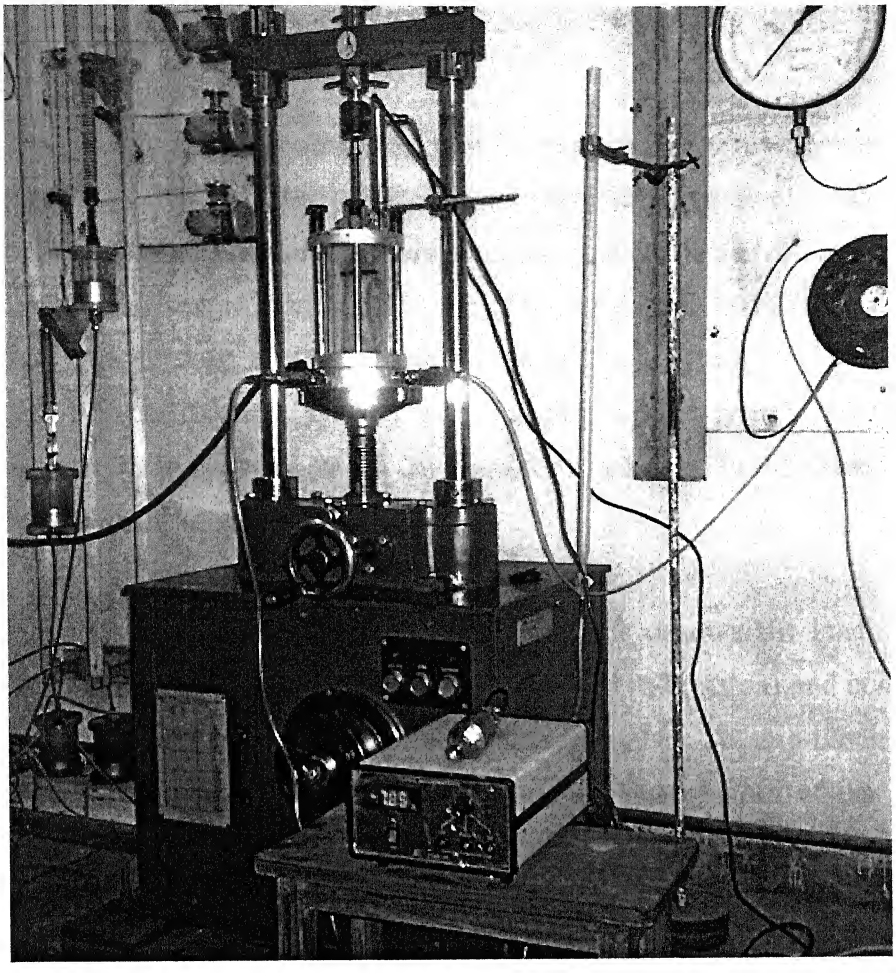

Fig. 2.4: Strain-controlled triaxial test setup with mounted sample

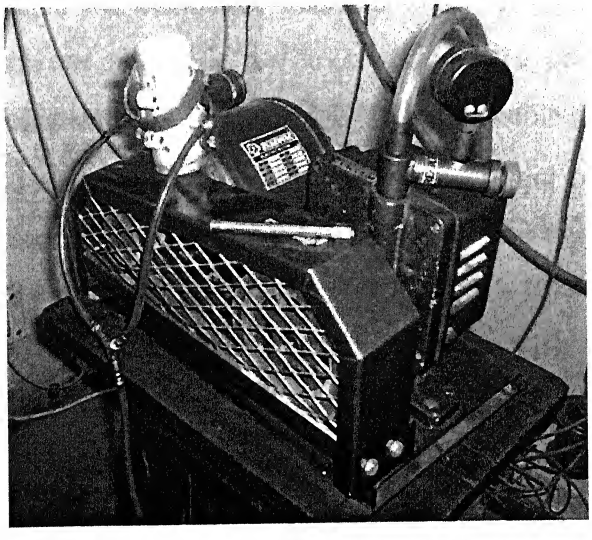

Fig. 2.5: Suction pump, split mold and tamper

2.4. Details of Method 2

The monotonic stress-controlled triaxial compression test with pore pressure measurement is used to determine the steady state strength. Poulos et al. (1985) provided details for evaluation of steady state strength and liquefaction behavior by this method. Here, instead of controlling the strain, load is applied to the specimen in increments. The loading equipment may be either (1) a pneumatic system, (2) a closed-loop electro-hydraulic system, or (3) a dead-weight system. A deadweight system is practical only for up to 3.8 cm diameter specimens. In the present study, a dead-weight system was used.

Fig. 2.6 shows a satisfactory arrangement for deadweight loading, which consists of a horizontal loading bar bearing on the load rod (piston) and connected to a weight hanger suspended beneath the triaxial chamber. A stop-block must be provided beneath the weight hanger that will permit deformation of the specimen equivalent to not less than 30 percent axial strain but will prevent contact of the horizontal loading bar with the top of the triaxial chamber. The loading assembly should be designed to support 150 kg so that stresses generated are large enough to produce steady state stage in the samples and fabricated with lightweight material.

The magnitude of the monotonic load increments is arbitrary but should be selected to provide several points on the stress-strain curve prior to peak deviator stress. For a confining pressure (σ_{3c}) of 50 kPa, a reasonable increment would be equivalent to about 30 kPa of deviator stress based on the initial area of the specimen. If the confining pressure is 50 kPa to 500 kPa, an increment equivalent to about 35 kPa is more practical; i.e. for the specimen diameter used, a load increment of 3 to 4 kg is suitable. The load increment value should be reduced as peak deviator stress is approached, so that the application of the last increment does not significantly exceed the true peak value. A few trial tests are conducted to develop skill and confidence before the actual tests. The test set up is shown in the following figure (Fig. 2.6).

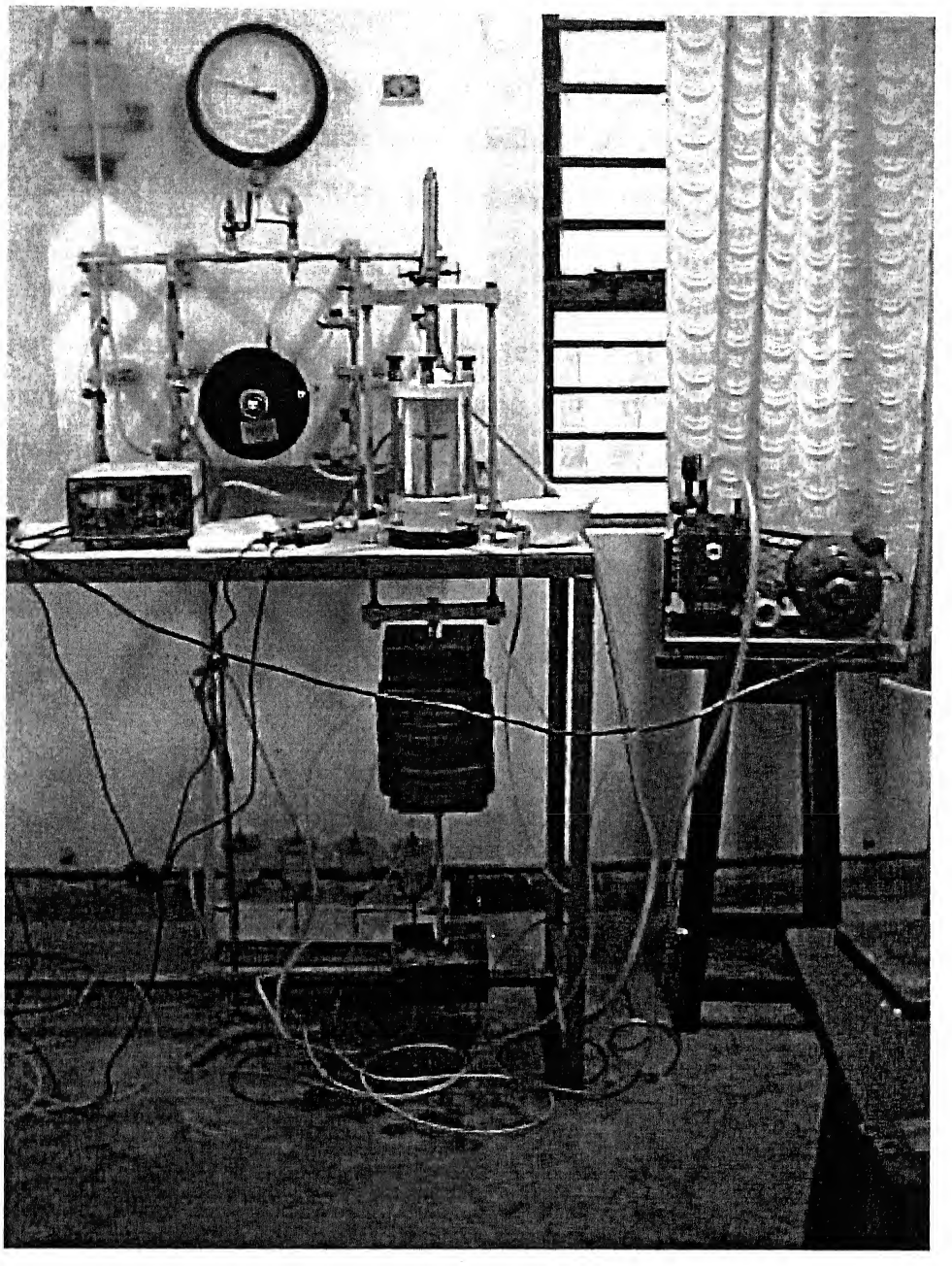

Fig. 2.6: Stress controlled triaxial apparatus with dead-weight loading system

Loading is continued with approximately l-min intervals until either (a) the specimen liquefies or partially liquefies, or (b) the specimen tends to dilate. A complete stress-strain record is difficult to obtain and requires experience. The clues to approaching rapid failure are an obvious increase in deformation rate and steadily accelerating increase in pore water pressure. If the specimen deforms steadily but not catastrophically, additional load increments may be applied as the straining tends to cease until the pore pressure begins to decline.

Assuming that the loading piston is not connected to the specimen cap, the static uplift load equal to the area of the loading piston multiplied by the chamber pressure must be accounted for when applying axial stresses.

Incomplete saturation resulting in low B values should be guarded. The following problems can cause low B values: (a) use of insufficiently de-aired water may prevent dissolving of air in the specimen without resorting to extremely high back pressures; (b) incomplete de-airing or saturation of pore pressure transducer and drainage lines (can be avoided by applying a vacuum); and (c) system leaks due to punctured membrane, poor membrane sealing to cap and base, loose fittings, or improperly designed O-ring grooves.

Insufficient air or hydraulic fluid at failure conditions will cause unacceptable load reduction. Misalignment between the loading rod piston of the triaxial cell and load actuator or air piston through which load is transferred to the loading piston may also cause unacceptable loading conditions.

2.5. Properties of Ganga Sand

In the present study, Ganga sand has been used for finding its steady state strength characteristics. The basic properties as determined in the laboratory are as follows:

Specific Gravity = G = 2.67

Maximum void ratio = $e_{max} = 0.97$

Minimum void ratio = $e_{min} = 0.64$

The grain size distribution curve for the soil is shown in Fig.2.7

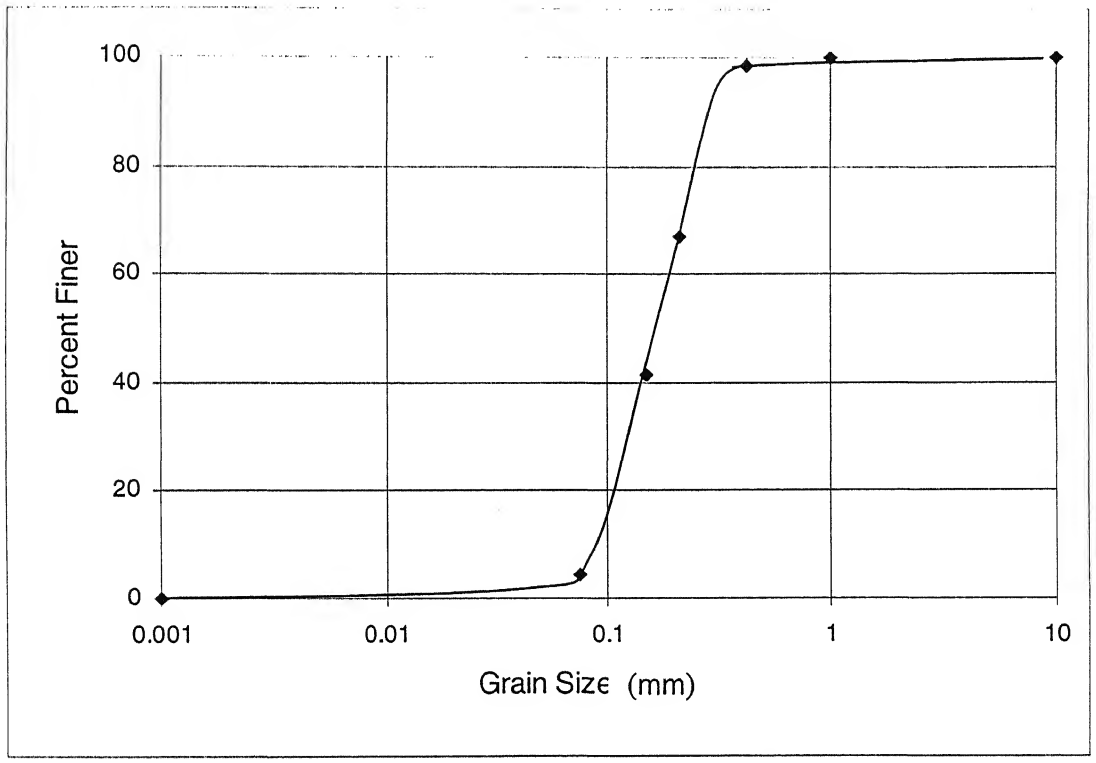

Fig. 2.7: Particle Size Distribution curve

The characteristic sizes as determined from the curve are as follows.

$D_{10} = 0.10$ mm

$D_{30} = 0.12$ mm

$D_{60} = 0.19$ mm

Uniformity Coefficient = $C_u = 1.9$

Coefficient of Curvature = $C_c = 0.76$

As per IS 1498-1970 (Unified Soil Classification System), it can be classified as SP, i.e. poorly graded sand with little fine content.

To observe the grain shapes of Ganga sand, the grains were studied under a stereo-microscope. A photograph of the grains at around 125 times zoom under the stereo-microscope is shown in Fig. 2.8. It can be seen that the boundaries of many particles can be traversed by only three or four tangents and although there are some sub-angular and subrounded particles, the grains together can be best described as angular.

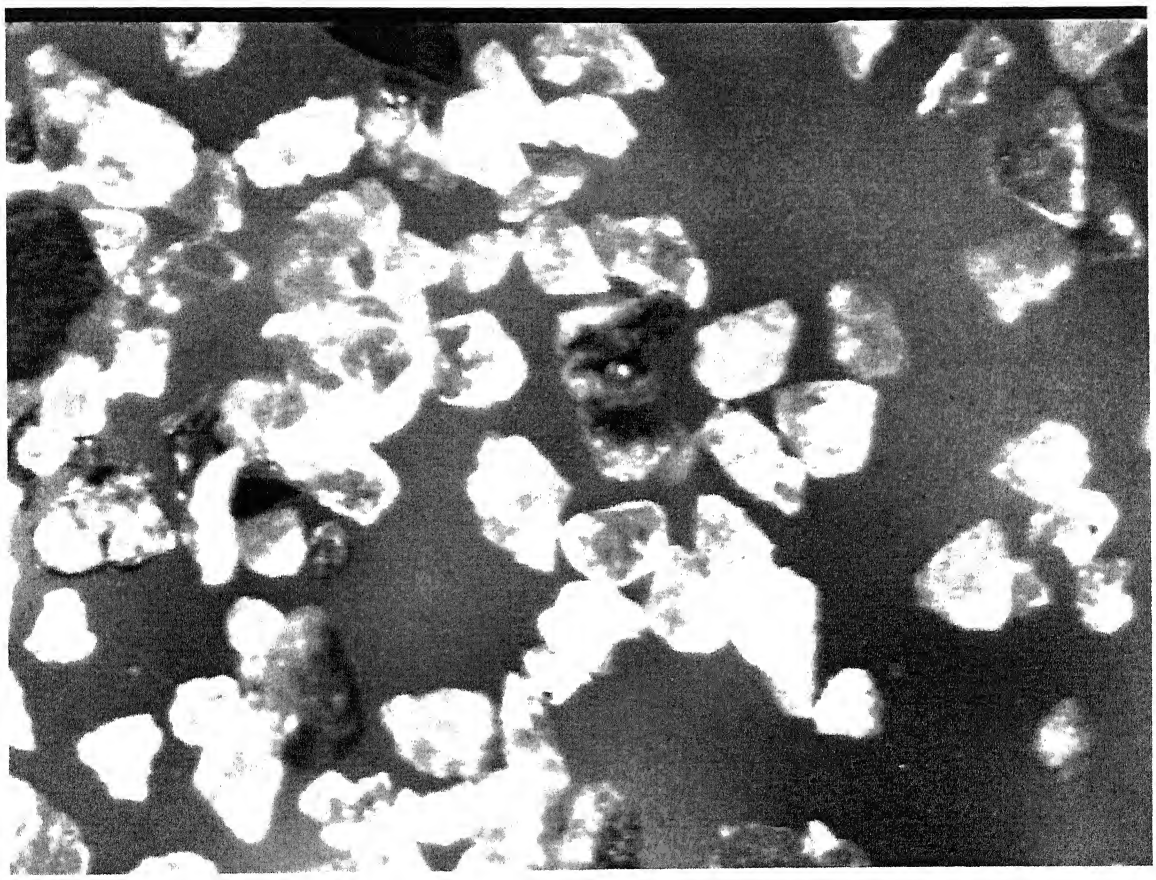

Fig. 2.8: Grain shape of Ganga sand

2.6. Planning of experiment:

Different samples were prepared and tested in triaxial apparatus. Ganga sands at three relative densities of around 20%, 45% and 75% were tested for steady state strength characteristics. The values of relative densities chosen were such that they can cover a wide range of state of compactness namely loose, medium and dense sands and would exhibit varying steady state behavior. The maximum initial consolidation pressure that could be applied by the available equipment was of the order of 350 kPa. Based on this, the samples were tested at different rebounded cell pressures of 50 kPa, 100 kPa, 150 kPa, 200 kPa, 250 kPa and 300 kPa; i.e. at overconsolidation ratios between 1.17 to 7. Forty-five samples were tested by method 1 at the mentioned relative densities, at initial consolidation stresses of 350, 300 and 250 kPa with possible mentioned rebounded pressures. Some of these results were verified by method 2. As the initial consolidation stress becomes lower, the rebounded cell pressures become very low and hence the generation of the undrained curve from consolidated drained tests becomes more difficult. Tests were conducted with utmost care and all the inconsistent ones were repeated. The results are presented in the next chapter with brief discussion.

CHAPTER 3

RESULTS AND DISCUSSION

3.1. Stress-Strain and Volumetric Strain-Axial Strain behavior in Strain-controlled drained triaxial tests

Fig. 3.1 depicts the stress-strain characteristics of five samples of initial relative density, $(D_r)_i$ of 75%, which were all initially consolidated to a stress of 350 kPa and then rebounded to 300 kPa, 250 kPa, 200 kPa, 150 kPa and 100 kPa separately and then subjected to deviator stress under drained condition. Fig. 3.2 depicts the volume change characteristics of the same samples. From Fig. 3.1 and Fig. 3.2 and from the volumetric strain data during isotropic consolidation as presented in Table 3.1, the whole undrained response was evaluated by the method as discussed earlier in section 2.3 and is shown in the bold line. This process is conducted for samples prepared at other relative densities and for samples initially consolidated to other cell pressures. Any curve in Fig. 3.2 is entered with the corresponding isotropic volumetric strain data from Table 3.1 and the point where it cuts the volume change curve of that particular rebounded stress, is located. A point on the curve depicting the undrained response can be located by moving vertically up from the above point described earlier until the drained test stress-strain curve of the corresponding rebounded sample is intersected.

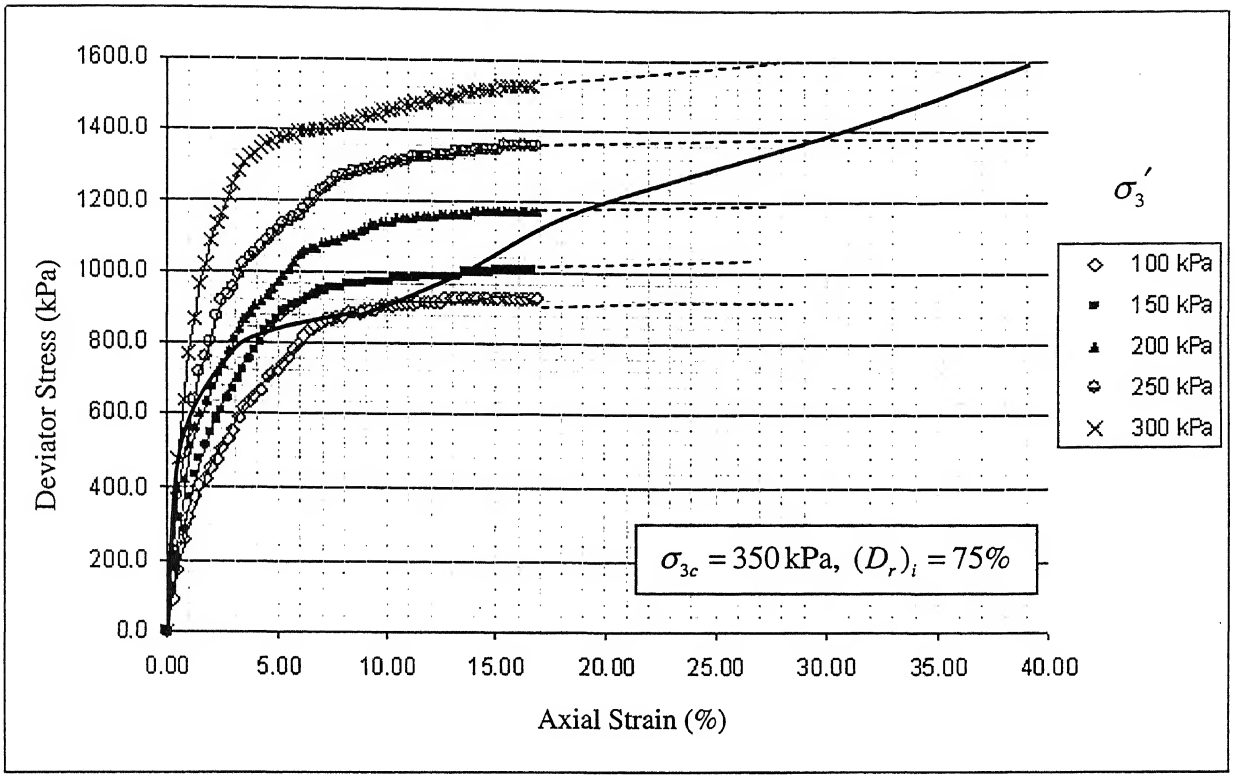

Fig. 3.1: Stress-Strain behavior

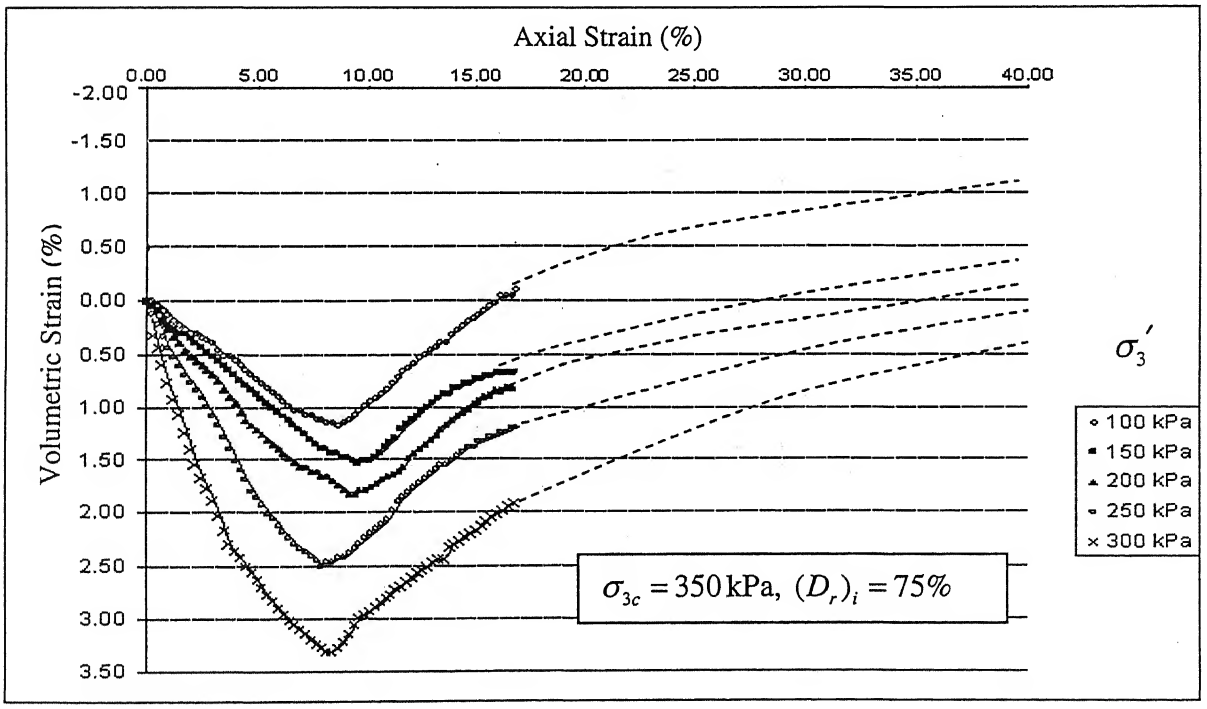

Fig. 3.2: Volume change behavior

Rebounded cell pressure (kPa)	Volumetric strain during rebound (%)
300	0.17
250	0.44
200	0.61
150	0.95
100	1.13

Table 3.1: Volumetric strain during rebound to lower cell pressures

The steady state is obtained where the undrained as well as corresponding rebounded drained stress-strain response become horizontal. If this does not happen within the strain levels up to which testing were done, then the stress-strain as well as volumetric strain-axial strain curves for the drained tests may have to be extrapolated to obtain the steady state. This is particularly true when the density becomes larger. Also a sample with rebounded cell pressure lying between two actually conducted rebounded tests may have to be interpolated to obtain the steady state. Also some data can be redundant, for example, here the sample rebounded to 50 kPa is not shown since no point of the undrained response would be located on it.

Similarly Fig. 3.3 and Fig. 3.4 represent stress-strain and volume change data from strain-controlled rebounded CD tests for $(D_r)_i$ of 45 %. Fig. 3.5 and Fig. 3.6 represent the same respectively for $(D_r)_i$ of 20 %. It can be noted from the volumetric strain-axial strain curves (Fig. 3.2, Fig. 3.4 and Fig. 3.6) that volume change behavior depends greatly on the initial relative density of the soil sample. While loose sand shows completely contractive behavior, medium or dense sand tend to expand beyond a certain axial strain. This dilative tendency increases with increase in relative density. Also this method of determination of steady state strength clearly depicts the importance of this volume change characteristics. It can be seen that the undrained response can rise after formation of a quasi-steady state to even beyond the initial peak stress for medium or dense samples. This is possible only if the drained response of a particular rebounded sample is intersected twice by the vertical lines generated from corresponding volumetric strain curve, which in turn, is possible only if this corresponding volume change curve of the rebounded sample shows dilative tendency.

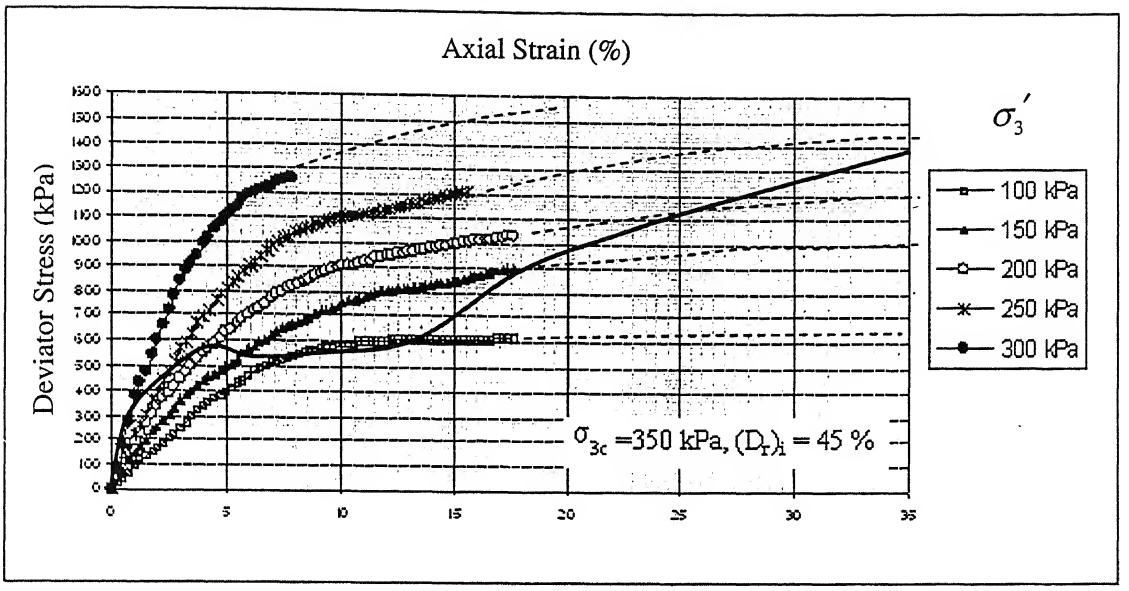

Fig. 3.3: Stress-Strain behavior

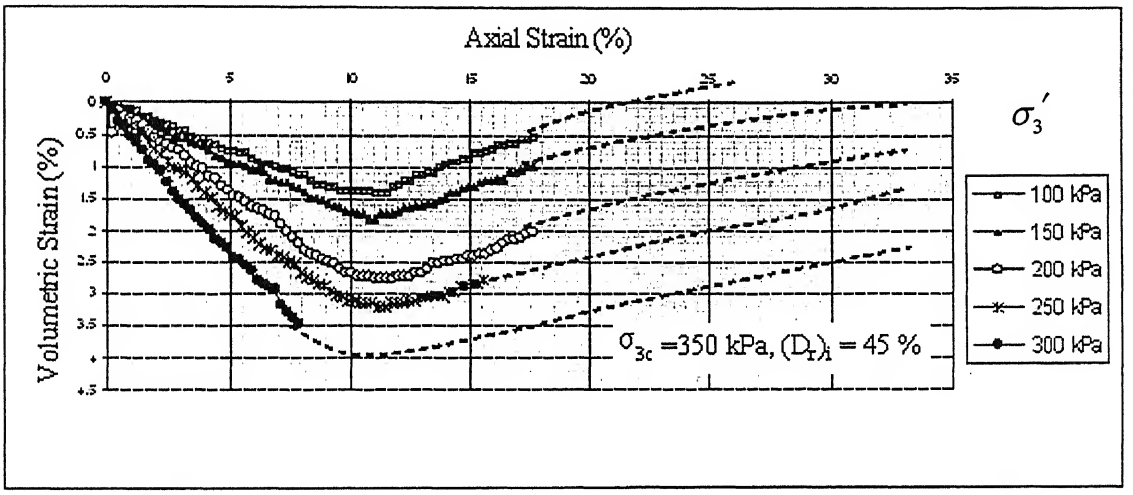

Fig. 3.4: Volume change behavior

Rebounded cell pressure (kPa)	Volumetric strain during rebound (%)
300	0.60
250	0.79
200	1.13
150	1.21
100	1.47

Table 3.2: Volumetric strain during rebound to lower cell pressures

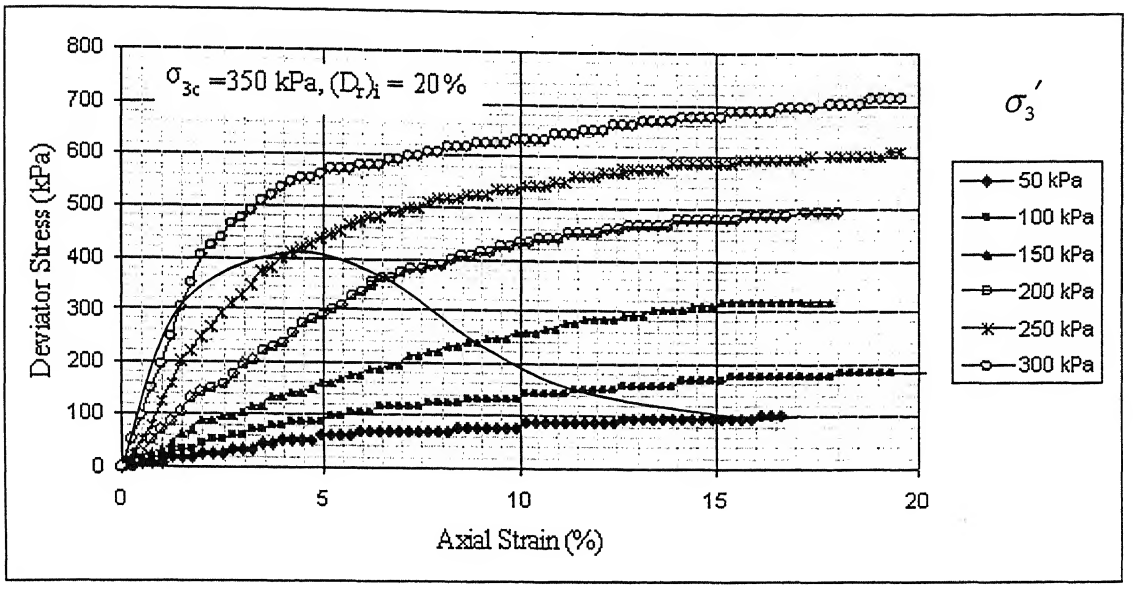

Fig. 3.5: Stress-Strain behavior

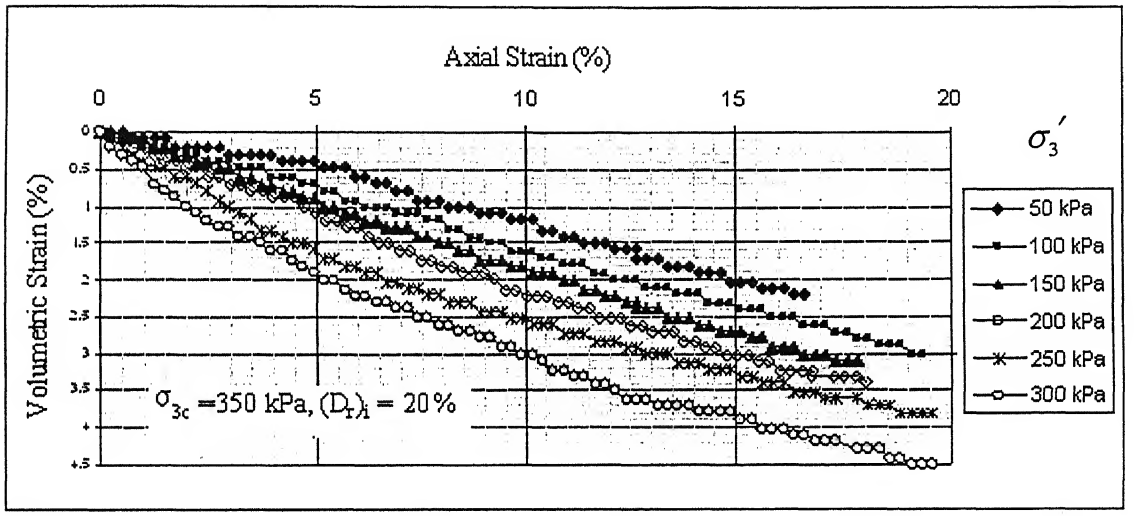

Fig. 3.6: Volume change behavior

Rebounded cell pressure (kPa)	Volumetric strain during rebound (%)
300	1.01
250	1.32
200	1.50
150	1.72
100	1.92
50	2.11

Table 3.3: Volumetric strain during rebound to lower cell pressures

3.2. Stress-Strain behavior and Effective Stress Path in Stress-controlled Consolidated Undrained triaxial tests

Stress-controlled consolidated undrained tests were conducted on samples with three relative densities, subject to different consolidation stress. The stress-strain results are presented in Fig. 3.7 and the corresponding stress paths are shown in Fig. 3.8.

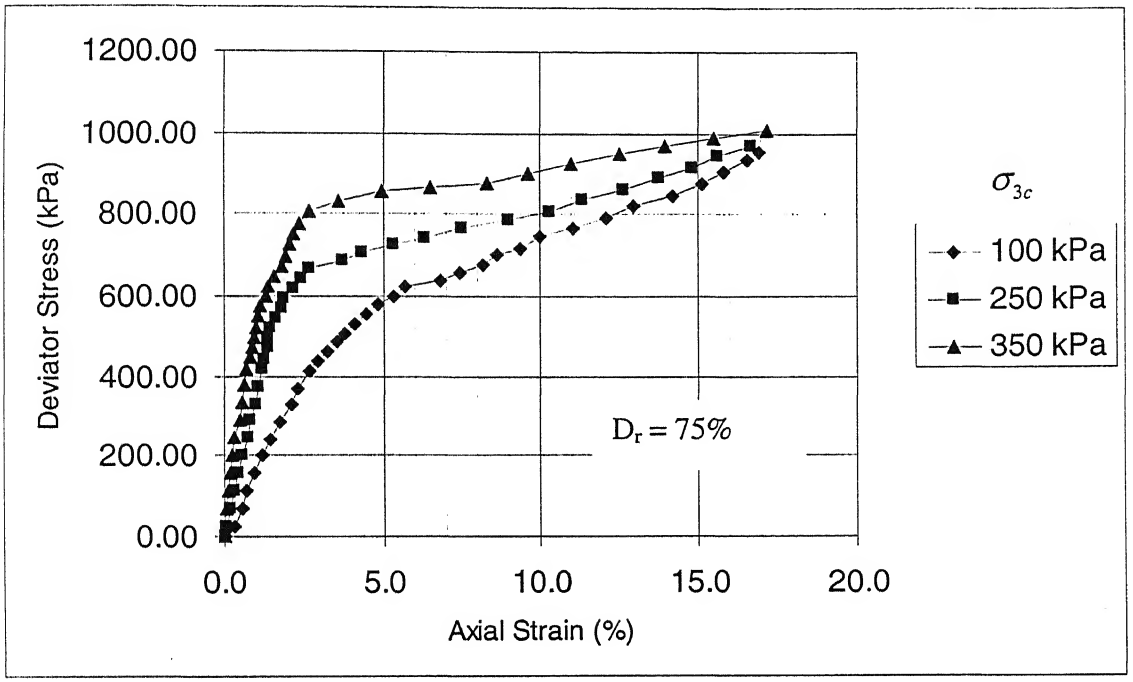

Fig. 3.7: Stress-strain behaviors at different consolidation stresses

With the dead-weight loading system used in this study it was very difficult to conduct the experiment after the peak stress, let alone up to the steady state point, particularly for samples with low relative density. It can be seen from Fig. 3.7 that samples with same initial relative density, when tested under different consolidation stresses, tend to converge to same stress at large strain levels. Thus the position of the ultimate steady state line is unique with respect to the initial mean stresses but the position of the quasi steady state lines for different initial mean stresses are different. They deviate more from the ultimate steady state line for lower initial mean stresses.

It was observed that the quasi steady state appears only when the consolidation stress is high enough and the range of quasi steady state is limited to a narrow range of void ratio, just below the ultimate steady state line. This is due to the high

sensitivity of the behavior to the density. For example quasi steady state was not generally observed below initial mean stress of 250 kPa.

Fig. 3.8 shows the Effective stress path for different initial confining stresses of 100, 250 and 350 kPa for samples of relative density 75%, from stress-controlled consolidated undrained triaxial tests. It can be seen from Fig. 3.8 that the nature of the effective stress paths for samples with different initial confining stresses tend to be of similar nature if the relative density is same.

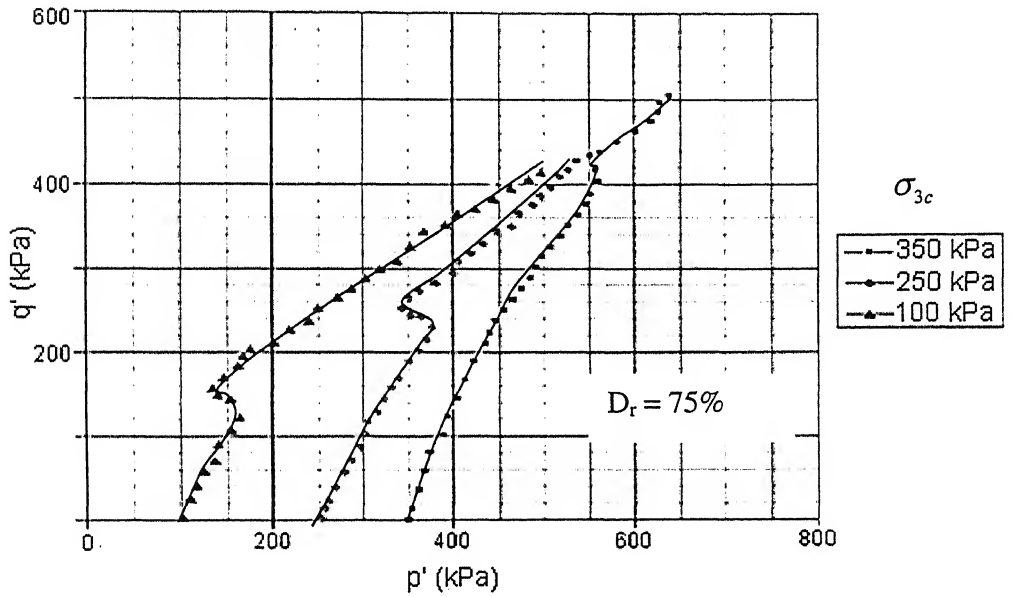

Fig. 3.8: Effective stress paths at different consolidation stresses

3.3. Comparison of undrained stress path and steady state strength determined by the two methods

Fig. 3.9 shows the comparison of steady state strength as well as the complete undrained behavior (variation of deviatoric stress with axial strain) as evaluated from series of strain-controlled drained triaxial tests and stress-controlled consolidated undrained test, at initial relative density of 75%.

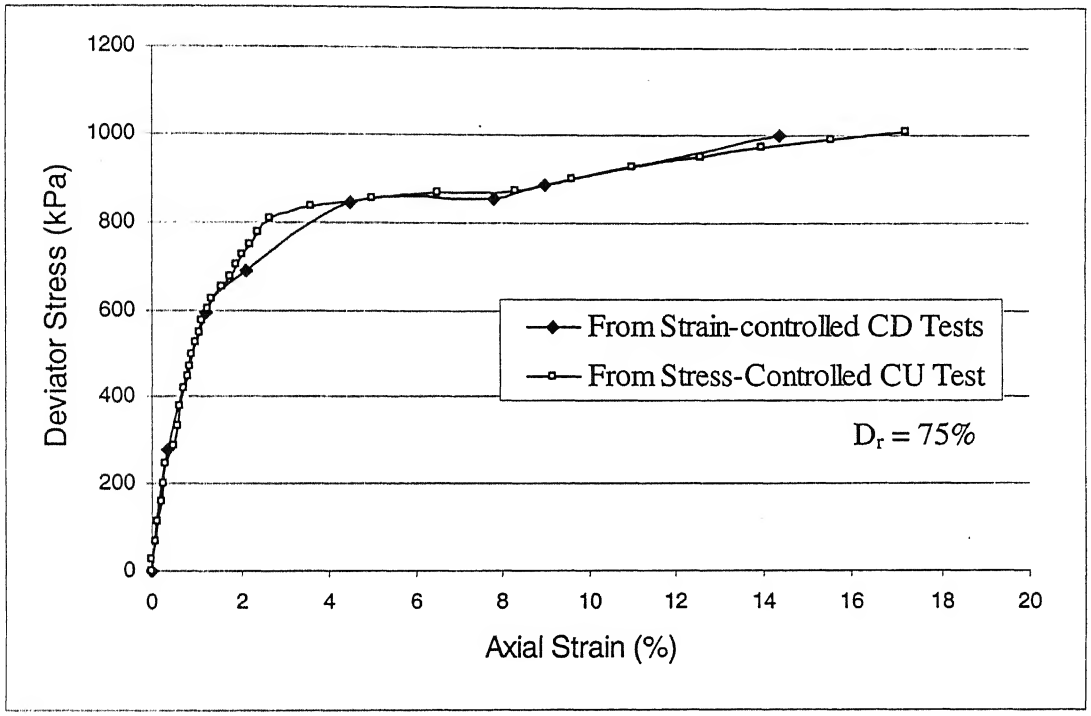

Fig. 3.9: Stress-strain behavior at 75% relative density

Fig. 3.10 shows the comparison of steady state strength as well as the complete undrained behavior (variation of deviatoric stress with axial strain) as evaluated from series of strain-controlled drained triaxial tests and stress-controlled consolidated undrained test, at initial relative density of 45%.

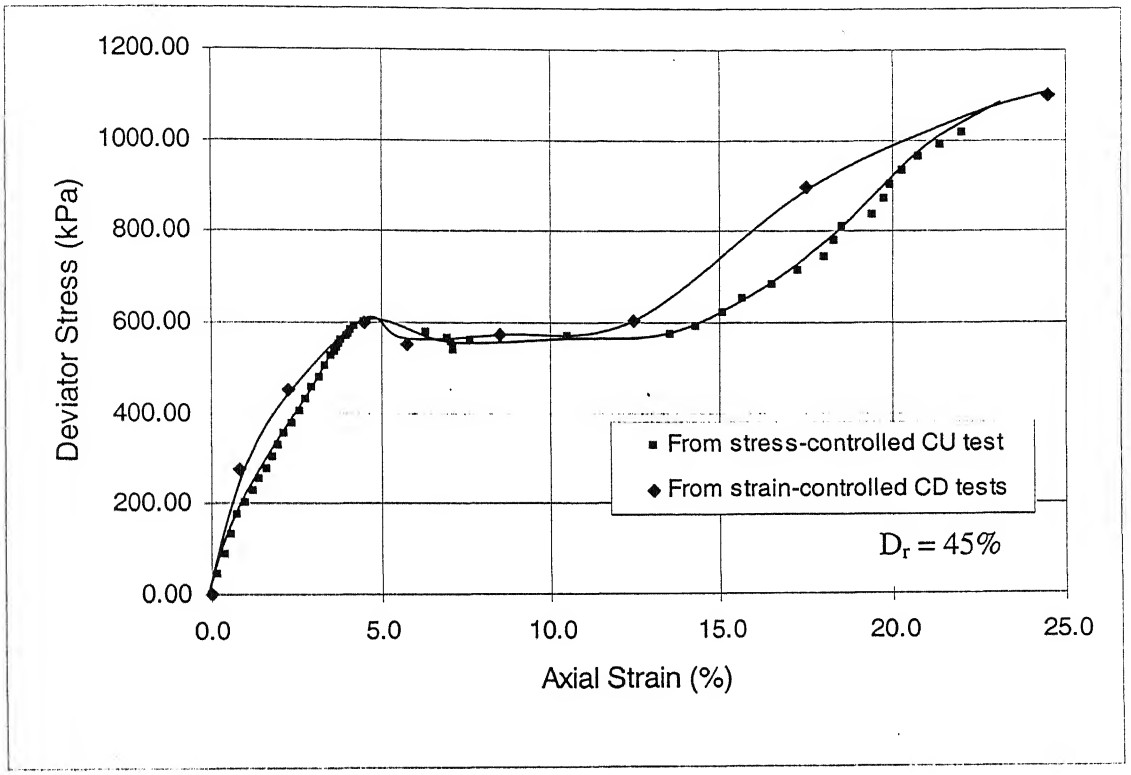

Fig. 3.10: Stress-strain behavior at 45% relative density

Fig. 3.11 shows the comparison of steady state strength as well as the complete undrained behavior (variation of deviatoric stress with axial strain) as evaluated from series of strain-controlled drained triaxial tests and stress-controlled consolidated undrained test, at initial relative density of 20%.

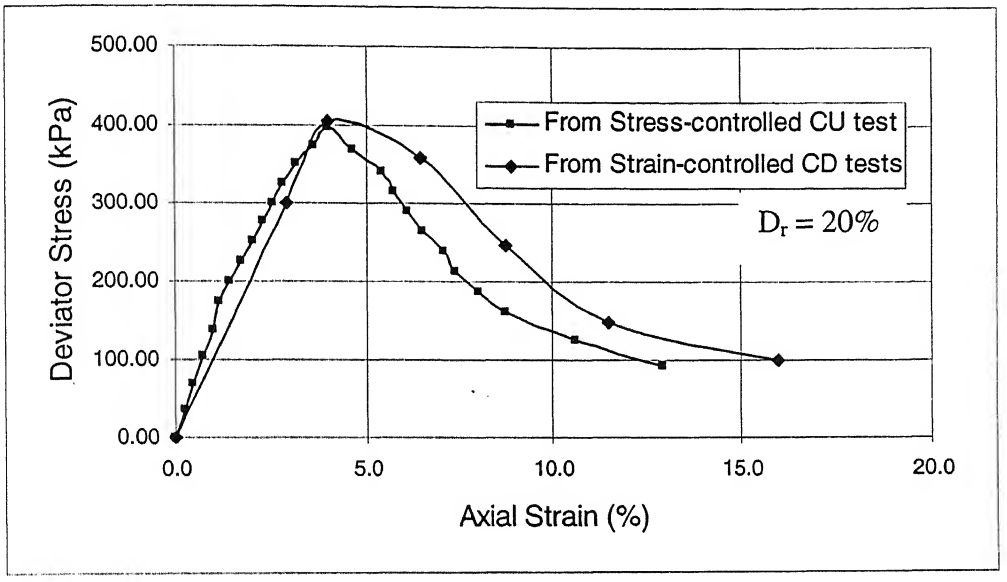

Fig. 3.11: Stress-strain behavior at 20% relative density

It is quite clear that the behavior evaluated from the series of strain-controlled consolidated drained tests on rebounded samples with volume change measurements, is in excellent agreement with the result from the stress-controlled consolidated undrained tests. Little variation that is observed can not be attributed to the shortcomings of the method involving strain-controlled consolidated drained tests with volume change measurements, because the stress-controlled consolidated undrained tests had limitations like a dead-weight equipment and low recording speed (since it was not an automatic recorder and had to be operated manually). As two different types of tests gave excellent similarity between the behaviors, it can be concluded that the sample preparation and measurements made are reliable.

3.4. Comparison of behavior at different relative densities:

Fig. 3.12 shows stress-strain behavior of samples prepared at three different relative densities which were initially subjected to the same consolidation stress and Fig. 3.13 shows the corresponding effective stress path.

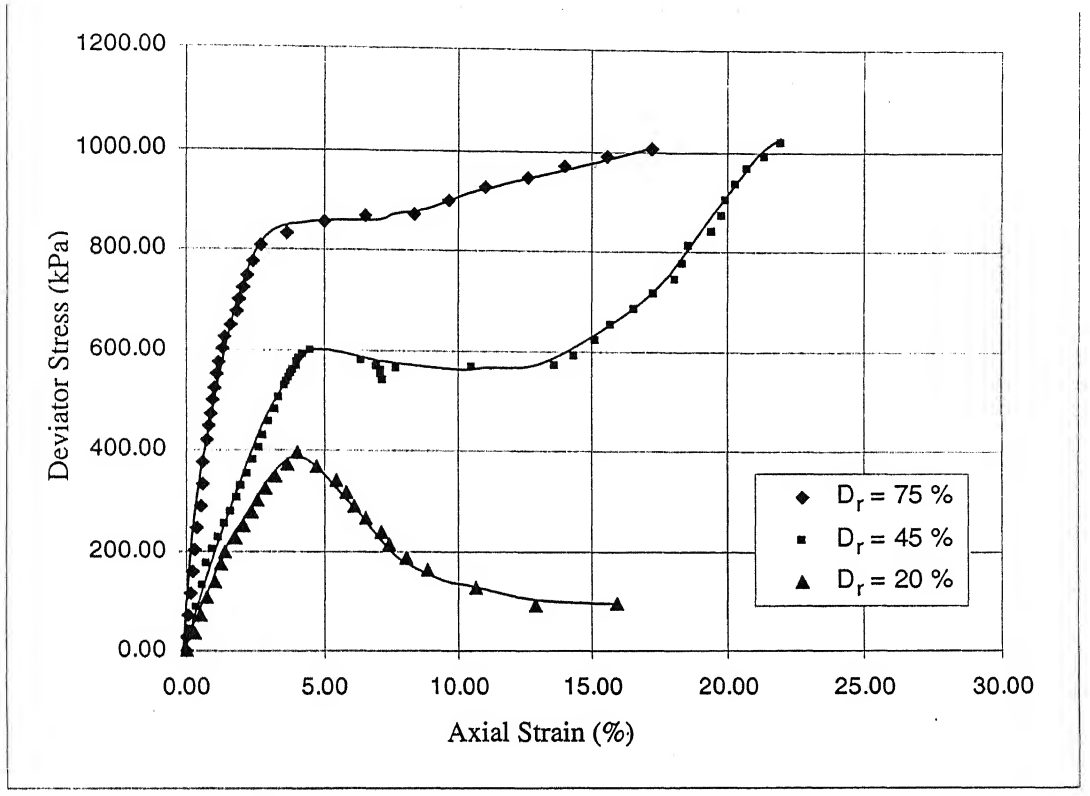

Fig. 3.12: Stress-strain behavior at different relative densities

It is seen that as density increases the true or ultimate steady state is obtained at a larger strain level. For example, Fig. 3.1, 3.3 and 3.5 shows, for same initial consolidation stress of 350 kPa, ultimate steady state was obtained after 55%, at 45% and at 15% strain respectively for relative density of around 75%, 45% and 20% with steady state strength of around 2000 kPa, 1500 kPa and 120 kPa respectively.

Also the undrained behaviors corresponding to the three relative densities as shown in Fig. 3.12 are distinct from each other. At loose state (Dr=20%), immediately after the peak stress is attained, the shear strength drops steeply until it reaches the ultimate steady state, indicating complete liquefaction behavior. For sands with medium relative density (45%), after the peak shear stress is attained the same drops, but not abruptly, till a quasi steady state is attained, after which the sample regains

strength and takes more stress till the ultimate steady state is obtained at large strain level. At dense state (Dr =75%), there is hardly any drop in shear stress till the ultimate steady state is obtained at very large strain. Similar behavior is depicted also in the effective stress paths shown in Fig. 3.13. The effective stress path at 20% relative density shows continuous loss in shear strength as it traces towards the origin showing complete liquefaction behavior where as the same at 45% relative density shows some loss in q as it starts moving towards origin before it shoots back again showing limited liquefaction behavior. But the effective stress path at 75% relative density shows hardly any drop in shear strength.

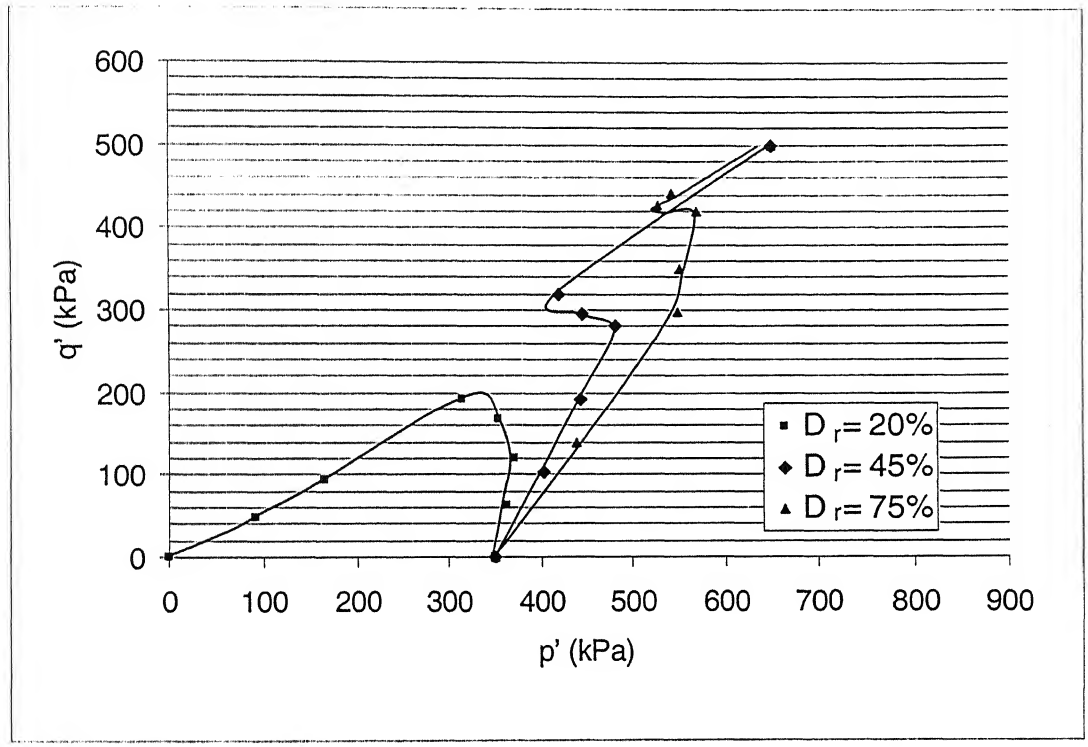

Fig. 3.13: Effective stress paths at different relative densities

3.5. Comparison between ultimate steady state line and quasi-steady state lines

Fig. 3.14 shows quasi steady state lines at two different consolidation stresses and the ultimate steady state line for Ganga sand.

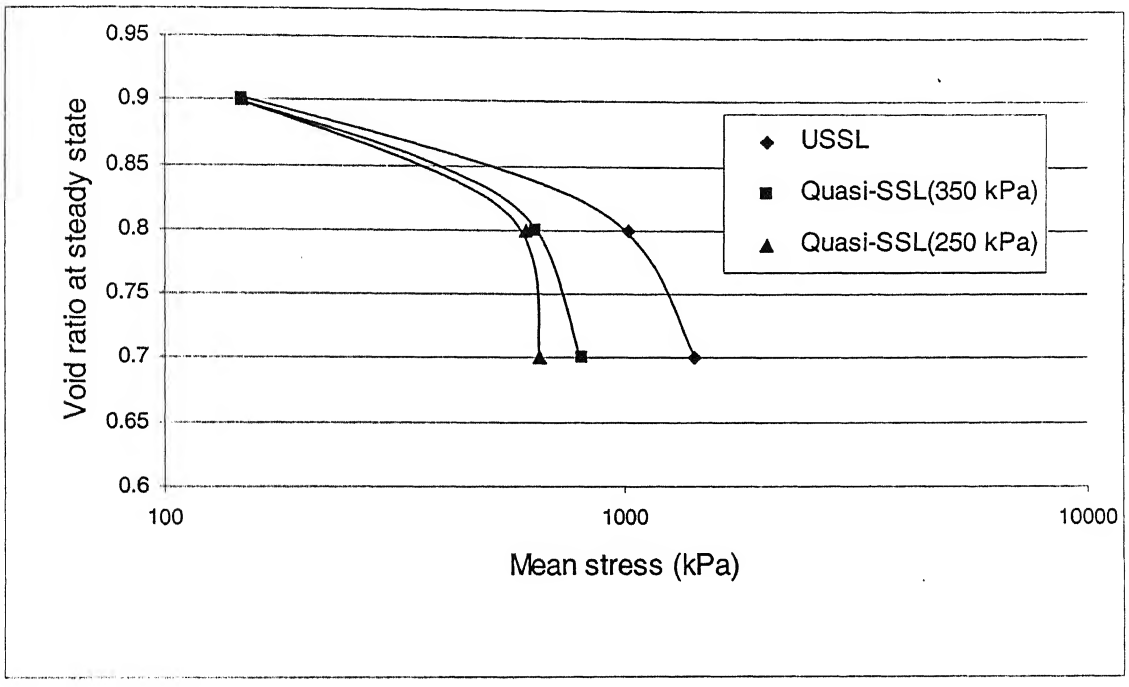

Fig. 3.14: Steady state line

In triaxial compression tests, in the range of initial effective mean stresses up to 500 kPa, the rates of decrease in void ratio with mean stress are lesser in comparison to the same there after. This implies that during undrained loading the initial effective mean stresses in this range have less effect on the compressibility behavior of sand than in the higher range. As the samples were prepared in different ways to attain different relative densities, it is assumed here that the position of the ultimate steady state line is independent of the method of sample preparation.

3.6. Comparison of the behavior of Ganga sand with Toyoura sand

In Fig. 3.15 to Fig. 3.19 the test data of Ganga sand is compared with the same on Toyoura sand (Yoshimine and Ishihara, 1998). Fig. 3.15 shows the comparison between the grain size distributions of the two sands. The two curves are very close showing almost no variation in this respect. However it has been pointed out earlier that the Ganga sand is angular where as it has been reported that Toyoura sand is subrounded.

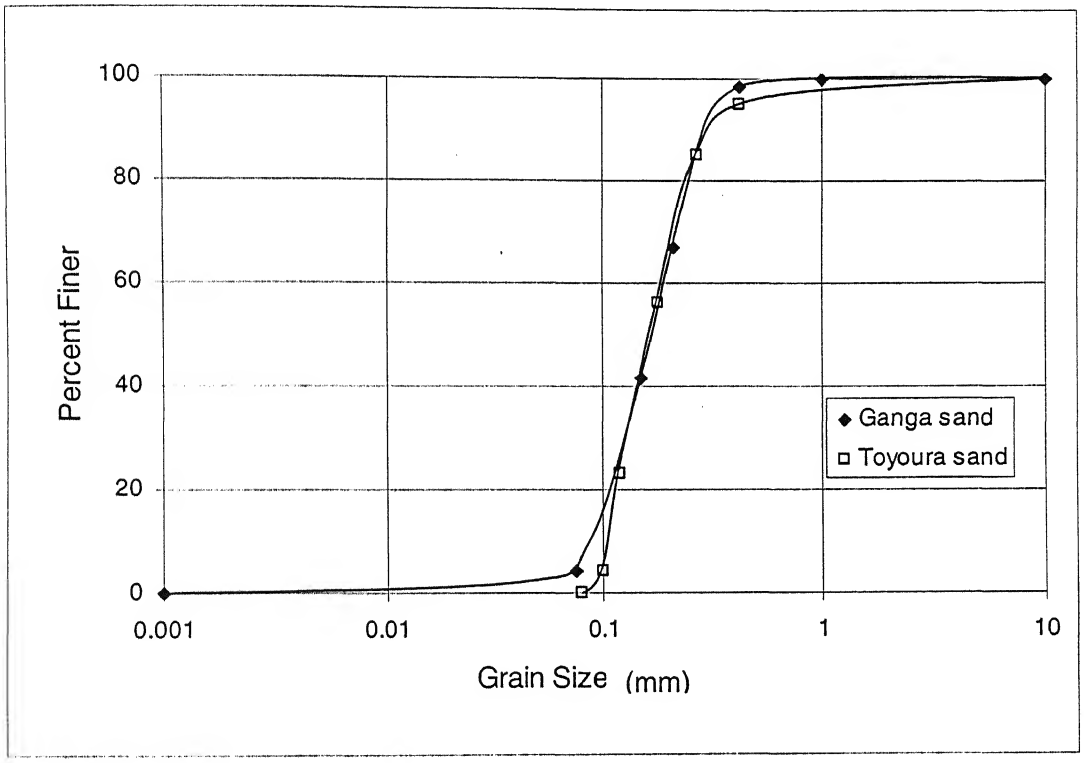

Fig. 3.15: Comparison of grain size distribution

Fig. 3.16 represents undrained stress-strain behavior at different void ratios for a particular confining stress and Fig. 3.17 represents the effective stress paths for the same set. Fig. 3.18 represents undrained stress-strain behavior at a particular void ratio and at different confining stresses. Finally Fig. 3.19 compares the ultimate steady state line of the two sands.

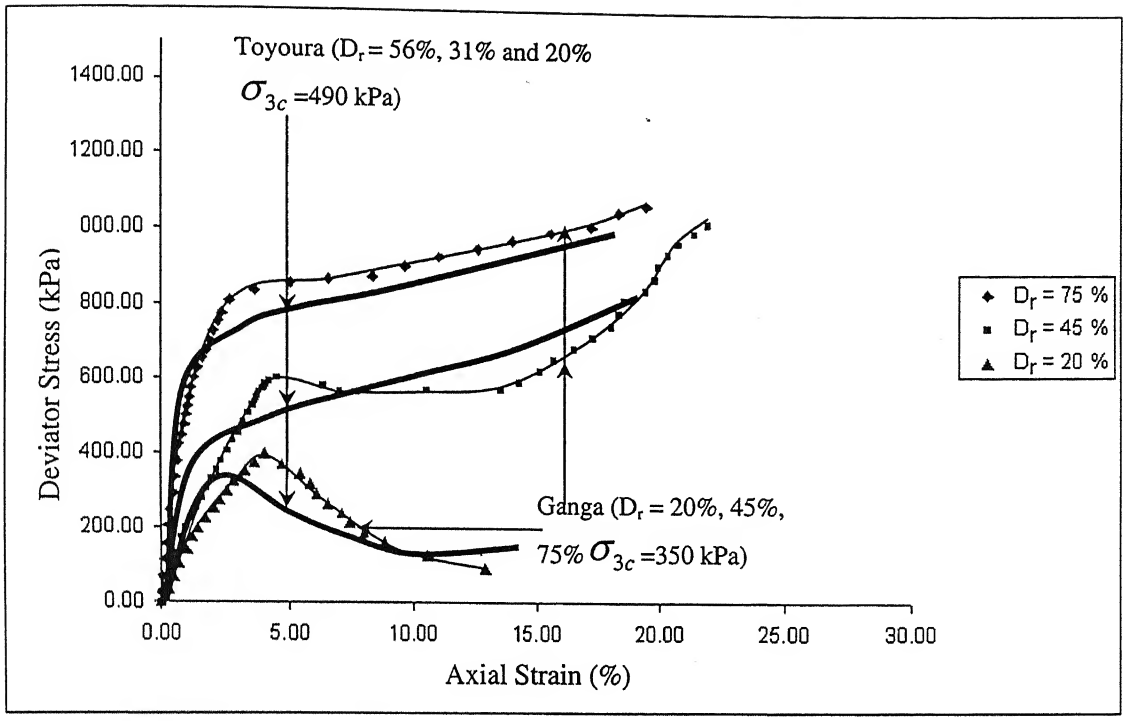

Fig. 3.16: Comparison of stress-strain behavior at different relative densities

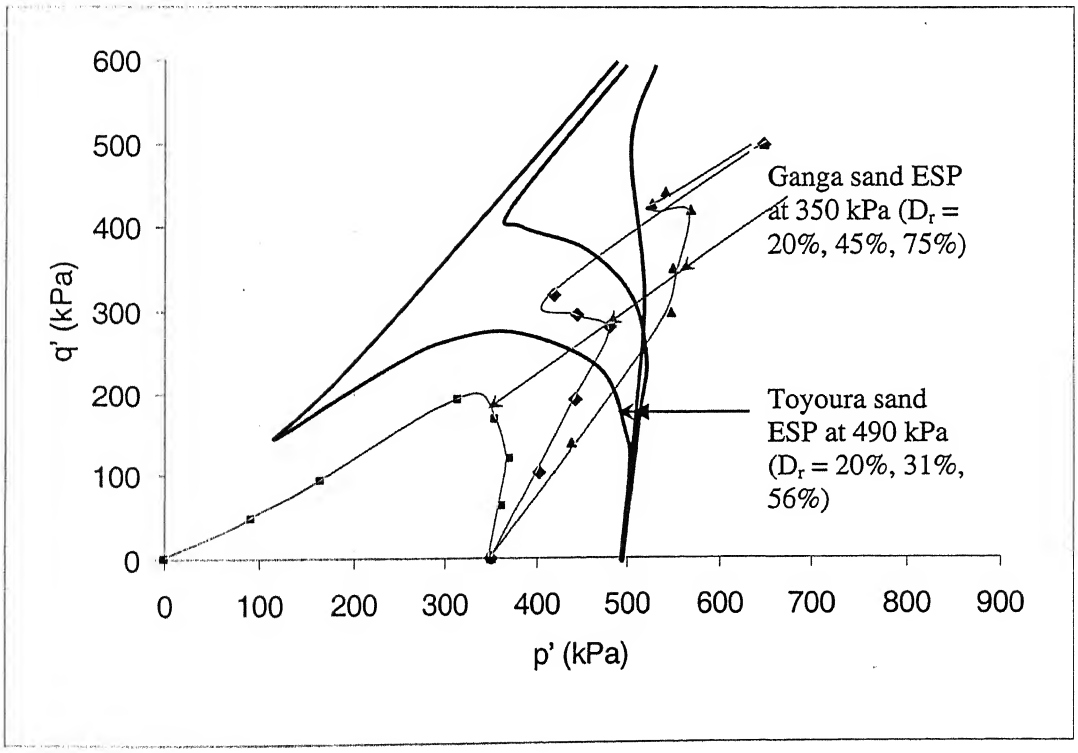

Fig. 3.17: Comparison of variation of effective stress path with relative densities

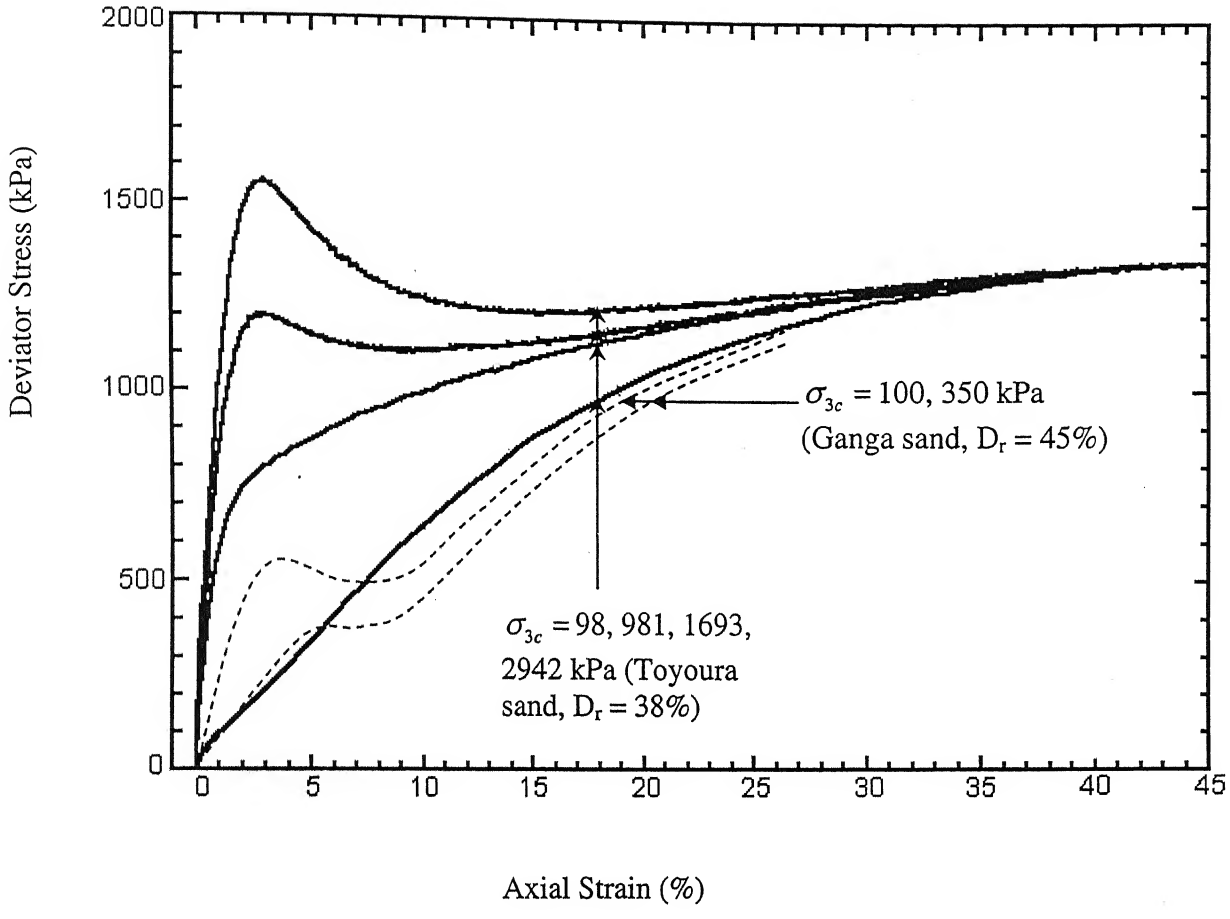

Fig. 3.18: Comparison of stress-strain behavior at different consolidation stresses

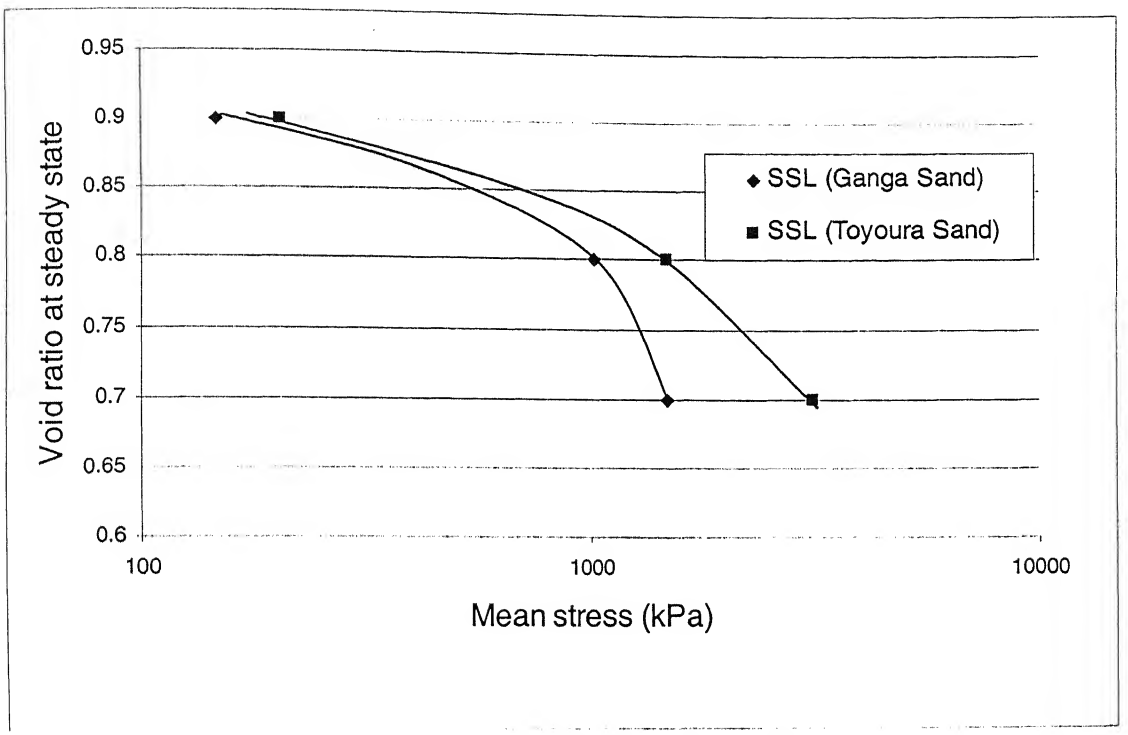

Fig. 3.19: Comparison of steady state line

It can be seen from the above figures that the stress-strain behavior, variation of effective stress path, steady state strength and such other characteristics of Ganga sand show similar trend although the range of values are different from those of Toyoura sand. It can be mentioned here that the grain size distribution of Toyoura sand is almost similar to that of Ganga sand (presented in Fig. 3.15) with e_{max} and e_{min} for Toyoura sand being 0.98 and 0.59 respectively and the corresponding values for the Ganga sand are 0.97 and 0.64. The grains of Ganga sand being angular, its steady state line is expected to have higher slope indicating greater compressibility in comparison to Toyoura sand whose particles are subrounded. Had the relative densities and consolidation stresses for the two sands been very close better agreement among the stress-strain diagrams and effective stress paths showing the complete loading history up to the steady state point would have been attained. Also, due to limitation of the equipment in the present study samples could not be tested over such a wide range of consolidation stresses as was done by Ishihara et al. (1998). But the qualitative trend of steady state strength behavior of Ganga sand matches reasonably well with that of Toyoura sand.

3.7. Comparison with model behavior

Ganga sand is clean sand with around 2% fines content. For clean sand having fines content less than 5%, as proposed by Cubrinovski and Ishihara (2000), the void ratio range $e_{max} - e_{min}$ is expected to lie within 0.25 to 0.50 with lower values expected for lower fines content. So a void ratio range of 0.33 for Ganga sand is fairly consistent with this observation.

The Ganga sand particles as shown in Fig. 2.8 illustrate several features of particle appearance. The particle shapes range from angular, subangular to subrounded but the grains of Ganga sand are predominantly angular in nature.

Based on the model study, Cubrinovski and Ishihara (2000) suggested the following expression (for angular grains) to estimate the slope of steady state line in e - log p' curve.

$$\lambda = -0.02 + 0.25(e_{max} - e_{min})$$

This is valid in the range of p' =10 to 200 kPa

$e_{max} - e_{min}$ = 0.33 in our case.

Putting that we get $\lambda = 0.0625$

Steady state line diagram from experiment indicates a slope of 0.0633 in the mentioned range of p', which is in excellent agreement with the result from the model.

Steady state line in the relative density-p' diagram for the range of p' =10 to 200 kPa was given as

$$D_{rs} = -0.4 + 1.4(e_{max} - e_{min}) + \frac{.01 - (1 - \log p')\{-0.02 + 0.25(e_{max} - e_{min})}{(e_{max} - e_{min})}$$

Here D_{rs} is the relative density at the steady state line expressed as a ratio, not as a percentage. D_{r0}, the relative density of the steady state line, in percentage, at p' = 0 is given as

D_{r0} = - 40 + 140($e_{max} - e_{min}$)

D_{r0} becomes 6.2% for our case by putting the void ratio range as 0.33 in the given relationship. The comparison between steady state lines as obtained from the model and experiments, in the relative density-p' plot is shown in Fig. 3.20.

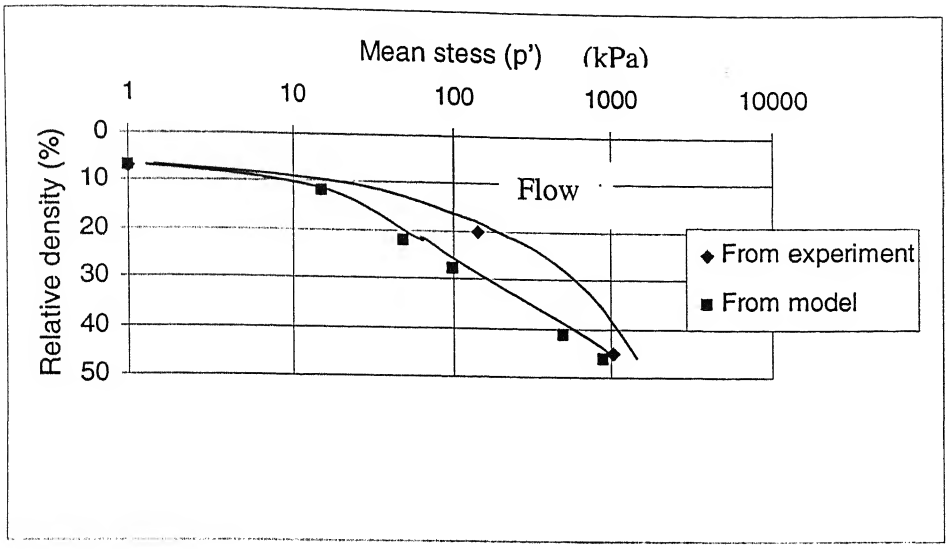

Fig. 3.20: Steady state line in the relative density-p' diagram for Ganga sand

Cubrinovski and Ishihara (2000) stated that the slope of the steady state line, as given by λ is not valid for inconsequential values of consolidating pressure (p' < 10 kPa range) and expressed the steady state line as combination of two straight lines within and beyond 10 kPa in the e-log p' curve. However, it can be observed from the experimental steady state line of Ganga sand, as well as Toyoura sand that the slope is steeper than the above value for p' > 200 kPa. The slope of the experimental steady state line in e-log p' curve is constantly changing with change in p' and cannot be approximated as a combination of two straight lines. However it is observed the steady state line in e-log p' curve can be approximated in a much better way by a quadratic form. So either separate equations for slopes are needed to be developed for different p' ranges or a quadratic equation can be fitted. The equation of steady state lines for Ganga sand and Toyoura sand can be expressed for p' > 200 kPa, respectively as

$e = -0.323 \log p'^2 + 1.544 \log p' - 0.945$ and

$e = -0.1267 \log p'^2 + 0.5795 \log p' + 0.2373$.

The dependence of the coefficients of the quadratic form depends on the properties and parameters of the soils and can be found if data on steady state strength behavior of several sands are available.

3.8 Conclusion

Based on the results and discussions presented in the above sections the following conclusions are drawn:

1. The results obtained by an alternative effective stress approach involving traditional consolidated drained triaxial tests with volume change measurements on rebounded samples was in good agreement with that found by stress-controlled consolidated undrained tests with pore pressure measurements.
2. The steady state behavior of the Ganga sand has been found to be of similar trend as described in literature for Toyoura sand especially in the lower strain region and tend to be different at higher strain levels. As the grain size distribution characteristics are pretty similar, this difference may be attributed to difference in grain shape.
3. The position and slope of steady state line for Ganga sand matches well with the model as proposed by Cubrinovski and Ishihara (2000), for the mean stress value less than 200 kPa. However, the steady state line slope is much steeper in higher stress range and changes at an increasing rate. Approximation in this range is erroneous and a quadratic fit of data in this range is better.
4. As expected undrained behavior of soil at different consolidation stresses are different and so also the drained behavior of soils. But the drained stress-strain as well as volumetric strain-axial strain behavior, of soil samples which were initially consolidated to the same stress before being rebounded to different higher stresses, is of similar nature. So, just conducting a few tests many of these curves can be obtained by interpolation and extrapolation. This provides an opportunity to reduce the number of tests to a great extent, particularly if only the peak stress or only the steady state strength is required, instead of the complete undrained stress-strain response.
5. If at any strata the in-situ void ratio of the Ganga sand is known the possibility of liquefaction of the same can be found out from the steady strength properties as determined in this study.

3.9 Scope of Future studies

1. Similar studies can be taken up with other sands of the country where possibility of liquefaction exists.
2. Experimental data with higher effective mean stresses, for different sands, can be collected for developing better correlations over the entire range of void ratio change with mean stress.
3. Tests may be conducted under dynamic loading to determine the critical shear stress for liquefaction and compare the same with the corresponding steady state strength values.
4. Effect of sample disturbance, sample preparation, presence of non-plastic fines on the steady state strength of local sand may be studied.
5. Effect of anisotropic consolidation and type of tests (compression and extension) on steady state strength need to be studied.

REFERENCES

Alarcon-Guzman, A., Leonards, G. A., and Chameau J. L. (1988), 'Undrained monotonic and cyclic strength of sands', Journal of Geotechnical Engineering, ASCE, Vol. 114, No. 10, pp. 1089-1109.

Been, K. and Jefferies, M. G. (1985), 'A state parameter for sands', Geotechnique, Vol. 35, No. 2, pp. 99-112.

Bishop, A.W., Green, G.E., Garga, V.K., Andersen, A., Brown, J.D.(1971), 'A new ring shear apparatus and its application to the measurement of residual strength', Geotechnique, Vol. 21 pp. 273-328

Castro, G. (1975), 'Liquefaction and Cyclic Mobility of Saturated Sands', Journal of Geotechnical Engineering Division, ASCE, Vol. 101, No. 6, pp. 551-569.

Castro, G. (1977), 'Factors affecting Liquefaction and Cyclic Mobility', Journal of Geotechnical Engineering Division, ASCE, Vol. 103, No. 6, pp. 501-506.

Castro, G., Poulos, S. J., and Francis, D. L. (1985), 'Re-Examination of Slide of Lower San Fernando Dam', Journal of Geotechnical Engineering, Vol. 111, No. 9, pp. 1093-1107.

Castro, G., Seed, R. B., Keller, T. O., and Seed, H. B. (1985), 'Steady-State Strength Analysis of Lower San Fernando Dam Slide', Journal of Geotechnical Engineering, Vol. 118, No. 3, pp. 406-427.

Crawford, H. S. (1984), 'An Experimental Investigation of Factors Influencing Static Liquefaction', MS Thesis, University of Western Ontario, London.

Cubrinovski, M., and Ishihara, K. (1998), 'Modeling of Sand Behavior based on State Concept', Soils and Foundations, Vol. 38, No. 3, pp. 115-127.

Cubrinovski, M., and Ishihara K. (1998), 'State Concept and Modified Elastoplasticity for Sand Modeling', Soils and Foundations, Vol. 38, No. 4, pp. 213-225.

Cubrinovski, M., and Ishihara K. (2000), 'Flow Potential of Sandy Soils with different Grain Compositions', Soils and Foundations, Vol. 40, No. 4, pp. 103-119.

Hyodo, M., Tanimizu, H., Yasufuku, N., and Murata, H. (1994), 'Undrained cyclic and monotonic triaxial behavior of saturated loose sand', Soils and Foundations, Vol. 34, No. 1, pp. 19-32.

Konrad, J. M. (1990), 'Minimum Undrained Strength Versus Steady-State Strength of Sands', Journal of Geotechnical Engineering, Vol. 116, No. 6, pp. 948-963.

Mohamad, R., and Dorby, R. (1986), 'Undrained monotonic and cyclic triaxial strength of sand', Journal of Geotechnical Engineering, ASCE, Vol. 112, No. 10, pp. 941-958.

Norris, G., Madhu, R., Valeschini, R., and Ashour, M. (1997), 'Liquefaction and Residual Strength of Sands from Drained Triaxial Tests', Rep. 2, Rep. No. CCEER-95-2, Engineering Department, University of Nevada.

Norris, G., Siddharthan, R., Zafir, Z., Madhu, R. (1997), 'Liquefaction and Residual Strength of Sands from Drained Triaxial Tests', Journal of Geotechnical and Geoenvironmental Engineering, ASCE, Vol. 123, No. GT3, pp. 220-228.

Poulos, S. J. (1981), 'The Steady State of Deformation', Journal of Geotechnical Engineering Division, ASCE, Vol. 107, No. 5, pp. 553-562.

Poulos, S. J., Castro, G., and France, J. W. (1985), 'Liquefaction Evaluation Procedure', Journal of Geotechnical Engineering Division, ASCE, Vol. 111, No. 6, pp. 772-791.

Riemer, M.F., and Seed, R.B. (1997), 'Factors affecting apparent position of steady-state line', Journal of Geotechnical Engineering, ASCE, Vol. 123, pp.281-288.

Seed, H. B., Tokimatsu, K., Harder, L. F., and Chung, R. M. (1985), 'Influence of SPT Procedures in Soil Liquefaction Resistance Evaluations', Journal of Geotechnical Engineering, ASCE, Vol. 111, No. 12, pp. 1425-1445.

Sitharam, T. G., Govinda Raju, L., and Srinivasa Murthy, B. R. (2004), 'Cyclic and monotonic undrained shear response of silty sand from Bhuj region in India', ISET Journal of Earthquake Technology, Vol. 41, N0. 2-4, pp. 249-260.

Stark, T. D., and Mesri, G. (1992), 'Undrained Shear Strength of Liquefied Sands for Stability Analysis', Journal of Geotechnical Engineering Division, ASCE, Vol. 118, No. 11, pp. 1727-1747.

Vaid, Y.P., and Chern, J. C. (1983), 'Effect of Static Shear in Resistance to Liquefaction', Soils and Foundations, Vol. 23, No. 1, pp. 47-60.

Vaid, Y.P., and Chern, J. C. (1985), 'Closure to Effect of Static Shear in Resistance to Liquefaction', Soils and Foundations, Vol. 25, No. 3, pp. 154-156.

Vaid, Y. P., and Chern, J. C. (1985), 'Cyclic and monotonic undrained response of saturated sands', Advances in the Art of Testing Soils Under Cyclic Conditions, ASCE, pp. 120-147.

Verdugo, R. (1992), 'Characterization of sandy soil behavior under large deformation', Ph.D. thesis, University of Tokyo.

Verdugo, R., and Ishihara, K. (1996), 'The Steady State of Sandy Soils', Soils and Foundations, Japanese Geotechnical Society, Vol. 36, No. 2, pp. 81-91.

Vincent B. D. (1990), 'Loading Systems, Sample Preparation, and Liquefaction', Journal of Geotechnical Engineering, Vol. 116, No. 5, pp. 805-821.

Yoshimine, M., and Ishihara, K. (1998), 'Flow potential of sand during liquefaction', Soils and Foundations, Vol. 38, No. 3, pp. 187-196.

Yoshimine, M., Ishihara, K., and Vargas, W. (1998), 'Effects of principal stress direction and intermediate principal stress on undrained shear behavior of sand', Soils and Foundations, Vol. 38, No. 3, pp. 179-188.

APPENDIX

Consolidated Drained triaxial test with volume change measurements on rebounded sample

Initial Length (cm)	10.2	Initial void ratio	0.72
Initial Diameter (cm)	3.8	Initial Relative density	77.00
Initial c/s area (sq. cm)	11.34	Initial Cell Pressure (kPa)	350
Initial Volume (cc)	115.68	Rebounded Cell Pressure (kPa)	100
Weight of sample taken (gm)	180	Back Pressure (kPa)	50
Dry density (gm/cc)	1.56	Volume Change during rebound (cc)	1.3
Specific Gravity	2.67	Volumetric strain during rebound (%)	1.12

Displacement (mm)	Load (kN)	Axial Strain (%)	Stress (kPa)	Volume Change (Comp) (cc)	Volumetric Strain (%)
0.00	0.00	0.00	0.0	0.00	0.00
0.25	0.10	0.25	88.2	0.00	0.00
0.50	0.20	0.49	176.3	0.05	0.04
0.75	0.29	0.74	255.7	0.10	0.09
1.00	0.36	0.98	317.4	0.15	0.13
1.25	0.42	1.23	370.3	0.20	0.17
1.50	0.46	1.47	405.6	0.25	0.22
1.75	0.48	1.72	423.2	0.30	0.26
2.00	0.51	1.96	449.7	0.35	0.30
2.25	0.54	2.21	476.1	0.35	0.30
2.50	0.57	2.45	502.6	0.40	0.35
2.75	0.60	2.70	529.0	0.40	0.35
3.00	0.63	2.94	555.5	0.45	0.39
3.25	0.67	3.19	590.8	0.55	0.48
3.50	0.70	3.43	617.2	0.60	0.52
3.75	0.72	3.68	634.9	0.60	0.52
4.00	0.74	3.92	652.5	0.65	0.56
4.25	0.76	4.17	670.1	0.70	0.61
4.50	0.80	4.41	705.4	0.75	0.65
4.75	0.81	4.66	714.2	0.80	0.69
5.00	0.82	4.90	723.0	0.85	0.73
5.25	0.84	5.15	740.7	0.90	0.78
5.50	0.86	5.39	758.3	0.95	0.82
5.75	0.89	5.64	784.8	1.00	0.86

Displacement (mm)	Load (kN)	Axial Strain (%)	Stress (kPa)	Volume Change (Comp) (cc)	Volumetric Strain (%)
6.00	0.91	5.88	802.4	1.05	0.91
6.25	0.93	6.13	820.0	1.10	0.95
6.50	0.95	6.37	837.7	1.15	0.99
6.75	0.96	6.62	846.5	1.20	1.04
7.00	0.97	6.86	855.3	1.20	1.04
7.25	0.98	7.11	864.1	1.25	1.08
7.50	0.98	7.35	864.1	1.25	1.08
7.75	0.99	7.60	872.9	1.30	1.12
8.00	0.99	7.84	872.9	1.30	1.12
8.25	1.00	8.09	881.7	1.30	1.12
8.50	1.00	8.33	881.7	1.30	1.12
8.75	1.00	8.58	881.7	1.35	1.17
9.00	1.01	8.82	890.6	1.30	1.12
9.25	1.01	9.07	890.6	1.30	1.12
9.50	1.01	9.31	890.6	1.25	1.08
9.75	1.02	9.56	899.4	1.20	1.04
10.00	1.02	9.80	899.4	1.15	0.99
10.25	1.02	10.05	899.4	1.10	0.95
10.50	1.03	10.29	908.2	1.05	0.91
10.75	1.03	10.54	908.2	1.00	0.86
11.00	1.03	10.78	908.2	0.95	0.82
11.25	1.03	11.03	908.2	0.90	0.78
11.50	1.04	11.27	917.0	0.80	0.69
11.75	1.04	11.52	917.0	0.75	0.65
12.00	1.04	11.76	917.0	0.70	0.61
12.25	1.04	12.01	917.0	0.70	0.61
12.50	1.04	12.25	917.0	0.60	0.52
12.75	1.05	12.50	925.8	0.55	0.48
13.00	1.05	12.75	925.8	0.55	0.48
13.25	1.05	12.99	925.8	0.50	0.43
13.50	1.05	13.24	925.8	0.45	0.39
13.75	1.05	13.48	925.8	0.45	0.39
14.00	1.05	13.73	925.8	0.35	0.30
14.25	1.05	13.97	925.8	0.30	0.26
14.50	1.05	14.22	925.8	0.25	0.22
14.75	1.05	14.46	925.8	0.25	0.22
15.00	1.05	14.71	925.8	0.20	0.17
15.25	1.05	14.95	925.8	0.15	0.13
15.50	1.05	15.20	925.8	0.10	0.09
15.75	1.05	15.44	925.8	0.05	0.04
16.00	1.05	15.69	925.8	0.00	0.00
16.25	1.05	15.93	925.8	-0.05	-0.04
16.50	1.05	16.18	925.8	-0.05	-0.04
16.75	1.05	16.42	925.8	-0.05	-0.04
17.00	1.05	16.67	925.8	-0.10	-0.09

Consolidated Drained triaxial test with volume change measurements on rebounded sample

Initial Length (cm)	10.25	Initial void ratio	0.72
Initial Diameter (cm)	3.8	Initial Relative density	74.45
Initial c/s area (sq. cm)	11.34	Initial Cell Pressure (kPa)	350
Initial Volume (cc)	116.25	Rebounded Cell Pressure (kPa)	150
Weight of sample taken (gm)	180	Back Pressure (kPa)	50
Dry density (gm/cc)	1.55	Volume Change during rebound (cc)	1.1
Specific Gravity	2.67	Volumetric strain during rebound (%)	0.95

Displacement (mm)	Load (kN)	Axial Strain (%)	Stress (kPa)	Volume Change (Comp) (cc)	Volumetric Strain (%)
0.00	0.00	0.00	0.0	0.00	0.00
0.25	0.12	0.24	105.8	0.05	0.04
0.50	0.23	0.49	202.8	0.10	0.09
0.75	0.32	0.73	282.2	0.20	0.17
1.00	0.42	0.98	370.3	0.25	0.22
1.25	0.49	1.22	432.1	0.30	0.26
1.50	0.54	1.46	476.1	0.35	0.30
1.75	0.58	1.71	511.4	0.35	0.30
2.00	0.62	1.95	546.7	0.40	0.34
2.25	0.66	2.20	582.0	0.45	0.39
2.50	0.69	2.44	608.4	0.50	0.43
2.75	0.73	2.68	643.7	0.55	0.47
3.00	0.76	2.93	670.1	0.60	0.52
3.25	0.79	3.17	696.6	0.65	0.56
3.50	0.82	3.41	723.0	0.70	0.60
3.75	0.85	3.66	749.5	0.75	0.65
4.00	0.88	3.90	775.9	0.80	0.69
4.25	0.91	4.15	802.4	0.85	0.73
4.50	0.94	4.39	828.8	0.90	0.77
4.75	0.96	4.63	846.5	0.95	0.82
5.00	0.98	4.88	864.1	1.00	0.86
5.25	1.00	5.12	881.7	1.05	0.90
5.50	1.01	5.37	890.6	1.10	0.95
5.75	1.02	5.61	899.4	1.15	0.99

Displacement (mm)	Load (kN)	Axial Strain (%)	Stress (kPa)	Volume Change (Comp) (cc)	Volumetric Strain (%)
6.00	1.03	5.85	908.2	1.20	1.03
6.25	1.04	6.10	917.0	1.25	1.08
6.50	1.05	6.34	925.8	1.30	1.12
6.75	1.06	6.59	934.7	1.35	1.16
7.00	1.07	6.83	943.5	1.40	1.20
7.25	1.07	7.07	943.5	1.45	1.25
7.50	1.08	7.32	952.3	1.50	1.29
7.75	1.08	7.56	952.3	1.55	1.33
8.00	1.08	7.80	952.3	1.60	1.38
8.25	1.09	8.05	961.1	1.60	1.38
8.50	1.09	8.29	961.1	1.65	1.42
8.75	1.09	8.54	961.1	1.65	1.42
9.00	1.09	8.78	961.1	1.70	1.46
9.25	1.10	9.02	969.9	1.70	1.46
9.50	1.10	9.27	969.9	1.75	1.51
9.75	1.10	9.51	969.9	1.80	1.55
10.00	1.10	9.76	969.9	1.75	1.51
10.25	1.10	10.00	969.9	1.75	1.51
10.50	1.11	10.24	978.7	1.70	1.46
10.75	1.11	10.49	978.7	1.65	1.42
11.00	1.11	10.73	978.7	1.60	1.38
11.25	1.11	10.98	978.7	1.55	1.33
11.50	1.11	11.22	978.7	1.50	1.29
11.75	1.12	11.46	987.6	1.40	1.20
12.00	1.12	11.71	987.6	1.35	1.16
12.25	1.12	11.95	987.6	1.30	1.12
12.50	1.12	12.20	987.6	1.25	1.08
12.75	1.12	12.44	987.6	1.20	1.03
13.00	1.12	12.68	987.6	1.15	0.99
13.25	1.12	12.93	987.6	1.10	0.95
13.50	1.12	13.17	987.6	1.05	0.90
13.75	1.13	13.41	996.4	1.00	0.86
14.00	1.13	13.66	996.4	1.00	0.86
14.25	1.13	13.90	996.4	0.95	0.82
14.50	1.13	14.15	996.4	0.95	0.82
14.75	1.13	14.39	996.4	0.90	0.77
15.00	1.13	14.63	996.4	0.90	0.77
15.25	1.14	14.88	1005.2	0.85	0.73
15.50	1.14	15.12	1005.2	0.85	0.73
15.75	1.14	15.37	1005.2	0.80	0.69
16.00	1.14	15.61	1005.2	0.80	0.69
16.25	1.14	15.85	1005.2	0.80	0.69
16.50	1.14	16.10	1005.2	0.80	0.69
16.75	1.14	16.34	1005.2	0.80	0.69
17.00	1.14	16.59	1005.2	0.80	0.69

Consolidated Drained triaxial test with volume change measurements on rebounded sample

Initial Length (cm)	10.25	Initial void ratio	0.72
Initial Diameter (cm)	3.8	Initial Relative density	74.45
Initial c/s area (sq. cm)	11.34	Initial Cell Pressure (kPa)	350
Initial Volume (cc)	116.25	Rebounded Cell Pressure (kPa)	200
Weight of sample taken (gm)	180	Back Pressure (kPa)	50
Dry density (gm/cc)	1.55	Volume Change during rebound (cc)	0.7
Specific Gravity	2.67	Volumetric strain during rebound (%)	0.60

Displacement (mm)	Load (kN)	Axial Strain (%)	Stress (kPa)	Volume Change (Comp) (cc)	Volumetric Strain (%)
0.00	0.00	0.00	0.0	0.00	0.00
0.25	0.21	0.24	185.2	0.05	0.04
0.50	0.36	0.49	317.4	0.10	0.09
0.75	0.48	0.73	423.2	0.20	0.17
1.00	0.59	0.98	520.2	0.30	0.26
1.25	0.64	1.22	564.3	0.40	0.34
1.50	0.68	1.46	599.6	0.45	0.39
1.75	0.72	1.71	634.9	0.55	0.47
2.00	0.77	1.95	678.9	0.60	0.52
2.25	0.81	2.20	714.2	0.65	0.56
2.50	0.84	2.44	740.7	0.70	0.60
2.75	0.88	2.68	775.9	0.75	0.65
3.00	0.92	2.93	811.2	0.80	0.69
3.25	0.95	3.17	837.7	0.85	0.73
3.50	0.98	3.41	864.1	0.95	0.82
3.75	1.00	3.66	881.7	1.05	0.90
4.00	1.02	3.90	899.4	1.10	0.95
4.25	1.04	4.15	917.0	1.20	1.03
4.50	1.06	4.39	934.7	1.30	1.12
4.75	1.08	4.63	952.3	1.35	1.16
5.00	1.10	4.88	969.9	1.40	1.20
5.25	1.12	5.12	987.6	1.45	1.25
5.50	1.14	5.37	1005.2	1.50	1.29
5.75	1.16	5.61	1022.8	1.55	1.33

Displacement (mm)	Load (kN)	Axial Strain (%)	Stress (kPa)	Volume Change (Comp) (cc)	Volumetric Strain (%)
6.00	1.19	5.85	1049.3	1.60	1.38
6.25	1.20	6.10	1058.1	1.65	1.42
6.50	1.21	6.34	1066.9	1.70	1.46
6.75	1.21	6.59	1066.9	1.75	1.51
7.00	1.22	6.83	1075.7	1.80	1.55
7.25	1.22	7.07	1075.7	1.80	1.55
7.50	1.23	7.32	1084.5	1.85	1.59
7.75	1.23	7.56	1084.5	1.85	1.59
8.00	1.24	7.80	1093.4	1.90	1.63
8.25	1.25	8.05	1102.2	1.90	1.63
8.50	1.25	8.29	1102.2	1.95	1.68
8.75	1.26	8.54	1111.0	2.00	1.72
9.00	1.27	8.78	1119.8	2.05	1.76
9.25	1.28	9.02	1128.6	2.10	1.81
9.50	1.28	9.27	1128.6	2.10	1.81
9.75	1.29	9.51	1137.5	2.05	1.76
10.00	1.29	9.76	1137.5	2.05	1.76
10.25	1.29	10.00	1137.5	2.00	1.72
10.50	1.30	10.24	1146.3	2.00	1.72
10.75	1.30	10.49	1146.3	1.95	1.68
11.00	1.30	10.73	1146.3	1.90	1.63
11.25	1.30	10.98	1146.3	1.90	1.63
11.50	1.31	11.22	1155.1	1.85	1.59
11.75	1.31	11.46	1155.1	1.80	1.55
12.00	1.31	11.71	1155.1	1.70	1.46
12.25	1.31	11.95	1155.1	1.65	1.42
12.50	1.32	12.20	1163.9	1.60	1.38
12.75	1.32	12.44	1163.9	1.55	1.33
13.00	1.32	12.68	1163.9	1.50	1.29
13.25	1.32	12.93	1163.9	1.45	1.25
13.50	1.32	13.17	1163.9	1.40	1.20
13.75	1.32	13.41	1163.9	1.35	1.16
14.00	1.33	13.66	1172.7	1.30	1.12
14.25	1.33	13.90	1172.7	1.25	1.08
14.50	1.33	14.15	1172.7	1.20	1.03
14.75	1.33	14.39	1172.7	1.15	0.99
15.00	1.33	14.63	1172.7	1.10	0.95
15.25	1.33	14.88	1172.7	1.10	0.95
15.50	1.33	15.12	1172.7	1.05	0.90
15.75	1.33	15.37	1172.7	1.00	0.86
16.00	1.33	15.61	1172.7	0.95	0.82
16.25	1.33	15.85	1172.7	0.95	0.82
16.50	1.33	16.10	1172.7	0.95	0.82
16.75	1.33	16.34	1172.7	0.95	0.82
17.00	1.33	16.59	1172.7	0.95	0.82

Consolidated Drained triaxial test with volume change measurements on rebounded sample

Initial Length (cm)	10.2	Initial void ratio	0.72
Initial Diameter (cm)	3.8	Initial Relative density	77.00
Initial c/s area (sq. cm)	11.34	Initial Cell Pressure (kPa)	350
Initial Volume (cc)	115.68	Rebounded Cell Pressure (kPa)	250
Weight of sample taken (gm)	180	Back Pressure (kPa)	50
Dry density (gm/cc)	1.56	Volume Change during rebound (cc)	0.5
Specific Gravity	2.67	Volumetric strain during rebound (%)	0.43

Displacement (mm)	Load (kN)	Axial Strain (%)	Stress (kPa)	Volume Change (Comp) (cc)	Volumetric Strain (%)
0.00	0.00	0.00	0.0	0.00	0.00
0.25	0.26	0.25	229.3	0.15	0.13
0.50	0.43	0.49	379.2	0.25	0.22
0.75	0.55	0.74	485.0	0.40	0.35
1.00	0.62	0.98	546.7	0.50	0.43
1.25	0.72	1.23	634.9	0.60	0.52
1.50	0.81	1.47	714.2	0.70	0.61
1.75	0.86	1.72	758.3	0.80	0.69
2.00	0.91	1.96	802.4	0.90	0.78
2.25	0.99	2.21	872.9	0.95	0.82
2.50	1.04	2.45	917.0	1.05	0.91
2.75	1.06	2.70	934.7	1.15	0.99
3.00	1.08	2.94	952.3	1.25	1.08
3.25	1.12	3.19	987.6	1.35	1.17
3.50	1.15	3.43	1014.0	1.50	1.30
3.75	1.17	3.68	1031.6	1.60	1.38
4.00	1.19	3.92	1049.3	1.75	1.51
4.25	1.21	4.17	1066.9	1.85	1.60
4.50	1.23	4.41	1084.5	1.95	1.69
4.75	1.25	4.66	1102.2	2.05	1.77
5.00	1.26	4.90	1111.0	2.15	1.86
5.25	1.28	5.15	1128.6	2.20	1.90
5.50	1.29	5.39	1137.5	2.30	1.99
5.75	1.30	5.64	1146.3	2.35	2.03

Displacement (mm)	Load (kN)	Axial Strain (%)	Stress (kPa)	Volume Change (Comp) (cc)	Volumetric Strain (%)
6.00	1.31	5.88	1155.1	2.45	2.12
6.25	1.33	6.13	1172.7	2.50	2.16
6.50	1.35	6.37	1190.4	2.55	2.20
6.75	1.37	6.62	1208.0	2.60	2.25
7.00	1.39	6.86	1225.6	2.65	2.29
7.25	1.40	7.11	1234.4	2.70	2.33
7.50	1.42	7.35	1252.1	2.75	2.38
7.75	1.43	7.60	1260.9	2.80	2.42
8.00	1.44	7.84	1269.7	2.85	2.46
8.25	1.44	8.09	1269.7	2.80	2.42
8.50	1.45	8.33	1278.5	2.80	2.42
8.75	1.45	8.58	1278.5	2.75	2.38
9.00	1.46	8.82	1287.3	2.75	2.38
9.25	1.46	9.07	1287.3	2.70	2.33
9.50	1.47	9.31	1296.2	2.65	2.29
9.75	1.47	9.56	1296.2	2.60	2.25
10.00	1.48	9.80	1305.0	2.55	2.20
10.25	1.48	10.05	1305.0	2.50	2.16
10.50	1.49	10.29	1313.8	2.45	2.12
10.75	1.49	10.54	1313.8	2.40	2.07
11.00	1.49	10.78	1313.8	2.35	2.03
11.25	1.50	11.03	1322.6	2.25	1.95
11.50	1.50	11.27	1322.6	2.15	1.86
11.75	1.50	11.52	1322.6	2.10	1.82
12.00	1.50	11.76	1322.6	2.10	1.82
12.25	1.51	12.01	1331.4	2.05	1.77
12.50	1.51	12.25	1331.4	2.00	1.73
12.75	1.51	12.50	1331.4	1.95	1.69
13.00	1.51	12.75	1331.4	1.90	1.64
13.25	1.52	12.99	1340.3	1.85	1.60
13.50	1.52	13.24	1340.3	1.80	1.56
13.75	1.52	13.48	1340.3	1.80	1.56
14.00	1.52	13.73	1340.3	1.75	1.51
14.25	1.53	13.97	1349.1	1.70	1.47
14.50	1.53	14.22	1349.1	1.65	1.43
14.75	1.53	14.46	1349.1	1.60	1.38
15.00	1.53	14.71	1349.1	1.60	1.38
15.25	1.53	14.95	1349.1	1.55	1.34
15.50	1.54	15.20	1357.9	1.55	1.34
15.75	1.54	15.44	1357.9	1.50	1.30
16.00	1.54	15.69	1357.9	1.50	1.30
16.25	1.54	15.93	1357.9	1.45	1.25
16.50	1.54	16.18	1357.9	1.45	1.25
16.75	1.54	16.42	1357.9	1.40	1.21
17.00	1.54	16.67	1357.9	1.40	1.21

Consolidated Drained triaxial test with volume change measurements on rebounded sample

Initial Length (cm)	10.3	Initial void ratio	0.73
Initial Diameter (cm)	3.8	Initial Relative density	71.90
Initial c/s area (sq. cm)	11.34	Initial Cell Pressure (kPa)	350
Initial Volume (cc)	116.81	Rebounded Cell Pressure (kPa)	300
Weight of sample taken (gm)	180	Back Pressure (kPa)	50
Dry density (gm/cc)	1.54	Volume Change during rebound (cc)	0.2
Specific Gravity	2.67	Volumetric strain during rebound (%)	0.17

Displacement (mm)	Load (kN)	Axial Strain (%)	Stress (kPa)	Volume Change (Comp) (cc)	Volumetric Strain (%)
0.00	0.00	0.00	0.0	0.00	0.00
0.25	0.26	0.24	229.3	0.35	0.30
0.50	0.54	0.49	476.1	0.50	0.43
0.75	0.72	0.73	634.9	0.70	0.60
1.00	0.87	0.97	767.1	0.90	0.77
1.25	0.98	1.21	864.1	1.10	0.94
1.50	1.09	1.46	961.1	1.25	1.07
1.75	1.15	1.70	1014.0	1.45	1.24
2.00	1.23	1.94	1084.5	1.60	1.37
2.25	1.28	2.18	1128.6	1.80	1.54
2.50	1.32	2.43	1163.9	1.95	1.67
2.75	1.37	2.67	1208.0	2.05	1.75
3.00	1.41	2.91	1243.3	2.20	1.88
3.25	1.45	3.16	1278.5	2.35	2.01
3.50	1.48	3.40	1305.0	2.50	2.14
3.75	1.50	3.64	1322.6	2.65	2.27
4.00	1.51	3.88	1331.4	2.75	2.35
4.25	1.53	4.13	1349.1	2.80	2.40
4.50	1.54	4.37	1357.9	2.90	2.48
4.75	1.55	4.61	1366.7	2.95	2.53
5.00	1.56	4.85	1375.5	3.05	2.61
5.25	1.56	5.10	1375.5	3.15	2.70
5.50	1.57	5.34	1384.3	3.20	2.74
5.75	1.57	5.58	1384.3	3.30	2.83

Displacement (mm)	Load (kN)	Axial Strain (%)	Stress (kPa)	Volume Change (Comp) (cc)	Volumetric Strain (%)
6.00	1.58	5.83	1393.2	3.35	2.87
6.25	1.58	6.07	1393.2	3.40	2.91
6.50	1.58	6.31	1393.2	3.50	3.00
6.75	1.59	6.55	1402.0	3.55	3.04
7.00	1.59	6.80	1402.0	3.60	3.08
7.25	1.59	7.04	1402.0	3.65	3.12
7.50	1.60	7.28	1410.8	3.70	3.17
7.75	1.60	7.52	1410.8	3.75	3.21
8.00	1.61	7.77	1419.6	3.80	3.25
8.25	1.61	8.01	1419.6	3.85	3.30
8.50	1.62	8.25	1428.4	3.85	3.30
8.75	1.62	8.50	1428.4	3.80	3.25
9.00	1.63	8.74	1437.2	3.70	3.17
9.25	1.63	8.98	1437.2	3.65	3.12
9.50	1.64	9.22	1446.1	3.55	3.04
9.75	1.64	9.47	1446.1	3.45	2.95
10.00	1.65	9.71	1454.9	3.40	2.91
10.25	1.65	9.95	1454.9	3.40	2.91
10.50	1.66	10.19	1463.7	3.35	2.87
10.75	1.66	10.44	1463.7	3.30	2.83
11.00	1.67	10.68	1472.5	3.25	2.78
11.25	1.67	10.92	1472.5	3.20	2.74
11.50	1.68	11.17	1481.3	3.15	2.70
11.75	1.68	11.41	1481.3	3.10	2.65
12.00	1.68	11.65	1481.3	3.05	2.61
12.25	1.69	11.89	1490.2	3.00	2.57
12.50	1.69	12.14	1490.2	2.95	2.53
12.75	1.69	12.38	1490.2	2.95	2.53
13.00	1.70	12.62	1499.0	2.90	2.48
13.25	1.70	12.86	1499.0	2.85	2.44
13.50	1.70	13.11	1499.0	2.80	2.40
13.75	1.71	13.35	1507.8	2.80	2.40
14.00	1.71	13.59	1507.8	2.70	2.31
14.25	1.71	13.83	1507.8	2.65	2.27
14.50	1.72	14.08	1516.6	2.60	2.23
14.75	1.72	14.32	1516.6	2.60	2.23
15.00	1.72	14.56	1516.6	2.55	2.18
15.25	1.72	14.81	1516.6	2.50	2.14
15.50	1.73	15.05	1525.4	2.45	2.10
15.75	1.73	15.29	1525.4	2.40	2.05
16.00	1.73	15.53	1525.4	2.35	2.01
16.25	1.73	15.78	1525.4	2.35	2.01
16.50	1.73	16.02	1525.4	2.30	1.97
16.75	1.73	16.26	1525.4	2.25	1.93
17.00	1.73	16.50	1525.4	2.20	1.88

Consolidated Drained triaxial test with volume change measurements on rebounded sample

Initial Length (cm)	10.15	Initial void ratio	0.81
Initial Diameter (cm)	3.8	Initial Relative density	49.11
Initial c/s area (sq. cm)	11.34	Initial Cell Pressure (kPa)	350
Initial Volume (cc)	115.11	Rebounded Cell Pressure (kPa)	100
Weight of sample taken (gm)	170	Back Pressure (kPa)	50
Dry density (gm/cc)	1.48	Volume Change during rebound (cc)	1.70
Specific Gravity	2.67	Volumetric strain during rebound (%)	1.47

Displacement (mm)	Load (kN)	Burette Reading (cc)	Axial Strain (%)	Stress (kPa)	Volume Change (Comp) (cc)	Volumetric Strain (%)
0.00	0.00	49.00	0.00	0.00	0.00	0.00
0.25	0.03	48.95	0.25	26.59	0.05	0.04
0.50	0.05	48.95	0.49	44.32	0.05	0.04
0.75	0.08	48.90	0.74	70.91	0.10	0.09
1.00	0.11	48.90	0.99	97.50	0.10	0.09
1.25	0.13	48.85	1.23	115.23	0.15	0.13
1.50	0.15	48.75	1.48	132.96	0.25	0.22
1.75	0.17	48.75	1.72	150.69	0.25	0.22
2.00	0.19	48.70	1.97	168.42	0.30	0.26
2.25	0.21	48.65	2.22	186.14	0.35	0.30
2.50	0.24	48.60	2.46	212.74	0.40	0.35
2.75	0.26	48.55	2.71	230.47	0.45	0.39
3.00	0.29	48.50	2.96	257.06	0.50	0.43
3.25	0.31	48.50	3.20	274.79	0.50	0.43
3.50	0.33	48.40	3.45	292.51	0.60	0.52
3.75	0.36	48.35	3.69	319.11	0.65	0.56
4.00	0.38	48.35	3.94	336.83	0.65	0.56
4.25	0.40	48.30	4.19	354.56	0.70	0.61
4.50	0.42	48.25	4.43	372.29	0.75	0.65
4.75	0.43	48.20	4.68	381.15	0.80	0.69
5.00	0.45	48.15	4.93	398.88	0.85	0.74
5.25	0.47	48.15	5.17	416.61	0.85	0.74
5.50	0.49	48.10	5.42	434.34	0.90	0.78
5.75	0.50	48.10	5.67	443.20	0.90	0.78
6.00	0.52	48.00	5.91	460.93	1.00	0.87
6.25	0.54	47.95	6.16	478.66	1.05	0.91
6.50	0.55	47.90	6.40	487.52	1.10	0.96

Displacement (mm)	Load (kN)	Burette Reading (cc)	Axial Strain (%)	Stress (kPa)	Volume Change (Comp) (cc)	Volumetric Strain (%)
6.75	0.56	47.90	6.65	496.39	1.10	0.96
7.00	0.58	47.85	6.90	514.11	1.15	1.00
7.25	0.58	47.80	7.14	514.11	1.20	1.04
7.50	0.59	47.80	7.39	522.98	1.20	1.04
7.75	0.60	47.75	7.64	531.84	1.25	1.09
8.00	0.61	47.70	7.88	540.71	1.30	1.13
8.25	0.62	47.70	8.13	549.57	1.30	1.13
8.50	0.63	47.60	8.37	558.43	1.40	1.22
8.75	0.64	47.55	8.62	567.30	1.45	1.26
9.00	0.64	47.55	8.87	567.30	1.45	1.26
9.25	0.65	47.50	9.11	576.16	1.50	1.30
9.50	0.66	47.50	9.36	585.03	1.50	1.30
9.75	0.66	47.45	9.61	585.03	1.55	1.35
10.00	0.67	47.45	9.85	593.89	1.55	1.35
10.25	0.67	47.45	10.10	593.89	1.55	1.35
10.50	0.67	47.45	10.34	593.89	1.55	1.35
10.75	0.67	47.45	10.59	593.89	1.55	1.35
11.00	0.68	47.45	10.84	602.76	1.55	1.35
11.25	0.68	47.40	11.08	602.76	1.60	1.39
11.50	0.68	47.40	11.33	602.76	1.60	1.39
11.75	0.68	47.40	11.58	602.76	1.60	1.39
12.00	0.68	47.50	11.82	602.76	1.50	1.30
12.25	0.68	47.55	12.07	602.76	1.45	1.26
12.50	0.69	47.60	12.32	611.62	1.40	1.22
12.75	0.69	47.60	12.56	611.62	1.40	1.22
13.00	0.69	47.70	12.81	611.62	1.30	1.13
13.25	0.69	47.70	13.05	611.62	1.30	1.13
13.50	0.69	47.75	13.30	611.62	1.25	1.09
13.75	0.69	47.75	13.55	611.62	1.25	1.09
14.00	0.69	47.85	13.79	611.62	1.15	1.00
14.25	0.69	47.90	14.04	611.62	1.10	0.96
14.50	0.69	47.95	14.29	611.62	1.05	0.91
14.75	0.69	47.95	14.53	611.62	1.05	0.91
15.00	0.69	48.00	14.78	611.62	1.00	0.87
15.25	0.69	48.00	15.02	611.62	1.00	0.87
15.50	0.69	48.10	15.27	611.62	0.90	0.78
15.75	0.69	48.10	15.52	611.62	0.90	0.78
16.00	0.69	48.15	15.76	611.62	0.85	0.74
16.25	0.69	48.20	16.01	611.62	0.80	0.69
16.50	0.69	48.25	16.26	611.62	0.75	0.65
16.75	0.69	48.25	16.50	611.62	0.75	0.65
17.00	0.69	48.30	16.75	611.62	0.70	0.61
17.25	0.70	48.30	17.00	620.48	0.70	0.61
17.50	0.70	48.35	17.24	620.48	0.65	0.56
17.75	0.70	48.35	17.49	620.48	0.65	0.56
18.00	0.70	48.40	17.73	620.48	0.60	0.52

Consolidated Drained triaxial test with volume change measurements on rebounded sample

Initial Length (cm)	10.2	Initial void ratio	0.81
Initial Diameter (cm)	3.79	Initial Relative density	49.30
Initial c/s area (sq. cm)	11.28	Initial Cell Pressure (kPa)	350
Initial Volume (cc)	115.07	Rebounded Cell Pressure (kPa)	150
Weight of sample taken (gm)	170	Back Pressure (kPa)	50
Dry density (gm/cc)	1.48	Volume Change during rebound (cc)	1.40
Specific Gravity	2.67	Volumetric strain during rebound (%)	1.21

Displacement (mm)	Load (kN)	Burette Reading (cc)	Axial Strain (%)	Stress (kPa)	Volume Change (Comp) (cc)	Volumetric Strain (%)
0.00	0.00	49.00	0.00	0.0	0.00	0.00
0.25	0.05	48.95	0.25	44.3	0.05	0.04
0.50	0.09	48.90	0.49	79.8	0.10	0.09
0.75	0.14	48.90	0.74	124.1	0.10	0.09
1.00	0.17	48.85	0.98	150.7	0.15	0.13
1.25	0.20	48.75	1.23	177.3	0.25	0.22
1.50	0.23	48.70	1.47	203.9	0.30	0.26
1.75	0.27	48.65	1.72	239.3	0.35	0.30
2.00	0.29	48.60	1.96	257.1	0.40	0.35
2.25	0.32	48.55	2.21	283.6	0.45	0.39
2.50	0.35	48.50	2.45	310.2	0.50	0.43
2.75	0.37	48.40	2.70	328.0	0.60	0.52
3.00	0.41	48.35	2.94	363.4	0.65	0.56
3.25	0.43	48.35	3.19	381.2	0.65	0.56
3.50	0.45	48.30	3.43	398.9	0.70	0.61
3.75	0.48	48.25	3.68	425.5	0.75	0.65
4.00	0.50	48.20	3.92	443.2	0.80	0.69
4.25	0.52	48.15	4.17	460.9	0.85	0.73
4.50	0.53	48.05	4.41	469.8	0.95	0.82
4.75	0.55	48.00	4.66	487.5	1.00	0.86
5.00	0.57	47.95	4.90	505.3	1.05	0.91
5.25	0.58	47.90	5.15	514.1	1.10	0.95
5.50	0.60	47.90	5.39	531.8	1.10	0.95
5.75	0.62	47.85	5.64	549.6	1.15	0.99
6.00	0.64	47.80	5.88	567.3	1.20	1.04
6.25	0.65	47.80	6.13	576.2	1.20	1.04

Displacement (mm)	Load (kN)	Burette Reading (cc)	Axial Strain (%)	Stress (kPa)	Volume Change (Comp) (cc)	Volumetric Strain (%)
6.50	0.67	47.75	6.37	593.9	1.25	1.09
6.75	0.68	47.65	6.62	602.8	1.35	1.17
7.00	0.70	47.60	6.86	620.5	1.40	1.22
7.25	0.72	47.55	7.11	638.2	1.45	1.26
7.50	0.74	47.55	7.35	655.9	1.45	1.26
7.75	0.75	47.50	7.60	664.8	1.50	1.30
8.00	0.76	47.45	7.84	673.7	1.55	1.35
8.25	0.77	47.40	8.09	682.5	1.60	1.39
8.50	0.78	47.30	8.33	691.4	1.70	1.48
8.75	0.79	47.30	8.58	700.3	1.70	1.48
9.00	0.81	47.25	8.82	718.0	1.75	1.52
9.25	0.82	47.20	9.07	726.9	1.80	1.56
9.50	0.82	47.15	9.31	726.9	1.85	1.61
9.75	0.83	47.10	9.56	735.7	1.90	1.65
10.00	0.84	47.05	9.80	744.6	1.95	1.69
10.25	0.85	47.05	10.05	753.4	1.95	1.69
10.50	0.86	47.00	10.29	762.3	2.00	1.74
10.75	0.86	47.00	10.54	762.3	2.00	1.74
11.00	0.87	46.90	10.78	771.2	2.10	1.82
11.25	0.88	46.90	11.03	780.0	2.10	1.82
11.50	0.89	47.00	11.27	788.9	2.00	1.74
11.75	0.90	47.00	11.52	797.8	2.00	1.74
12.00	0.91	47.00	11.76	806.6	2.00	1.74
12.25	0.91	47.05	12.01	806.6	1.95	1.69
12.50	0.91	47.10	12.25	806.6	1.90	1.65
12.75	0.92	47.10	12.50	815.5	1.90	1.65
13.00	0.92	47.15	12.75	815.5	1.85	1.61
13.25	0.92	47.15	12.99	815.5	1.85	1.61
13.50	0.93	47.20	13.24	824.4	1.80	1.56
13.75	0.93	47.20	13.48	824.4	1.80	1.56
14.00	0.94	47.25	13.73	833.2	1.75	1.52
14.25	0.94	47.30	13.97	833.2	1.70	1.48
14.50	0.95	47.40	14.22	842.1	1.60	1.39
14.75	0.95	47.40	14.46	842.1	1.60	1.39
15.00	0.95	47.45	14.71	842.1	1.55	1.35
15.25	0.96	47.50	14.95	850.9	1.50	1.30
15.50	0.96	47.50	15.20	850.9	1.50	1.30
15.75	0.97	47.55	15.44	859.8	1.45	1.26
16.00	0.98	47.60	15.69	868.7	1.40	1.22
16.25	0.99	47.60	15.93	877.5	1.40	1.22
16.50	0.99	47.65	16.18	877.5	1.35	1.17
16.75	1.00	47.65	16.42	886.4	1.35	1.17
17.00	1.00	47.75	16.67	886.4	1.25	1.09
17.25	1.01	47.75	16.91	895.3	1.25	1.09
17.50	1.01	47.80	17.16	895.3	1.20	1.04
17.75	1.02	47.85	17.40	904.1	1.15	1.00
18.00	1.02	47.85	17.65	904.1	1.15	1.00

Consolidated Drained triaxial test with volume change measurements on rebounded sample

Initial Length (cm)	10.2	Initial void ratio	0.82
Initial Diameter (cm)	3.8	Initial Relative density	46.41
Initial c/s area (sq. cm)	11.34	Initial Cell Pressure (kPa)	350
Initial Volume (cc)	115.68	Rebounded Cell Pressure (kPa)	200
Weight of sample taken (gm)	170	Back Pressure (kPa)	50
Dry density (gm/cc)	1.47	Volume Change during rebound (cc)	1.30
Specific Gravity	2.67	Volumetric strain during rebound (%)	1.13

Displacement (mm)	Load (kN)	Burette Reading (cc)	Axial Strain (%)	Stress (kPa)	Volume Change (Comp) (cc)	Volumetric Strain (%)
0.00	0.00	49.00	0.00	0.0	0.00	0.00
0.25	0.06	48.45	0.25	52.9	0.55	0.48
0.50	0.11	48.85	0.49	97.0	0.15	0.13
0.75	0.17	48.75	0.74	149.9	0.25	0.22
1.00	0.22	48.70	0.98	194.0	0.30	0.26
1.25	0.26	48.65	1.23	229.3	0.35	0.30
1.50	0.30	48.60	1.47	264.5	0.40	0.35
1.75	0.34	48.50	1.72	299.8	0.50	0.43
2.00	0.38	48.35	1.96	335.1	0.65	0.56
2.25	0.42	48.30	2.21	370.3	0.70	0.61
2.50	0.44	48.25	2.45	388.0	0.75	0.65
2.75	0.47	48.20	2.70	414.4	0.80	0.69
3.00	0.50	48.15	2.94	440.9	0.85	0.73
3.25	0.53	48.05	3.19	467.3	0.95	0.82
3.50	0.56	47.90	3.43	493.8	1.10	0.95
3.75	0.59	47.85	3.68	520.2	1.15	0.99
4.00	0.62	47.80	3.92	546.7	1.20	1.04
4.25	0.64	47.70	4.17	564.3	1.30	1.12
4.50	0.66	47.65	4.41	582.0	1.35	1.17
4.75	0.68	47.50	4.66	599.6	1.50	1.30
5.00	0.71	47.45	4.90	626.0	1.55	1.34
5.25	0.72	47.35	5.15	634.9	1.65	1.43
5.50	0.75	47.30	5.39	661.3	1.70	1.47
5.75	0.77	47.25	5.64	678.9	1.75	1.51
6.00	0.79	47.15	5.88	696.6	1.85	1.60
6.25	0.81	47.10	6.13	714.2	1.90	1.64
6.50	0.82	47.05	6.37	723.0	1.95	1.69

Displacement (mm)	Load (kN)	Burette Reading (cc)	Axial Strain (%)	Stress (kPa)	Volume Change (Comp) (cc)	Volumetric Strain (%)
6.75	0.84	47.00	6.62	740.7	2.00	1.73
7.00	0.86	46.95	6.86	758.3	2.05	1.77
7.25	0.88	46.85	7.11	775.9	2.15	1.86
7.50	0.89	46.70	7.35	784.8	2.30	1.99
7.75	0.91	46.60	7.60	802.4	2.40	2.07
8.00	0.92	46.50	7.84	811.2	2.50	2.16
8.25	0.93	46.35	8.09	820.0	2.65	2.29
8.50	0.94	46.30	8.33	828.8	2.70	2.33
8.75	0.95	46.25	8.58	837.7	2.75	2.38
9.00	0.97	46.20	8.82	855.3	2.80	2.42
9.25	0.98	46.15	9.07	864.1	2.85	2.46
9.50	0.99	46.10	9.31	872.9	2.90	2.51
9.75	1.00	46.00	9.56	881.7	3.00	2.59
10.00	1.01	45.95	9.80	890.6	3.05	2.64
10.25	1.02	45.95	10.05	899.4	3.05	2.64
10.50	1.02	45.90	10.29	899.4	3.10	2.68
10.75	1.02	45.90	10.54	899.4	3.10	2.68
11.00	1.03	45.90	10.78	908.2	3.10	2.68
11.25	1.04	45.85	11.03	917.0	3.15	2.72
11.50	1.04	45.85	11.27	917.0	3.15	2.72
11.75	1.05	45.85	11.52	925.8	3.15	2.72
12.00	1.05	45.85	11.76	925.8	3.15	2.72
12.25	1.06	45.90	12.01	934.7	3.10	2.68
12.50	1.06	45.90	12.25	934.7	3.10	2.68
12.75	1.07	45.90	12.50	943.5	3.10	2.68
13.00	1.07	45.95	12.75	943.5	3.05	2.64
13.25	1.08	45.95	12.99	952.3	3.05	2.64
13.50	1.08	46.00	13.24	952.3	3.00	2.59
13.75	1.09	46.10	13.48	961.1	2.90	2.51
14.00	1.09	46.10	13.73	961.1	2.90	2.51
14.25	1.10	46.15	13.97	969.9	2.85	2.46
14.50	1.10	46.15	14.22	969.9	2.85	2.46
14.75	1.11	46.20	14.46	978.7	2.80	2.42
15.00	1.11	46.20	14.71	978.7	2.80	2.42
15.25	1.12	46.25	14.95	987.6	2.75	2.38
15.50	1.12	46.25	15.20	987.6	2.75	2.38
15.75	1.13	46.30	15.44	996.4	2.70	2.33
16.00	1.13	46.30	15.69	996.4	2.70	2.33
16.25	1.14	46.35	15.93	1005.2	2.65	2.29
16.50	1.14	46.40	16.18	1005.2	2.60	2.25
16.75	1.14	46.50	16.42	1005.2	2.50	2.16
17.00	1.14	46.55	16.67	1005.2	2.45	2.12
17.25	1.15	46.55	16.91	1014.0	2.45	2.12
17.50	1.15	46.60	17.16	1014.0	2.40	2.07
17.75	1.16	46.65	17.40	1022.8	2.35	2.03
18.00	1.16	46.70	17.65	1022.8	2.30	1.99

Consolidated Drained triaxial test with volume change measurements on rebounded sample

Initial Length (cm)	10.2	Initial void ratio	0.82
Initial Diameter (cm)	3.8	Initial Relative density	46.41
Initial c/s area (sq. cm)	11.34	Initial Cell Pressure (kPa)	350
Initial Volume (cc)	115.68	Rebounded Cell Pressure (kPa)	250
Weight of sample taken (gm)	170	Back Pressure (kPa)	50
Dry density (gm/cc)	1.47	Volume Change during rebound (cc)	0.90
Specific Gravity	2.67	Volumetric strain during rebound (%)	0.79

Displacement (mm)	Load (kN)	Burette Reading (cc)	Axial Strain (%)	Stress (kPa)	Volume Change (Comp) (cc)	Volumetric Strain (%)
0.00	0.00	49.00	0.00	0.0	0.00	0.00
0.25	0.06	48.90	0.25	52.9	0.10	0.09
0.50	0.12	48.75	0.49	105.8	0.25	0.22
0.75	0.18	48.65	0.74	158.7	0.35	0.30
1.00	0.25	48.60	0.98	220.4	0.40	0.35
1.25	0.30	48.50	1.23	264.5	0.50	0.43
1.50	0.35	48.45	1.47	308.6	0.55	0.48
1.75	0.41	48.30	1.72	361.5	0.70	0.61
2.00	0.45	48.20	1.96	396.8	0.80	0.69
2.25	0.50	48.10	2.21	440.9	0.90	0.78
2.50	0.54	47.95	2.45	476.1	1.05	0.91
2.75	0.59	47.85	2.70	520.2	1.15	0.99
3.00	0.64	47.80	2.94	564.3	1.20	1.04
3.25	0.67	47.75	3.19	590.8	1.25	1.08
3.50	0.71	47.65	3.43	626.0	1.35	1.17
3.75	0.76	47.50	3.68	670.1	1.50	1.30
4.00	0.79	47.40	3.92	696.6	1.60	1.38
4.25	0.82	47.30	4.17	723.0	1.70	1.47
4.50	0.86	47.15	4.41	758.3	1.85	1.60
4.75	0.89	47.05	4.66	784.8	1.95	1.69
5.00	0.92	47.00	4.90	811.2	2.00	1.73
5.25	0.94	46.95	5.15	828.8	2.05	1.77
5.50	0.97	46.80	5.39	855.3	2.20	1.90
5.75	1.00	46.70	5.64	881.7	2.30	1.99
6.00	1.02	46.60	5.88	899.4	2.40	2.07

Displacement (mm)	Load (kN)	Burette Reading (cc)	Axial Strain (%)	Stress (kPa)	Volume Change (Comp) (cc)	Volumetric Strain (%)
6.25	1.04	46.50	6.13	917.0	2.50	2.16
6.50	1.07	46.40	6.37	943.5	2.60	2.25
6.75	1.09	46.35	6.62	961.1	2.65	2.29
7.00	1.11	46.25	6.86	978.7	2.75	2.38
7.25	1.13	46.20	7.11	996.4	2.80	2.42
7.50	1.15	46.15	7.35	1014.0	2.85	2.46
7.75	1.16	46.10	7.60	1022.8	2.90	2.51
8.00	1.18	45.95	7.84	1040.5	3.05	2.64
8.25	1.19	45.90	8.09	1049.3	3.10	2.68
8.50	1.20	45.80	8.33	1058.1	3.20	2.77
8.75	1.21	45.75	8.58	1066.9	3.25	2.81
9.00	1.22	45.70	8.82	1075.7	3.30	2.85
9.25	1.23	45.60	9.07	1084.5	3.40	2.94
9.50	1.24	45.55	9.31	1093.4	3.45	2.98
9.75	1.25	45.50	9.56	1102.2	3.50	3.03
10.00	1.25	45.45	9.80	1102.2	3.55	3.07
10.25	1.26	45.45	10.05	1111.0	3.55	3.07
10.50	1.26	45.40	10.29	1111.0	3.60	3.11
10.75	1.26	45.40	10.54	1111.0	3.60	3.11
11.00	1.27	45.40	10.78	1119.8	3.60	3.11
11.25	1.27	45.35	11.03	1119.8	3.65	3.16
11.50	1.28	45.35	11.27	1128.6	3.65	3.16
11.75	1.28	45.40	11.52	1128.6	3.60	3.11
12.00	1.29	45.40	11.76	1137.5	3.60	3.11
12.25	1.29	45.40	12.01	1137.5	3.60	3.11
12.50	1.30	45.45	12.25	1146.3	3.55	3.07
12.75	1.30	45.45	12.50	1146.3	3.55	3.07
13.00	1.31	45.45	12.75	1155.1	3.55	3.07
13.25	1.31	45.50	12.99	1155.1	3.50	3.03
13.50	1.32	45.50	13.24	1163.9	3.50	3.03
13.75	1.32	45.55	13.48	1163.9	3.45	2.98
14.00	1.33	45.55	13.73	1172.7	3.45	2.98
14.25	1.33	45.55	13.97	1172.7	3.45	2.98
14.50	1.34	45.60	14.22	1181.5	3.40	2.94
14.75	1.34	45.60	14.46	1181.5	3.40	2.94
15.00	1.35	45.70	14.71	1190.4	3.30	2.85
15.25	1.36	45.70	14.95	1199.2	3.30	2.85
15.50	1.36	45.75	15.20	1199.2	3.25	2.81
15.75	1.37	45.75	15.44	1208.0	3.25	2.81
16.00	1.37	45.80	15.69	1208.0	3.20	2.77

Consolidated Drained triaxial test with volume change measurements on rebounded sample

Initial Length (cm)	10.2	Initial void ratio	0.82
Initial Diameter (cm)	3.8	Initial Relative density	46.41
Initial c/s area (sq. cm)	11.34	Initial Cell Pressure (kPa)	350
Initial Volume (cc)	115.68	Rebounded Cell Pressure (kPa)	300
Weight of sample taken (gm)	170	Back Pressure (kPa)	50
Dry density (gm/cc)	1.47	Volume Change during rebound (cc)	0.70
Specific Gravity	2.67	Volumetric strain during rebound (%)	0.60

Displacement (mm)	Load (kN)	Burette Reading (cc)	Axial Strain (%)	Stress (kPa)	Volume Change (Comp) (cc)	Volumetric Strain (%)
0.00	0.00	49.00	0.00	0.0	0.00	0.00
0.25	0.09	48.85	0.25	79.4	0.15	0.13
0.50	0.20	48.65	0.49	176.3	0.35	0.30
0.75	0.31	48.55	0.74	273.3	0.45	0.39
1.00	0.43	48.40	0.98	379.2	0.60	0.52
1.25	0.49	48.30	1.23	432.1	0.70	0.61
1.50	0.54	48.15	1.47	476.1	0.85	0.73
1.75	0.61	47.95	1.72	537.9	1.05	0.91
2.00	0.68	47.85	1.96	599.6	1.15	0.99
2.25	0.75	47.75	2.21	661.3	1.25	1.08
2.50	0.82	47.55	2.45	723.0	1.45	1.25
2.75	0.88	47.40	2.70	775.9	1.60	1.38
3.00	0.95	47.25	2.94	837.7	1.75	1.51
3.25	1.00	47.15	3.19	881.7	1.85	1.60
3.50	1.03	47.05	3.43	908.2	1.95	1.69
3.75	1.07	46.90	3.68	943.5	2.10	1.82
4.00	1.12	46.80	3.92	987.6	2.20	1.90
4.25	1.15	46.70	4.17	1014.0	2.30	1.99
4.50	1.19	46.55	4.41	1049.3	2.45	2.12
4.75	1.22	46.45	4.66	1075.7	2.55	2.20
5.00	1.25	46.35	4.90	1102.2	2.65	2.29
5.25	1.28	46.20	5.15	1128.6	2.80	2.42
5.50	1.30	46.15	5.39	1146.3	2.85	2.46
5.75	1.33	46.05	5.64	1172.7	2.95	2.55
6.00	1.35	45.95	5.88	1190.4	3.05	2.64
6.25	1.36	45.80	6.13	1199.2	3.20	2.77
6.50	1.37	45.70	6.37	1208.0	3.30	2.85
6.75	1.38	45.65	6.62	1216.8	3.35	2.90
7.00	1.39	45.60	6.86	1225.6	3.40	2.94
7.25	1.41	45.35	7.11	1243.3	3.65	3.16
7.50	1.42	45.20	7.35	1252.1	3.80	3.28
7.75	1.43	45.10	7.60	1260.9	3.90	3.37
8.00	1.43	45.00	7.84	1260.9	4.00	3.46

Displacement (mm)	Load (kN)	Burette Reading (cc)	Axial Strain (%)	Stress (kPa)	Volume Change (Comp) (cc)	Volumetric Strain (%)
6.50	0.08	48.20	6.44	70.91	0.80	0.70
6.75	0.08	48.20	6.68	70.91	0.80	0.70
7.00	0.08	48.10	6.93	70.91	0.90	0.79
7.25	0.08	48.10	7.18	70.91	0.90	0.79
7.50	0.08	47.95	7.43	70.91	1.05	0.92
7.75	0.08	47.95	7.67	70.91	1.05	0.92
8.00	0.08	47.95	7.92	70.91	1.05	0.92
8.25	0.08	47.85	8.17	70.91	1.15	1.01
8.50	0.09	47.85	8.42	79.78	1.15	1.01
8.75	0.09	47.85	8.66	79.78	1.15	1.01
9.00	0.09	47.75	8.91	79.78	1.25	1.10
9.25	0.09	47.75	9.16	79.78	1.25	1.10
9.50	0.09	47.75	9.41	79.78	1.25	1.10
9.75	0.09	47.65	9.65	79.78	1.35	1.18
10.00	0.09	47.65	9.90	79.78	1.35	1.18
10.25	0.10	47.65	10.15	88.64	1.35	1.18
10.50	0.10	47.50	10.40	88.64	1.50	1.32
10.75	0.10	47.50	10.64	88.64	1.50	1.32
11.00	0.10	47.40	10.89	88.64	1.60	1.40
11.25	0.10	47.40	11.14	88.64	1.60	1.40
11.50	0.10	47.30	11.39	88.64	1.70	1.49
11.75	0.10	47.30	11.63	88.64	1.70	1.49
12.00	0.10	47.30	11.88	88.64	1.70	1.49
12.25	0.10	47.20	12.13	88.64	1.80	1.58
12.50	0.10	47.20	12.38	88.64	1.80	1.58
12.75	0.11	47.20	12.62	97.50	1.80	1.58
12.75	0.11	47.05	12.62	97.50	1.95	1.71
13.00	0.11	47.05	12.87	97.50	1.95	1.71
13.25	0.11	47.05	13.12	97.50	1.95	1.71
13.50	0.11	46.95	13.37	97.50	2.05	1.80
13.75	0.11	46.95	13.61	97.50	2.05	1.80
14.00	0.11	46.95	13.86	97.50	2.05	1.80
14.25	0.11	46.85	14.11	97.50	2.15	1.89
14.50	0.11	46.85	14.36	97.50	2.15	1.89
14.75	0.11	46.85	14.60	97.50	2.15	1.89
15.00	0.11	46.70	14.85	97.50	2.30	2.02
15.25	0.11	46.70	15.10	97.50	2.30	2.02
15.50	0.11	46.70	15.35	97.50	2.30	2.02
15.75	0.11	46.60	15.59	97.50	2.40	2.11
16.00	0.11	46.60	15.84	97.50	2.40	2.11
16.25	0.12	46.60	16.09	106.37	2.40	2.11
16.50	0.12	46.50	16.34	106.37	2.50	2.19
16.75	0.12	46.50	16.58	106.37	2.50	2.19

Consolidated Drained triaxial test with volume change measurements on rebounded sample

Initial Length (cm)	10.1	Initial void ratio	0.89
Initial Diameter (cm)	3.78	Initial Relative density	23.82
Initial c/s area (sq. cm)	11.22	Initial Cell Pressure (kPa)	350
Initial Volume (cc)	113.34	Rebounded Cell Pressure (kPa)	300
Weight of sample taken (gm)	160	Back Pressure (kPa)	50
Dry density (gm/cc)	1.41	Volume Change during rebound (cc)	2.20
Specific Gravity	2.67	Volumetric strain during rebound (%)	1.92

Displacement (mm)	Load (kN)	Burette Reading (cc)	Axial Strain (%)	Stress (kPa)	Volume Change (Comp) (cc)	Volumetric Strain (%)
0.00	0.00	46.5	0.00	0.0	0.00	0.00
0.25	0.00	46.5	0.25	0.0	0.00	0.00
0.50	0.01	46.4	0.50	8.9	0.10	0.09
0.75	0.02	46.4	0.74	17.8	0.10	0.09
1.00	0.02	46.25	0.99	17.8	0.25	0.22
1.25	0.03	46.25	1.24	26.7	0.25	0.22
1.50	0.04	46.25	1.49	35.6	0.25	0.22
1.75	0.04	46.15	1.73	35.6	0.35	0.31
2.00	0.05	46.15	1.98	44.6	0.35	0.31
2.25	0.06	46.15	2.23	53.5	0.35	0.31
2.50	0.06	46.05	2.48	53.5	0.45	0.40
2.75	0.07	46.05	2.72	62.4	0.45	0.40
3.00	0.07	46.05	2.97	62.4	0.45	0.40
3.25	0.08	45.95	3.22	71.3	0.55	0.49
3.50	0.08	45.95	3.47	71.3	0.55	0.49
3.75	0.09	45.95	3.71	80.2	0.55	0.49
4.00	0.09	45.8	3.96	80.2	0.70	0.62
4.25	0.10	45.8	4.21	89.1	0.70	0.62
4.50	0.10	45.8	4.46	89.1	0.70	0.62
4.75	0.10	45.7	4.70	89.1	0.80	0.71
5.00	0.10	45.7	4.95	89.1	0.80	0.71
5.25	0.11	45.6	5.20	98.0	0.90	0.79
5.50	0.11	45.6	5.45	98.0	0.90	0.79
5.75	0.12	45.45	5.69	106.9	1.05	0.93
6.00	0.12	45.45	5.94	106.9	1.05	0.93
6.25	0.12	45.35	6.19	106.9	1.15	1.01

Displacement (mm)	Load (kN)	Burette Reading (cc)	Axial Strain (%)	Stress (kPa)	Volume Change (Comp) (cc)	Volumetric Strain (%)
6.50	0.13	45.35	6.44	115.8	1.15	1.01
6.75	0.13	45.35	6.68	115.8	1.15	1.01
7.00	0.13	45.25	6.93	115.8	1.25	1.10
7.25	0.13	45.25	7.18	115.8	1.25	1.10
7.50	0.13	45.25	7.43	115.8	1.25	1.10
7.75	0.14	45.15	7.67	124.8	1.35	1.19
8.00	0.14	45.15	7.92	124.8	1.35	1.19
8.25	0.14	45	8.17	124.8	1.50	1.32
8.50	0.14	45	8.42	124.8	1.50	1.32
8.75	0.15	44.9	8.66	133.7	1.60	1.41
9.00	0.15	44.9	8.91	133.7	1.60	1.41
9.25	0.15	44.8	9.16	133.7	1.70	1.50
9.50	0.15	44.8	9.41	133.7	1.70	1.50
9.75	0.15	44.65	9.65	133.7	1.85	1.63
10.00	0.15	44.65	9.90	133.7	1.85	1.63
10.25	0.16	44.65	10.15	142.6	1.85	1.63
10.50	0.16	44.55	10.40	142.6	1.95	1.72
10.75	0.16	44.55	10.64	142.6	1.95	1.72
11.00	0.16	44.45	10.89	142.6	2.05	1.81
11.25	0.16	44.45	11.14	142.6	2.05	1.81
11.50	0.17	44.45	11.39	151.5	2.05	1.81
11.75	0.17	44.3	11.63	151.5	2.20	1.94
12.00	0.17	44.3	11.88	151.5	2.20	1.94
12.25	0.17	44.2	12.13	151.5	2.30	2.03
12.50	0.17	44.2	12.38	151.5	2.30	2.03
12.75	0.18	44.2	12.62	160.4	2.30	2.03
13.00	0.18	44.1	12.87	160.4	2.40	2.12
13.25	0.18	44.1	13.12	160.4	2.40	2.12
13.50	0.18	44.1	13.37	160.4	2.40	2.12
13.75	0.18	44	13.61	160.4	2.50	2.21
14.00	0.18	44	13.86	160.4	2.50	2.21
14.25	0.19	44	14.11	169.3	2.50	2.21
14.50	0.19	43.85	14.36	169.3	2.65	2.34
14.75	0.19	43.85	14.60	169.3	2.65	2.34
15.00	0.19	43.85	14.85	169.3	2.65	2.34
15.25	0.19	43.75	15.10	169.3	2.75	2.43
15.50	0.20	43.75	15.35	178.2	2.75	2.43
15.75	0.20	43.75	15.59	178.2	2.75	2.43
16.00	0.20	43.65	15.84	178.2	2.85	2.51
16.25	0.20	43.65	16.09	178.2	2.85	2.51
16.50	0.20	43.65	16.34	178.2	2.85	2.51
16.75	0.20	43.5	16.58	178.2	3.00	2.65
17.00	0.20	43.5	16.83	178.2	3.00	2.65
17.25	0.20	43.5	17.08	178.2	3.00	2.65
17.50	0.20	43.4	17.33	178.2	3.10	2.74
17.75	0.20	43.4	17.57	178.2	3.10	2.74
18.00	0.20	43.3	17.82	178.2	3.20	2.82
18.25	0.21	43.3	18.07	187.1	3.20	2.82
18.50	0.21	43.2	18.32	187.1	3.30	2.91
18.75	0.21	43.2	18.56	187.1	3.30	2.91
19.00	0.21	43.2	18.81	187.1	3.30	2.91
19.25	0.21	43.05	19.06	187.1	3.45	3.04
19.50	0.21	43.05	19.31	187.1	3.45	3.04
19.75	0.21	42.95	19.55	187.1	3.55	3.13
20.00	0.21	42.95	19.80	187.1	3.55	3.13
20.25	0.21	42.95	20.05	187.1	3.55	3.13

Consolidated Drained triaxial test with volume change measurements on rebounded sample

Initial Length (cm)	10.1	Initial void ratio	0.90
Initial Diameter (cm)	3.79	Initial Relative density	20.78
Initial c/s area (sq. cm)	11.28	Initial Cell Pressure (kPa)	350
Initial Volume (cc)	113.94	Rebounded Cell Pressure (kPa)	300
Weight of sample taken (gm)	160	Back Pressure (kPa)	50
Dry density (gm/cc)	1.40	Volume Change during rebound (cc)	1.95
Specific Gravity	2.67	Volumetric strain during rebound (%)	1.72

Displacement (mm)	Load (kN)	Burette Reading (cc)	Axial Strain (%)	Stress (kPa)	Volume Change (Comp) (cc)	Volumetric Strain (%)
0.00	0.00	52.00	0.00	0.0	0.00	0.00
0.25	0.01	52.00	0.25	8.9	0.00	0.00
0.50	0.02	51.90	0.50	17.7	0.10	0.09
0.75	0.03	51.90	0.74	26.6	0.10	0.09
1.00	0.04	51.90	0.99	35.5	0.10	0.09
1.25	0.05	51.75	1.24	44.3	0.25	0.22
1.50	0.07	51.75	1.49	62.0	0.25	0.22
1.75	0.08	51.65	1.73	70.9	0.35	0.31
2.00	0.10	51.65	1.98	88.6	0.35	0.31
2.25	0.10	51.55	2.23	88.6	0.45	0.40
2.50	0.11	51.55	2.48	97.5	0.45	0.40
2.75	0.11	51.45	2.72	97.5	0.55	0.49
3.00	0.12	51.45	2.97	106.4	0.55	0.49
3.25	0.13	51.30	3.22	115.2	0.70	0.62
3.50	0.13	51.30	3.47	115.2	0.70	0.62
3.75	0.15	51.20	3.71	133.0	0.80	0.71
4.00	0.15	51.20	3.96	133.0	0.80	0.71
4.25	0.16	51.10	4.21	141.8	0.90	0.79
4.50	0.16	51.10	4.46	141.8	0.90	0.79
4.75	0.17	51.00	4.70	150.7	1.00	0.88
5.00	0.18	51.00	4.95	159.6	1.00	0.88
5.25	0.18	50.85	5.20	159.6	1.15	1.01
5.50	0.19	50.85	5.45	168.4	1.15	1.01
5.75	0.20	50.75	5.69	177.3	1.25	1.10
6.00	0.20	50.75	5.94	177.3	1.25	1.10
6.25	0.21	50.65	6.19	186.1	1.35	1.19
6.50	0.21	50.65	6.44	186.1	1.35	1.19
6.75	0.22	50.55	6.68	195.0	1.45	1.28
7.00	0.22	50.55	6.93	195.0	1.45	1.28
7.25	0.24	50.55	7.18	212.7	1.45	1.28

Displacement (mm)	Load (kN)	Burette Reading (cc)	Axial Strain (%)	Stress (kPa)	Volume Change (Comp) (cc)	Volumetric Strain (%)
7.50	0.24	50.40	7.43	212.7	1.60	1.41
7.75	0.25	50.40	7.67	221.6	1.60	1.41
8.00	0.25	50.30	7.92	221.6	1.70	1.50
8.25	0.26	50.30	8.17	230.5	1.70	1.50
8.50	0.26	50.20	8.42	230.5	1.80	1.59
8.75	0.27	50.20	8.66	239.3	1.80	1.59
9.00	0.27	50.05	8.91	239.3	1.95	1.72
9.25	0.28	50.05	9.16	248.2	1.95	1.72
9.50	0.28	50.05	9.41	248.2	1.95	1.72
9.75	0.28	49.95	9.65	248.2	2.05	1.81
10.00	0.29	49.95	9.90	257.1	2.05	1.81
10.25	0.29	49.85	10.15	257.1	2.15	1.90
10.50	0.29	49.85	10.40	257.1	2.15	1.90
10.75	0.30	49.85	10.64	265.9	2.15	1.90
11.00	0.30	49.75	10.89	265.9	2.25	1.99
11.25	0.31	49.75	11.14	274.8	2.25	1.99
11.50	0.31	49.60	11.39	274.8	2.40	2.12
11.75	0.32	49.60	11.63	283.6	2.40	2.12
12.00	0.32	49.50	11.88	283.6	2.50	2.21
12.25	0.32	49.50	12.13	283.6	2.50	2.21
12.50	0.32	49.40	12.38	283.6	2.60	2.29
12.75	0.33	49.40	12.62	292.5	2.60	2.29
12.75	0.33	49.30	12.62	292.5	2.70	2.38
13.00	0.33	49.30	12.87	292.5	2.70	2.38
13.25	0.33	49.30	13.12	292.5	2.70	2.38
13.50	0.34	49.15	13.37	301.4	2.85	2.51
13.75	0.34	49.15	13.61	301.4	2.85	2.51
14.00	0.34	49.15	13.86	301.4	2.85	2.51
14.25	0.34	49.05	14.11	301.4	2.95	2.60
14.50	0.35	49.05	14.36	310.2	2.95	2.60
14.75	0.35	48.95	14.60	310.2	3.05	2.69
15.00	0.35	48.95	14.85	310.2	3.05	2.69
15.25	0.36	48.95	15.10	319.1	3.05	2.69
15.50	0.36	48.85	15.35	319.1	3.15	2.78
15.75	0.36	48.85	15.59	319.1	3.15	2.78
16.00	0.36	48.70	15.84	319.1	3.30	2.91
16.25	0.36	48.70	16.09	319.1	3.30	2.91
16.50	0.36	48.70	16.34	319.1	3.30	2.91
16.75	0.36	48.60	16.58	319.1	3.40	3.00
17.00	0.36	48.60	16.83	319.1	3.40	3.00
17.25	0.36	48.60	17.08	319.1	3.40	3.00
17.50	0.36	48.50	17.33	319.1	3.50	3.09
17.75	0.36	48.50	17.57	319.1	3.50	3.09
18.00	0.36	48.50	17.82	319.1	3.50	3.09

Consolidated Drained triaxial test with volume change measurements on rebounded sample

Initial Diameter (cm)	10.15	Initial Relative density	0.91
Initial c/s area (sq. cm)	3.79	Initial Diameter (cm)	17.93
Initial Volume (cc)	11.28	Initial Cell Pressure (kPa)	350
Weight of sample taken (gm)	114.51	Rebounded Cell Pressure (kPa)	300
Dry density (gm/cc)	160	Back Pressure (kPa)	50
Specific Gravity	1.40	Volume Change during rebound (cc)	1.70
Initial void ratio	2.67	Volumetric strain during rebound (%)	1.50

Displacement (mm)	Load (kN)	Burette Reading (cc)	Axial Strain (%)	Stress (kPa)	Volume Change (Comp) (cc)	Volumetric Strain (%)
0.00	0.00	45.80	0.00	0.0	0.00	0.00
0.25	0.02	45.70	0.25	17.7	0.10	0.09
0.50	0.03	45.70	0.49	26.6	0.10	0.09
0.75	0.06	45.55	0.74	53.2	0.25	0.22
1.00	0.08	45.55	0.99	70.9	0.25	0.22
1.25	0.10	45.45	1.23	88.6	0.35	0.31
1.50	0.12	45.35	1.48	106.4	0.45	0.39
1.75	0.15	45.35	1.72	133.0	0.45	0.39
2.00	0.16	45.25	1.97	141.8	0.55	0.48
2.25	0.17	45.25	2.22	150.7	0.55	0.48
2.50	0.18	45.10	2.46	159.6	0.70	0.61
2.75	0.20	45.10	2.71	177.3	0.70	0.61
3.00	0.22	45.00	2.96	195.0	0.80	0.70
3.25	0.23	45.00	3.20	203.9	0.80	0.70
3.50	0.25	44.90	3.45	221.6	0.90	0.79
3.75	0.26	44.90	3.69	230.5	0.90	0.79
4.00	0.27	44.80	3.94	239.3	1.00	0.87
4.25	0.29	44.80	4.19	257.1	1.00	0.87
4.50	0.31	44.80	4.43	274.8	1.00	0.87
4.75	0.32	44.65	4.68	283.6	1.15	1.00
5.00	0.33	44.55	4.93	292.5	1.25	1.09
5.25	0.34	44.45	5.17	301.4	1.35	1.18
5.50	0.35	44.45	5.42	310.2	1.35	1.18
5.75	0.37	44.35	5.67	328.0	1.45	1.27
6.00	0.38	44.35	5.91	336.8	1.45	1.27
6.25	0.39	44.20	6.16	345.7	1.60	1.40
6.50	0.40	44.20	6.40	354.6	1.60	1.40
6.75	0.41	44.10	6.65	363.4	1.70	1.48

Displacement (mm)	Load (kN)	Burette Reading (cc)	Axial Strain (%)	Stress (kPa)	Volume Change (Comp) (cc)	Volumetric Strain (%)
6.75	0.41	44.10	6.65	363.4	1.70	1.48
7.00	0.42	44.00	6.90	372.3	1.80	1.57
7.25	0.43	44.00	7.14	381.2	1.80	1.57
7.50	0.43	43.85	7.39	381.2	1.95	1.70
7.75	0.44	43.85	7.64	390.0	1.95	1.70
8.00	0.44	43.75	7.88	390.0	2.05	1.79
8.25	0.45	43.75	8.13	398.9	2.05	1.79
8.50	0.46	43.65	8.37	407.7	2.15	1.88
8.75	0.46	43.65	8.62	407.7	2.15	1.88
9.00	0.47	43.65	8.87	416.6	2.15	1.88
9.25	0.47	43.55	9.11	416.6	2.25	1.96
9.50	0.48	43.40	9.36	425.5	2.40	2.10
9.75	0.48	43.40	9.61	425.5	2.40	2.10
10.00	0.49	43.30	9.85	434.3	2.50	2.18
10.25	0.49	43.30	10.10	434.3	2.50	2.18
10.50	0.50	43.30	10.34	443.2	2.50	2.18
10.75	0.50	43.20	10.59	443.2	2.60	2.27
11.00	0.50	43.20	10.84	443.2	2.60	2.27
11.25	0.51	43.10	11.08	452.1	2.70	2.36
11.50	0.51	43.10	11.33	452.1	2.70	2.36
11.75	0.51	42.95	11.58	452.1	2.85	2.49
12.00	0.51	42.95	11.82	452.1	2.85	2.49
12.25	0.52	42.95	12.07	460.9	2.85	2.49
12.50	0.52	42.85	12.32	460.9	2.95	2.58
12.75	0.53	42.85	12.56	469.8	2.95	2.58
13.00	0.53	42.75	12.81	469.8	3.05	2.66
13.25	0.53	42.75	13.05	469.8	3.05	2.66
13.50	0.53	42.75	13.30	469.8	3.05	2.66
13.75	0.53	42.60	13.55	469.8	3.20	2.79
14.00	0.54	42.60	13.79	478.7	3.20	2.79
14.25	0.54	42.50	14.04	478.7	3.30	2.88
14.50	0.54	42.50	14.29	478.7	3.30	2.88
14.75	0.54	42.40	14.53	478.7	3.40	2.97
15.00	0.54	42.40	14.78	478.7	3.40	2.97
15.25	0.54	42.40	15.02	478.7	3.40	2.97
15.50	0.54	42.30	15.27	478.7	3.50	3.06
15.75	0.55	42.30	15.52	487.5	3.50	3.06
16.00	0.55	42.15	15.76	487.5	3.65	3.19
16.25	0.55	42.15	16.01	487.5	3.65	3.19
16.50	0.55	42.15	16.26	487.5	3.65	3.19
16.75	0.55	42.15	16.50	487.5	3.65	3.19
16.75	0.55	42.05	16.75	487.5	3.75	3.27
17.25	0.56	42.05	17.00	496.4	3.75	3.27
17.50	0.56	42.05	17.24	496.4	3.75	3.27
17.75	0.56	42.05	17.49	496.4	3.75	3.27
18.00	0.56	41.95	17.73	496.4	3.85	3.36

Consolidated Drained triaxial test with volume change measurements on rebounded sample

Initial Length (cm)	10.15	Initial void ratio	0.91
Initial Diameter (cm)	3.79	Initial Relative density	17.93
Initial c/s area (sq. cm)	11.28	Initial Cell Pressure (kPa)	350
Initial Volume (cc)	114.51	Rebounded Cell Pressure (kPa)	300
Weight of sample taken (gm)	160	Back Pressure (kPa)	50
Dry density (gm/cc)	1.40	Volume Change during rebound (cc)	1.50
Specific Gravity	2.67	Volumetric strain during rebound (%)	1.32

Displacement (mm)	Load (kN)	Burette Reading (cc)	Axial Strain (%)	Stress (kPa)	Volume Change (Comp) (cc)	Volumetric Strain (%)
0.00	0.00	49.00	0.00	0.0	0.00	0.00
0.25	0.03	48.90	0.25	26.6	0.10	0.09
0.50	0.06	48.75	0.49	53.2	0.25	0.22
0.75	0.09	48.65	0.74	79.8	0.35	0.31
1.00	0.14	48.55	0.99	124.1	0.45	0.39
1.25	0.18	48.45	1.23	159.6	0.55	0.48
1.50	0.23	48.45	1.48	203.9	0.55	0.48
1.75	0.25	48.30	1.72	221.6	0.70	0.61
2.00	0.28	48.30	1.97	248.2	0.70	0.61
2.25	0.30	48.20	2.22	265.9	0.80	0.70
2.50	0.33	48.10	2.46	292.5	0.90	0.79
2.75	0.35	47.95	2.71	310.2	1.05	0.92
3.00	0.37	47.85	2.96	328.0	1.15	1.00
3.25	0.39	47.75	3.20	345.7	1.25	1.09
3.50	0.42	47.65	3.45	372.3	1.35	1.18
3.75	0.43	47.50	3.69	381.2	1.50	1.31
4.00	0.45	47.50	3.94	398.9	1.50	1.31
4.25	0.46	47.40	4.19	407.7	1.60	1.40
4.50	0.47	47.30	4.43	416.6	1.70	1.48
4.75	0.48	47.30	4.68	425.5	1.70	1.48
5.00	0.49	47.20	4.93	434.3	1.80	1.57
5.25	0.50	47.05	5.17	443.2	1.95	1.70
5.50	0.51	47.05	5.42	452.1	1.95	1.70
5.75	0.52	46.95	5.67	460.9	2.05	1.79
6.00	0.53	46.95	5.91	469.8	2.05	1.79
6.25	0.54	46.85	6.16	478.7	2.15	1.88
6.50	0.54	46.85	6.40	478.7	2.15	1.88
6.75	0.55	46.70	6.65	487.5	2.30	2.01
7.00	0.55	46.70	6.90	487.5	2.30	2.01
7.25	0.56	46.60	7.14	496.4	2.40	2.10
7.50	0.56	46.60	7.39	496.4	2.40	2.10
7.75	0.57	46.50	7.64	505.3	2.50	2.18

Displacement (mm)	Load (kN)	Burette Reading (cc)	Axial Strain (%)	Stress (kPa)	Volume Change (Comp) (cc)	Volumetric Strain (%)
8.00	0.58	46.50	7.88	514.1	2.50	2.18
8.25	0.58	46.40	8.13	514.1	2.60	2.27
8.50	0.58	46.40	8.37	514.1	2.60	2.27
8.75	0.59	46.40	8.62	523.0	2.60	2.27
9.00	0.59	46.25	8.87	523.0	2.75	2.40
9.25	0.59	46.25	9.11	523.0	2.75	2.40
9.50	0.60	46.25	9.36	531.8	2.75	2.40
9.75	0.60	46.15	9.61	531.8	2.85	2.49
10.00	0.60	46.15	9.85	531.8	2.85	2.49
10.25	0.61	46.05	10.10	540.7	2.95	2.58
10.50	0.61	46.05	10.34	540.7	2.95	2.58
10.75	0.61	46.05	10.59	540.7	2.95	2.58
11.00	0.62	45.90	10.84	549.6	3.10	2.71
11.25	0.62	45.90	11.08	549.6	3.10	2.71
11.50	0.63	45.90	11.33	558.4	3.10	2.71
11.75	0.63	45.80	11.58	558.4	3.20	2.79
12.00	0.63	45.80	11.82	558.4	3.20	2.79
12.25	0.64	45.80	12.07	567.3	3.20	2.79
12.50	0.64	45.70	12.32	567.3	3.30	2.88
12.75	0.64	45.70	12.56	567.3	3.30	2.88
13.00	0.65	45.70	12.81	576.2	3.30	2.88
13.25	0.65	45.60	13.05	576.2	3.40	2.97
13.50	0.65	45.60	13.30	576.2	3.40	2.97
13.75	0.65	45.60	13.55	576.2	3.40	2.97
14.00	0.65	45.45	13.79	576.2	3.55	3.10
14.25	0.66	45.45	14.04	585.0	3.55	3.10
14.50	0.66	45.45	14.29	585.0	3.55	3.10
14.75	0.66	45.35	14.53	585.0	3.65	3.19
15.00	0.66	45.35	14.78	585.0	3.65	3.19
15.25	0.66	45.35	15.02	585.0	3.65	3.19
15.50	0.66	45.25	15.27	585.0	3.75	3.27
15.75	0.66	45.25	15.52	585.0	3.75	3.27
16.00	0.67	45.15	15.76	593.9	3.85	3.36
16.25	0.67	45.15	16.01	593.9	3.85	3.36
16.50	0.67	45.15	16.26	593.9	3.85	3.36
16.75	0.67	45.00	16.50	593.9	4.00	3.49
17.00	0.67	45.00	16.75	593.9	4.00	3.49
17.25	0.67	45.00	17.00	593.9	4.00	3.49
17.50	0.67	44.90	17.24	593.9	4.10	3.58
17.75	0.68	44.90	17.49	602.8	4.10	3.58
18.00	0.68	44.90	17.73	602.8	4.10	3.58
18.25	0.68	44.80	17.98	602.8	4.20	3.67
18.50	0.68	44.80	18.23	602.8	4.20	3.67
18.75	0.68	44.80	18.47	602.8	4.20	3.67
19.00	0.68	44.80	18.72	602.8	4.20	3.67
19.25	0.68	44.65	18.97	602.8	4.35	3.80
19.50	0.68	44.65	19.21	602.8	4.35	3.80
19.75	0.69	44.65	19.46	611.6	4.35	3.80
20.00	0.69	44.65	19.70	611.6	4.35	3.80

Consolidated Drained triaxial test with volume change measurements on rebounded sample

Initial Length (cm)	10.1	Initial void ratio	0.90
Initial Diameter (cm)	3.79	Initial Relative density	20.78
Initial c/s area (sq. cm)	11.28	Initial Cell Pressure (kPa)	350
Initial Volume (cc)	113.94	Rebounded Cell Pressure (kPa)	300
Weight of sample taken (gm)	160	Back Pressure (kPa)	50
Dry density (gm/cc)	1.40	Volume Change during rebound (cc)	1.15
Specific Gravity	2.67	Volumetric strain during rebound (%)	1.01

Displacement (mm)	Load (kN)	Burette Reading (cc)	Axial Strain (%)	Stress (kPa)	Volume Change (Comp) (cc)	Volumetric Strain (%)
0.00	0.00	49.00	0.00	0.0	0.00	0.00
0.25	0.06	48.75	0.25	53.2	0.25	0.22
0.50	0.11	48.65	0.50	97.5	0.35	0.31
0.75	0.17	48.55	0.74	150.7	0.45	0.39
1.00	0.22	48.45	0.99	195.0	0.55	0.48
1.25	0.28	48.20	1.24	248.2	0.80	0.70
1.50	0.34	48.10	1.49	301.4	0.90	0.79
1.75	0.39	48.00	1.73	345.7	1.00	0.88
2.00	0.45	47.85	1.98	398.9	1.15	1.01
2.25	0.47	47.75	2.23	416.6	1.25	1.10
2.50	0.49	47.65	2.48	434.3	1.35	1.18
2.75	0.52	47.55	2.72	460.9	1.45	1.27
3.00	0.53	47.55	2.97	469.8	1.45	1.27
3.25	0.55	47.40	3.22	487.5	1.60	1.40
3.50	0.57	47.40	3.47	505.3	1.60	1.40
3.75	0.58	47.30	3.71	514.1	1.70	1.49
4.00	0.60	47.20	3.96	531.8	1.80	1.58
4.25	0.61	47.20	4.21	540.7	1.80	1.58
4.50	0.62	47.05	4.46	549.6	1.95	1.71
4.75	0.62	46.95	4.70	549.6	2.05	1.80
5.00	0.63	46.85	4.95	558.4	2.15	1.89
5.25	0.64	46.75	5.20	567.3	2.25	1.97
5.50	0.64	46.75	5.45	567.3	2.25	1.97
5.75	0.64	46.60	5.69	567.3	2.40	2.11
6.00	0.65	46.50	5.94	576.2	2.50	2.19
6.25	0.65	46.50	6.19	576.2	2.50	2.19
6.50	0.65	46.40	6.44	576.2	2.60	2.28
6.75	0.66	46.40	6.68	585.0	2.60	2.28
7.00	0.66	46.30	6.93	585.0	2.70	2.37
7.25	0.67	46.30	7.18	593.9	2.70	2.37
7.50	0.67	46.15	7.43	593.9	2.85	2.50
7.75	0.68	46.15	7.67	602.8	2.85	2.50

Displacement (mm)	Load (kN)	Burette Reading (cc)	Axial Strain (%)	Stress (kPa)	Volume Change (Comp) (cc)	Volumetric Strain (%)
8.00	0.68	46.05	7.92	602.8	2.95	2.59
8.25	0.69	46.05	8.17	611.6	2.95	2.59
8.50	0.69	45.95	8.42	611.6	3.05	2.68
8.75	0.69	45.95	8.66	611.6	3.05	2.68
9.00	0.70	45.85	8.91	620.5	3.15	2.76
9.25	0.70	45.85	9.16	620.5	3.15	2.76
9.50	0.70	45.70	9.41	620.5	3.30	2.90
9.75	0.70	45.70	9.65	620.5	3.30	2.90
10.00	0.71	45.60	9.90	629.3	3.40	2.98
10.25	0.71	45.60	10.15	629.3	3.40	2.98
10.50	0.71	45.50	10.40	629.3	3.50	3.07
10.75	0.71	45.35	10.64	629.3	3.65	3.20
11.00	0.72	45.35	10.89	638.2	3.65	3.20
11.25	0.72	45.25	11.14	638.2	3.75	3.29
11.50	0.72	45.25	11.39	638.2	3.75	3.29
11.75	0.73	45.15	11.63	647.1	3.85	3.38
12.00	0.73	45.15	11.88	647.1	3.85	3.38
12.25	0.73	45.05	12.13	647.1	3.95	3.47
12.50	0.74	44.90	12.38	655.9	4.10	3.60
12.75	0.74	44.90	12.62	655.9	4.10	3.60
13.00	0.74	44.90	12.62	655.9	4.10	3.60
13.25	0.74	44.90	12.87	655.9	4.10	3.60
13.50	0.75	44.80	13.12	664.8	4.20	3.69
13.75	0.75	44.80	13.37	664.8	4.20	3.69
14.00	0.75	44.80	13.61	664.8	4.20	3.69
14.25	0.75	44.80	13.86	664.8	4.20	3.69
14.50	0.76	44.70	14.11	673.7	4.30	3.77
14.75	0.76	44.70	14.36	673.7	4.30	3.77
15.00	0.76	44.70	14.60	673.7	4.30	3.77
15.25	0.76	44.70	14.85	673.7	4.30	3.77
15.50	0.76	44.60	15.10	673.7	4.40	3.86
15.75	0.77	44.60	15.35	682.5	4.40	3.86
16.00	0.77	44.45	15.59	682.5	4.55	3.99
16.25	0.77	44.45	15.84	682.5	4.55	3.99
16.50	0.77	44.45	16.09	682.5	4.55	3.99
16.75	0.77	44.35	16.34	682.5	4.65	4.08
17.00	0.78	44.35	16.58	691.4	4.65	4.08
17.25	0.78	44.25	16.83	691.4	4.75	4.17
17.50	0.78	44.25	17.08	691.4	4.75	4.17
17.75	0.78	44.25	17.33	691.4	4.75	4.17
18.00	0.79	44.15	17.82	700.3	4.85	4.26
18.25	0.79	44.15	18.07	700.3	4.85	4.26
18.50	0.79	44.15	18.32	700.3	4.85	4.26
18.75	0.79	44.15	18.32	700.3	4.85	4.26
19.00	0.79	44.00	18.56	700.3	5.00	4.39
19.25	0.80	44.00	18.81	709.1	5.00	4.39
19.50	0.80	43.90	19.06	709.1	5.10	4.48
19.75	0.80	43.90	19.31	709.1	5.10	4.48
20.00	0.80	43.90	19.55	709.1	5.10	4.48

Stress-controlled Consolidated Undrained Triaxial Test Result (σ_{3c}=350 kPa, Initial Relative Density ≈20%)

Load (kg)	LVDT reading (mm)	Change in length (mm)	Strain (%)	Area (sq. cm)	Stress (kPa)	PWP Reading (bar)	PWP Change (kPa)	p' (kPa)	q (kPa)
0	4.6	0	0.0	11.34	0.00	-2.37	0	350.0	0.0
4	4.32	0.28	0.3	11.37	35.18	-2.12	25	342.6	17.6
8	4.11	0.49	0.5	11.40	70.20	-1.97	40	345.1	35.1
12	3.85	0.75	0.7	11.42	105.03	-1.90	47	355.5	52.5
16	3.62	0.98	1.0	11.45	139.72	-1.78	59	360.9	69.9
20	3.43	1.17	1.2	11.47	174.32	-1.63	74	363.2	87.2
23	3.18	1.42	1.4	11.50	199.97	-1.48	89	361.0	100.0
26	2.88	1.72	1.7	11.54	225.37	-1.38	99	363.7	112.7
29	2.56	2.04	2.0	11.57	250.57	-1.27	110	365.3	125.3
32	2.28	2.32	2.3	11.61	275.71	-1.11	126	361.9	137.9
35	2.04	2.56	2.5	11.63	300.82	-0.97	140	360.4	150.4
38	1.79	2.81	2.8	11.66	325.77	-0.86	151	361.9	162.9
41	1.41	3.19	3.2	11.71	350.13	-0.64	173	352.1	175.1
44	0.94	3.66	3.6	11.77	373.95	-0.46	191	346.0	187.0
47	0.59	4.01	4.0	11.81	398.01	-0.29	208	341.0	199.0
44	-0.12	4.72	4.7	11.90	369.87	-0.01	236	298.9	184.9
41	-0.89	5.49	5.4	11.99	341.90	0.07	244	276.9	170.9
38	-1.21	5.81	5.8	12.03	315.82	0.12	249	258.9	157.9
35	-1.58	6.18	6.1	12.08	289.76	0.19	256	238.9	144.9
32	-1.98	6.58	6.5	12.13	263.80	0.37	274	207.9	131.9
29	-2.57	7.17	7.1	12.21	237.58	0.31	268	200.8	118.8
26	-2.86	7.46	7.4	12.24	212.34	0.38	275	181.2	106.2
23	-3.52	8.12	8.0	12.33	186.52	0.39	276	167.3	93.3
20	-4.26	8.86	8.8	12.43	160.90	0.43	280	150.4	80.4
16	-6.12	10.72	10.6	12.69	126.12	0.56	293	120.1	63.1
12	-8.46	13.06	12.9	13.02	92.14	0.68	305	91.1	46.1

Stress-controlled Consolidated Undrained Triaxial Test Result (σ_{3c}=350 kPa, Initial Relative Density ≈45%)

Load (kg)	LVDT reading (mm)	Change in length (mm)	Strain (%)	Area (sq. cm)	Stress (kPa)	PWP Reading (bar)	PWP Change (kPa)	p' (kPa)	q (kPa)
0	4.6	0	0.0	11.34	0.00	-2.86	0	350	0.0
5	4.42	0.18	0.2	11.36	44.01	-2.76	10	362	22.0
10	4.22	0.38	0.4	11.38	87.85	-2.69	17	377	43.9
15	4.04	0.56	0.6	11.40	131.54	-2.54	32	384	65.8
20	3.84	0.76	0.8	11.43	175.04	-2.41	45	393	87.5
23	3.62	0.98	1.0	11.45	200.85	-2.36	50	400	100.4
26	3.4	1.2	1.2	11.48	226.55	-2.33	53	410	113.3
29	3.2	1.4	1.4	11.50	252.19	-2.25	61	415	126.1
32	3	1.6	1.6	11.52	277.72	-2.15	71	418	138.9
35	2.81	1.79	1.8	11.54	303.17	-2.08	78	424	151.6
38	2.63	1.97	2.0	11.57	328.56	-2.01	85	429	164.3
41	2.43	2.17	2.1	11.59	353.78	-1.95	91	436	176.9
44	2.21	2.39	2.4	11.61	378.83	-1.87	99	440	189.4
47	2	2.6	2.6	11.64	403.79	-1.79	107	445	201.9
50	1.8	2.8	2.8	11.66	428.69	-1.73	113	451	214.3
53	1.62	2.98	3.0	11.68	453.58	-1.69	117	460	226.8
56	1.42	3.18	3.1	11.71	478.28	-1.62	124	465	239.1
59	1.23	3.37	3.3	11.73	502.92	-1.55	131	470	251.5
62	1.04	3.56	3.5	11.75	527.47	-1.50	136	478	263.7
63	0.95	3.65	3.6	11.77	535.48	-1.46	140	478	267.7
64	0.88	3.72	3.7	11.77	543.59	-1.43	143	479	271.8
65	0.81	3.79	3.8	11.78	551.68	-1.40	146	480	275.8
66	0.74	3.86	3.8	11.79	559.77	-1.36	150	480	279.9
67	0.62	3.98	3.9	11.81	567.55	-1.27	159	475	283.8
68	0.56	4.04	4.0	11.81	575.66	-1.19	167	471	287.8
69	0.48	4.12	4.1	11.82	583.65	-1.09	177	465	291.8
70	0.39	4.21	4.2	11.83	591.55	-1.00	186	460	295.8
71	0.05	4.55	4.5	11.87	597.90	-0.92	194	455	298.9
70	-1.8	6.4	6.3	12.11	578.17	-0.97	189	450	289.1
69	-2.42	7.02	7.0	12.19	566.17	-0.98	188	445	283.1
68	-2.53	7.13	7.1	12.20	557.32	-0.87	199	430	278.7
67	-2.58	7.18	7.1	12.21	548.83	-0.82	204	420	274.4
66	-2.61	7.21	7.1	12.21	540.46	-0.76	210	410	270.2
69	-3.12	7.72	7.6	12.28	561.96	-0.47	239	392	281.0
72	-6.02	10.62	10.5	12.67	568.16	-0.47	239	395	284.1
75	-9.1	13.7	13.6	13.12	571.66	-0.52	234	402	285.8
78	-9.84	14.44	14.3	13.23	589.49	-0.53	233	412	294.7
83	-10.65	15.25	15.1	13.36	621.41	-0.45	241	420	310.7
88	-11.24	15.84	15.7	13.45	654.31	-0.40	246	431	327.2
93	-12.11	16.71	16.5	13.59	684.42	-0.40	246	446	342.2
98	-12.85	17.45	17.3	13.71	714.89	-0.36	250	457	357.4
103	-13.63	18.23	18.0	13.84	744.35	-0.35	251	471	372.2
108	-13.91	18.51	18.3	13.88	777.84	-0.31	255	484	388.9
113	-14.16	18.76	18.6	13.93	811.39	-0.50	236	520	405.7
118	-15.02	19.62	19.4	14.07	838.43	-0.56	230	539	419.2
123	-15.38	19.98	19.8	14.14	870.09	-0.62	224	561	435.0
128	-15.56	20.16	20.0	14.17	903.45	-0.76	210	592	451.7
133	-15.91	20.51	20.3	14.23	934.67	-0.73	213	604	467.3
138	-16.35	20.95	20.7	14.31	964.51	-0.75	211	621	482.3
143	-17.02	21.62	21.4	14.43	991.09	-0.79	207	639	495.5
148	-17.61	22.21	22.0	14.54	1018.12	-0.90	196	663	509.1

Stress-controlled Consolidated Undrained Triaxial Test Result (σ_{3c}=350 kPa, Initial Relative Density ≈75%)

Load (kg)	LVDT reading (mm)	Change in length (mm)	Strain (%)	Area (sq. cm)	Stress (kPa)	PWP Reading (bar)	PWP Change (kPa)	p' (kPa)	q (kPa)
0	5.7	0	0.0	11.34	0.00	-2.42	0	100.0	0.0
3	5.41	0.29	0.3	11.37	26.38	-2.42	0	108.8	26.4
8	5.11	0.59	0.6	11.41	70.13	-2.41	1	123.4	70.1
13	4.98	0.72	0.7	11.42	113.82	-2.21	21	137.9	113.8
18	4.73	0.97	1.0	11.45	157.21	-1.86	56	152.4	157.2
23	4.51	1.19	1.2	11.48	200.43	-1.58	84	166.8	200.4
28	4.23	1.47	1.5	11.51	243.32	-1.64	78	181.1	243.3
33	3.96	1.74	1.7	11.54	285.99	-1.71	71	195.3	286.0
38	3.59	2.11	2.1	11.58	328.10	-1.76	66	209.4	328.1
43	3.36	2.34	2.3	11.61	370.40	-1.80	62	223.5	370.4
48	3.02	2.68	2.7	11.65	412.05	-1.84	58	237.3	412.0
51	2.74	2.96	2.9	11.68	436.56	-1.89	53	245.5	436.6
54	2.41	3.29	3.3	11.72	460.68	-1.94	48	253.6	460.7
57	2.11	3.59	3.6	11.76	484.78	-2.00	42	261.6	484.8
60	1.85	3.85	3.8	11.79	508.93	-2.04	38	269.6	508.9
63	1.56	4.14	4.1	11.82	532.78	-2.10	32	277.6	532.8
66	1.17	4.53	4.5	11.87	555.91	-2.14	28	285.3	555.9
69	0.78	4.92	4.9	11.92	578.83	-2.18	24	292.9	578.8
72	0.32	5.38	5.3	11.98	601.10	-2.23	19	300.4	601.1
75	-0.06	5.76	5.7	12.03	623.66	-2.27	15	307.9	623.7
78	-1.21	6.91	6.8	12.17	640.77	-2.31	11	313.6	640.8
81	-1.82	7.52	7.4	12.25	661.10	-2.36	6	320.4	661.1
84	-2.56	8.26	8.2	12.35	680.16	-2.41	1	326.7	680.2
87	-3.01	8.71	8.6	12.41	701.03	-2.47	-5	333.7	701.0
90	-3.78	9.48	9.4	12.51	719.16	-2.53	-11	339.7	719.2
94	-4.42	10.12	10.0	12.60	745.87	-2.57	-15	348.6	745.9
98	-5.45	11.15	11.0	12.75	768.79	-2.66	-24	356.3	768.8
102	-6.55	12.25	12.1	12.91	790.38	-2.70	-28	363.5	790.4
107	-7.43	13.13	13.0	13.03	820.90	-2.73	-31	373.6	820.9
112	-8.65	14.35	14.2	13.22	847.33	-2.81	-39	382.4	847.3
117	-9.63	15.33	15.2	13.37	875.15	-2.84	-42	391.7	875.1
122	-10.31	16.01	15.9	13.48	905.30	-2.88	-46	401.8	905.3
127	-11.02	16.72	16.6	13.59	934.53	-2.96	-54	411.5	934.5
130	-11.44	17.14	17.0	13.66	951.84	-3.03	-61	417.3	951.8

Stress-controlled Consolidated Undrained Triaxial Test Result (σ_{3c}=250 kPa, Initial Relative Density ≈75%)

Load (kg)	LVDT reading (mm)	Change in length (mm)	Strain (%)	Area (sq. cm)	Stress (kPa)	PWP Reading (bar)	PWP Change (kPa)	p' (kPa)	q (kPa)
0	4.6	0	0.0	11.34	0.00	-2.45	0	250.0	0.0
3	4.51	0.09	0.1	11.35	26.43	-2.40	5	258.8	26.4
8	4.43	0.17	0.2	11.36	70.43	-2.29	16	273.5	70.4
13	4.28	0.32	0.3	11.38	114.28	-2.09	36	288.1	114.3
18	4.15	0.45	0.4	11.39	158.02	-1.59	86	302.7	158.0
23	4.02	0.58	0.6	11.41	201.66	-0.97	148	317.2	201.7
28	3.87	0.73	0.7	11.42	245.13	-0.76	169	331.7	245.1
33	3.76	0.84	0.8	11.44	288.59	-0.71	174	346.2	288.6
38	3.62	0.98	1.0	11.45	331.85	-0.76	169	360.6	331.8
43	3.54	1.06	1.0	11.46	375.21	-0.83	162	375.1	375.2
48	3.42	1.18	1.2	11.47	418.34	-0.97	148	389.4	418.3
51	3.36	1.24	1.2	11.48	444.21	-0.99	146	398.1	444.2
54	3.25	1.35	1.3	11.49	469.83	-1.02	143	406.6	469.8
57	3.19	1.41	1.4	11.50	495.63	-1.10	135	415.2	495.6
60	3.15	1.45	1.4	11.51	521.50	-1.15	130	423.8	521.5
63	2.97	1.63	1.6	11.53	546.59	-1.21	124	432.2	546.6
66	2.76	1.84	1.8	11.55	571.41	-1.31	114	440.5	571.4
69	2.69	1.91	1.9	11.56	596.96	-1.47	99	449.0	597.0
72	2.4	2.2	2.2	11.59	621.09	-1.56	90	457.0	621.1
75	2.18	2.42	2.4	11.62	645.53	-1.70	75	465.2	645.5
78	1.9	2.7	2.7	11.65	669.44	-1.78	67	473.1	669.4
81	0.81	3.79	3.8	11.78	687.48	-1.86	59	479.2	687.5
84	0.22	4.38	4.3	11.85	708.62	-1.90	55	486.2	708.6
87	-0.8	5.4	5.3	11.98	726.18	-1.93	52	492.1	726.2
90	-1.8	6.4	6.3	12.11	743.36	-1.97	48	497.8	743.4
94	-3	7.6	7.5	12.26	766.55	-2.00	45	505.5	766.5
98	-4.5	9.1	9.0	12.46	786.33	-2.07	39	512.1	786.3
102	-5.8	10.4	10.3	12.64	806.85	-2.13	32	519.0	806.9
107	-6.9	11.5	11.4	12.80	836.13	-2.16	29	528.7	836.1
112	-8.2	12.8	12.7	12.99	862.49	-2.20	25	537.5	862.5
117	-9.3	13.9	13.8	13.15	889.75	-2.25	20	546.6	889.8
122	-10.4	15	14.9	13.32	916.06	-2.30	15	555.4	916.1
127	-11.2	15.8	15.6	13.44	944.73	-2.34	11	564.9	944.7
132	-12.3	16.9	16.7	13.62	969.25	-2.39	6	573.1	969.2

Stress-controlled Consolidated Undrained Triaxial Test Result (σ_{3c}=100 kPa, Initial Relative Density ≈75%)

Load (kg)	LVDT reading (mm)	Change in length (mm)	Strain (%)	Area (sq. cm)	Stress (kPa)	PWP Reading (bar)	PWP Change (kPa)	p' (kPa)	q (kPa)
0	6.5	0	0.0	11.34	0.00	-2.56	0	350.0	0.0
3	6.48	0.02	0.0	11.34	26.45	-2.56	0	358.8	26.4
8	6.42	0.08	0.1	11.35	70.49	-2.44	12	361.5	70.5
13	6.35	0.15	0.1	11.36	114.47	-2.42	14	374.2	114.5
18	6.29	0.21	0.2	11.36	158.40	-2.32	24	378.8	158.4
23	6.22	0.28	0.3	11.37	202.26	-2.26	30	387.4	202.3
28	6.16	0.34	0.3	11.38	246.08	-2.26	30	402.0	246.1
33	6.01	0.49	0.5	11.40	289.59	-2.17	39	407.5	289.6
38	5.93	0.57	0.6	11.40	333.21	-2.11	45	416.1	333.2
43	5.88	0.62	0.6	11.41	376.86	-2.11	45	430.6	376.9
48	5.79	0.71	0.7	11.42	420.30	-2.06	50	440.1	420.3
51	5.67	0.83	0.8	11.43	446.04	-2.00	56	442.7	446.0
54	5.63	0.87	0.9	11.44	472.09	-1.94	62	445.4	472.1
57	5.57	0.93	0.9	11.45	498.02	-1.87	69	447.0	498.0
60	5.48	1.02	1.0	11.46	523.76	-1.81	75	449.6	523.8
63	5.41	1.09	1.1	11.46	549.56	-1.70	86	447.2	549.6
66	5.35	1.15	1.1	11.47	575.38	-1.69	87	454.8	575.4
69	5.21	1.29	1.3	11.49	600.69	-1.61	95	455.2	600.7
72	5.12	1.38	1.4	11.50	626.25	-1.52	104	454.7	626.2
75	4.91	1.59	1.6	11.52	650.96	-1.43	113	454.0	651.0
78	4.71	1.79	1.8	11.54	675.64	-1.34	122	453.2	675.6
81	4.58	1.92	1.9	11.56	700.71	-1.28	128	455.6	700.7
84	4.46	2.04	2.0	11.57	725.78	-1.19	137	454.9	725.8
87	4.29	2.21	2.2	11.59	750.41	-1.1	146	454.1	750.4
90	4.11	2.39	2.4	11.61	774.87	-0.91	165	443.3	774.9
94	3.82	2.68	2.7	11.65	806.93	-0.76	180	439.0	806.9
98	2.87	3.63	3.6	11.76	833.14	-0.36	220	407.7	833.1
102	1.48	5.02	5.0	11.93	854.76	-0.16	240	394.9	854.8
105	-0.08	6.58	6.5	12.13	865.60	-0.27	229	409.5	865.6
108	-1.9	8.4	8.3	12.37	873.17	-0.32	224	417.1	873.2
113	-3.2	9.7	9.6	12.54	900.77	-0.37	219	431.3	900.8
118	-4.6	11.1	11.0	12.74	926.21	-0.45	211	447.7	926.2
123	-6.2	12.7	12.6	12.97	948.27	-0.52	204	462.1	948.3
128	-7.6	14.1	14.0	13.18	971.17	-0.48	208	465.7	971.2